Technische Universität München
Lehrstuhl für Mathematische Statistik
Fakultät für Mathematik

Turbulence Modelling by Time-Series Methods: a Non-Parametric Approach

Vincenzo Ferrazzano

Vollständiger Abdruck der von der Fakultät für Mathematik der Technischen Universität München zur Erlangung des akademischen Grades eines

Doktors der Naturwissenschaften (Dr. rer. nat.)

genehmigten Dissertation.

Vorsitzender:		Univ.-Prof. Dr. Massimo Fornasier
Prüfer der Dissertation:	1.	Univ.-Prof. Dr. Claudia Klüppelberg
	2.	Prof. Peter Brockwell (em.) Colorado State University, Fort Collins, CO, USA (schriftliche Beurteilung)
	3.	Prof. Jürgen Schmiegel Universität Aarhus, Dänemark

Die Dissertation wurde am 12.12.2012 bei der Technischen Universität München eingereicht und durch die Fakultät für Mathematik am 19.12.2012 angenommen.

LA STATISTICA

di Trilussa

Sai ched'è la statistica? È na' cosa
che serve pe fà un conto in generale
de la gente che nasce, che sta male,
che more, che va in carcere e che spósa.

Ma pè me la statistica curiosa
è dove c'entra la percentuale,
pè via che, lì, la media è sempre eguale
puro co' la persona bisognosa.

Me spiego: da li conti che se fanno
seconno le statistiche d'adesso
risurta che te tocca un pollo all'anno:

e, se nun entra nelle spese tue,
t'entra ne la statistica lo stesso
perch'è c'è un antro che ne magna due.

Abstract

Turbulence is a wide and fascinating subject, dating back to over two centuries, and still offering new challenges to the scientific community as a whole. The theory of turbulence involves a wide range of fields, from very applied disciplines, such as engineering and climatology, to fundamental theoretical questions, such as the uniqueness of a strong solution of the three-dimensional Navier-Stokes equation. As a consequence, a considerable deal of attention has been paid to turbulence, engaging physicists and mathematicians alike. The phenomenological similarities between turbulent time-series and high-frequency financial data, together with the importance of wind as an energy resource, have more recently triggered a huge amount of interest on the subject. Classical simulation methods of a turbulent flow, based on discretising the Navier-Stokes equation, involve daunting calculations, defying the computational power of most recent supercomputers. There is, therefore, an interest in obtaining a parsimonious stochastic model, which is able to reproduce the rich phenomenology of turbulence. Since the most interesting aspect of turbulence lies in its behaviour at the smallest scale, a large number of high-frequency time-series are available.

The asymptotic behaviour of second order properties of CARMA processes, as the frequency of observation tends to infinity, is investigated in Chapter 1. A CARMA process is an element of the larger class of the continuous-time moving average processes (CMA) $X_t = \int_{-\infty}^{\infty} g(t-s)dW_s$, for $t \in \mathbb{R}$, where the kernel function g is deterministic, square integrable, and W is a process with stationary and uncorrelated increments and finite variance. Under some necessary and sufficient conditions, classical non-parametric time-series methods can be employed to estimate the kernel function g and the increments of the driving noise W, when X is a CARMA process. The flexibility of CARMA processes and the non-parametric nature of the employed methods hint that our results hold for a larger subclass of CMA processes. In Chapters 2 and 3. we show the consistency of the kernel and of the driving process estimation procedures, respectively. In Chapter 4, the processing techniques commonly employed to obtain samples of the velocity of a turbulent flow are reviewed. In Chapter 5, the results obtained in the previous Chapters are applied to atmospheric turbulence datasets. Based on the results of the estimation methods mentioned earlier, a parametric model reproducing the most commonly observed features of turbulence is proposed.

Acknowledgment

Coming from an engineering background, to achieve such results would have been impossible without the contribution of many persons.

First of all my thanks go to Prof. Claudia Klüppelberg for giving me the opportunity to undertake the doctoral studies. Without her always helpful advices, kind patience and encouragement throughout the years, this thesis would not have been possible. I am especially grateful to her for introducing me to many distinguished scholars. Among these I would like to thank Prof. Ole Barndorff-Nielsen, Prof. Richard Davis, Prof. Peter Brockwell, Prof. Jürgen Schmiegel and Dr. Gunnar Chr. Larsen for making my stays in Aarhus, New York City and Roskilde possible and productive. I will remember these days as fruitful and enjoyable. In particular, I am indebted to Prof. Benoit Chabaud, Prof. Jürgen Schmiegel and Dr. Beat Lüthi for sharing their data with us.

A special acknowledgment goes to Dr. Parag Vyas, Dr. Michael Schmitt and Dr. Marianne Hartung of GE Global Research for suggesting the vast and interesting problem of turbulence.

Furthermore, I am grateful to my colleagues at the Chair of Mathematical Statistics for their support and for the enjoyable company during the past years. I would like to especially thank my fellows students Christina Steinkohl, Florian Fuchs and Florian Uelzthöfer for all the time spent discussing mathematics and more mundane topics as well.

The financial support of GE Global Research through the "International Graduate School of Science and Engineering", project "Energie 2020", is also gratefully acknowledged.

Un ringraziamento particolare va a tutti gli amici incontrati a Monaco. In particolare alla nostra Luce, maestro di stile ed eleganza, che ci guida in questa valle di lacrime e impedisce che il Warp ottunda le nostre menti. Un riconoscimento speciale va a tutte le donne della mia vita, in particolare (in ordine di apparizione) a mia madre, Monica, Elisa, Fiorella e Barbara. Senza di voi, la strada fin qui sarebbe stata certamente più tetra e difficoltosa.

Contents

Introduction

In this Introduction we will illustrate some of the concepts employed throughout this thesis, giving when needed reference to the literature detailed in the bibliography at the end of this thesis.

In Section I we give a brief account of the theory of stationary turbulence, relevant for this thesis, presenting some stylised facts and theoretical results.

In Section II we shall recall the basic properties of continuous-time moving average (CMA) processes with finite variance. These processes constitute a general class of stationary processes, which have been proposed as possible models for the time-wise behaviour of turbulence (see e.g. Barndorff-Nielsen et al. (2011), Barndorff-Nielsen and Schmiegel (2009, 2008a)).

From a mathematical point of view, most of the results of this thesis will be obtained for a specific yet flexible subclass of CMA processes, namely the class of the continuous-time autoregressive moving-average (CARMA) processes. One of the advantages of this kind of processes is that many relevant quantities can be explicitly calculated. The definition of a CARMA process and basic properties are given in Section III.

Throughout this thesis we will investigate the asymptotic behaviour of the samples of the underlying continuous-time processes, when the sampling frequency tends to infinity. A brief overview of the subject will be given in Section IV.

We conclude this Introduction with a chapter-by-chapter outline of the thesis in Section V.

I. Turbulence

Turbulence is the complex behaviour of a particle in a fluid, under certain conditions, described by its velocity. Its modelling is a long-standing problem in both physics and mathematics. The Navier–Stokes equations, the basic mathematical equations describing turbulence, are well-known since the 19th century. Actual comprehension of this phenomenon, however, is scarce. Since the seminal work of Kolmogorov (1941a,b, 1942), henceforth referred to as *K41 theory*, there is a wide-spread conviction that turbulence can be regarded and analysed as a random phenomenon. In particular, the velocity of a turbulent flow can be modelled as a spatio-temporal stochastic process which preserves some statistical structure. We emphasise that high-resolution measurements with actual

probes in both space and time, are difficult to gather. The theory developed in a spatio-temporal setting is reduced to a time-series framework by utilising Taylor frozen-field hypothesis (Pope 2000, p. 223), which allows to exchange spatial with time increments. For an exhaustive account of the turbulence theory we refer to Frisch (1996) and Pope (2000). For a more intuitive description of turbulence we refer to Tsinober (2009). We note that virtually every observed turbulent flow displays several stylised statistical facts. Experimental investigations highlighted that the magnitude of these features only depends on a control parameter called the *Reynolds number*; it is proportional to the mean flow velocity over the kinematic viscosity. The final goal of this thesis is to analyse and model turbulent flows with a Reynolds number above a critical threshold, called *fully developed* turbulence. We focus on the modelling of the velocity $V = \{V_t\}_{t\in\mathbb{R}}$ along the main flow direction at some fixed point in space of a weakly stationary turbulent flow.

As customary in both statistics and physics, our analysis is mostly data driven. Therefore in the latter Chapter of this thesis we shall consider many dataset, coming from high-quality physical experiments. The most remarkable amongst the dataset employed is the so-called Brookhaven wind speed data set (see Drhuva 2000). It consists of measurements taken at the atmospheric boundary layer, about 35m above the ground and it displays a rather high Reynolds number.

The transmission and dissipation of energy are of paramount importance in the description of turbulence. In the K41 theory, the former is based on the phenomenology called *energy cascade* (see Richardson 2007). It is suggested that the kinetic energy enters the turbulent motion at its largest scale, called *energy containing range*. An example can be fall winds (e. g., Föhn in the Bavarian alps) downwards flowing from the top of a mountain, due to the pressure difference between the peak and the valley. These large scale phenomena are, in general, non-stationary and very specific models are needed. The kinetic energy is then transmitted by an inviscid mechanism to smaller scale vortices in the so-called *inertial range*, until it gets dissipated at its smallest scale, called *dissipation range*. In the frequency domain, these partitions correspond to low (energy containing range), intermediate (inertial range), and high frequencies (dissipation range). The extent of these ranges depends on the Reynolds number. Kolmogorov assumed that the transmission and dissipation mechanisms are independent from the one injecting the kinetic energy; moreover, he supposed that these mechanisms is universal for every fully developed turbulent flow. Along with other simplifications such as stationarity, the K41 theory gives an elegant and quantitative description of the energy transmission mechanism. It is essentially based on second order properties, in particular spectral density and autocovariance; the behaviour of the energy dissipation mostly remains unspecified. The most prominent result is *Kolmogorov 5/3-law*: in the inertial range, the spectral density of the velocity of a turbulent flow decays as $\omega^{-5/3}$ with the frequency ω.

In the development of his theory Kolmogorov did not take into account that turbulence is a highly non-Gaussian phenomenon. Although the K41 theory has been proven

to be correct to a fair degree concerning second order properties, it fails to make accurate predictions regarding higher-order statistics. Physicists subsume all phenomena deviating from the predictions of the K41 theory under the term *intermittency*. Our paramount aim in this thesis is to advocate a statistical model, which is able to reproduce the following key "intermittent" features, virtually observed in every fully developed turbulent flow. First, sample paths are rather smooth; physicists' conjecture that they are infinitely often differentiable in the L^2-sense. Unfortunately, to obtain experimental data with a good resolution at very small scales is still a daunting task, so no last word has been said on this matter. Nevertheless, the Navier–Stokes equation to be well defined requires that the turbulent velocity is an – at least – twice continuously differentiable process. Second, the velocity increments display a distinctive clustering: the phenomenon is originally called *intermittency*. In particular, the squared increments of turbulent flow velocities are significantly correlated; their autocorrelation is positive and slowly decaying. Third, the velocity increments are semi-heavy tailed and display a distinctive scaling. Their distribution is approximately Gaussian on large time-scales, but has exponential tails and is positively skewed on small time-scales. The skewness is given by *Kolmogorov 4/5-law*; for all $t \in \mathbb{R}$ and a $s > 0$ in the inertial range, we have

$$\mathbb{E}[(V_{t+s} - V_t)^3] \approx \frac{4}{5}\epsilon s,$$

where $\epsilon > 0$ is the mean rate of energy dissipation. Under some ideal conditions, ϵ is proportional to $\mathbb{E}[(\partial_t V)^2]$; it is the physical analogue of return volatility in finance. This law is a direct consequence of Navier–Stokes equations; it is one of the few exact results in turbulence theory. For a different approach to connect the classical Navier–Stokes equation with stochastic processes, see Birnir (2013).

II. Continuous-time moving average processes

We are concerned in this thesis with continuous-time moving average processes of the form

$$X_t := \int_{-\infty}^{\infty} g(t-s)dW_s, \quad t \in \mathbb{R}, \tag{II.i}$$

where $g \in L^2(\mathbb{R})$ and $\{W_t\}_{t\in\mathbb{R}}$ is a process stationary and uncorrelated increments, such that $\mathbb{E}[W_1] = 0$, $\mathbb{E}[W_1^2] = \sigma^2 < \infty$ and $W_0 = 0$ a.s.. The process X defined by (II.i) is then a stationary process with mean zero and finite variance $\sigma^2\|g\|_{L^2}^2$. Throughout this thesis, we will employ the weak concept of second order (weak) stationarity, that is, $\mathbb{E}[X_t]$ is constant for every t and the autocovariance function

$$\gamma_X(\tau) := \mathbb{E}[(X_{t+\tau} - \mathbb{E}[X_{t+\tau}])(X_t - \mathbb{E}[X_t])], \quad \tau \in \mathbb{R},$$

is independent of t. For every second order stationary process the spectral density f_X is defined as the inverse Fourier transform of the autocovariance function. i.e.

$$f_X(\omega) = \mathcal{F}^{-1}\{\gamma_X(\cdot)\}(\omega), \quad \omega \in \mathbb{R}.$$

The operator $\mathcal{F}$ is the linear Fourier-transform operator, $\mathcal{F}\{g(\cdot)\}(\omega) := \int_{\mathbb{R}} g(s)e^{i\omega s}ds$, defined for every function $g \in L^2(\mathbb{R})$ (see Hörmander (1990), Ch. VII and references therein for a review of the properties of the Fourier operator). A detailed account of the spectral theory of second order stationary processes can be found in Priestley (1981). The integral in (II.i) is understood in the L^2-sense, as in Doob (1990) Ch. IX. More specifically, for a CMA process the second order properties can be obtained with the convenient formulas (Doob (1990), Ch XI, Section 8).

$$\gamma_X(\tau) = \sigma^2 \int_{\mathbb{R}} g(s)g(s+\tau)ds, \qquad \tau \in \mathbb{R},$$
$$f_X(\omega) = \frac{\sigma^2}{2\pi}|\mathcal{F}\{g(\cdot)\}|^2(\omega), \qquad \omega \in \mathbb{R}.$$

The class of continuous-time moving average constitute a large subclass of the second order stationary processes. To be more precise, every process having a spectral density f_X has a representation in the L^2-sense as a CMA process, that is, there exists a CMA process having the same autocorrelation function and spectral density (Doob (1990), pg. 533).

From a time-series perspective, the case of causal continuous-time moving average processes is of particular interest, that is, when the kernel function g is assumed to be zero on $(-\infty, 0]$. Since g is deterministic, the randomness in a causal model is solely given by the driving process W. In many time-series applications a causal model, i.e. a model depending only on the past values of W, have a strong intuitive motivation.

The class of causal CMA process, although appealing from a modelling point of view, is slightly smaller than the one of continuous-time moving average. In order for a process to have a causal moving average representation (II.i), it must satisfy the Paley-Wiener condition (Yaglom (2005), Section 26.8), that is, its spectral density satisfies

$$\int_{\mathbb{R}} \frac{|\log f_X(\omega)|}{1+\omega^2} d\omega < \infty. \tag{II.ii}$$

The Paley-Wiener condition clearly rules out spectral densities either decaying as or faster than $e^{-|\omega|}$ or vanishing on sets having positive measure. This result descents from some beautiful results of Paley and Wiener (1934), equivalent to those of Titchmarsh (1948), connecting the behaviour of a function g with some regularity of its Fourier transform, when extended to the complex plane.

The rates of decay of the spectral density also relates to the order of differentiability of the process. As shown in Doob (1990), Example 1, pg. 535, if $\int_{\mathbb{R}} \omega^{2p} f_X(\omega)d\omega < \infty$

for some $p \in \mathbb{N}$, then the process X admits p derivatives in the L^2-sense. That implies differentiability of the sample paths in probability. Let us assume without any loss of generality that there exist an ϵ such that $f_X(\omega) > \epsilon$ for every fixed $\omega \in \mathbb{R}$. The differentiability condition, in conjunction with the Paley-Wiener condition (II.ii), tells us that processes having infinitely differentiable sample paths might not have a causal representation, while, on the other hand, processes with only a finite number of derivatives will always have one. This is a crucial point in turbulence, since it is still not clear whether the turbulent time-series are infinitely differentiable or not. An additional layer of confusion is given by the fact that most of the turbulence theory is developed in space; these results are often translated into a time context employing the Taylor hypothesis. We shall investigate the matter in Chapter 5.

In this thesis we assume that the driving noise W of a causal CMA process is a weak Lévy process L. By weak Lévy process, we understand a Lévy process (see e.g. Sato (1999)), where the hypothesis of independent increments is relaxed to the weaker one of *uncorrelated* increments. The assumptions of independent increments is too restrictive to incorporate non-linear effects in the model, such as volatility clustering, which is widely observed in turbulent and financial data.

Examples of causal CMA processes are the Ornstein-Uhlenbeck process, with $g(t) = e^{-\lambda t}\mathbf{1}_{(0,\infty)}$, where $\lambda > 0$, and the more general continuous-time autoregressive moving average (CARMA) processes studied by Doob (1944) for Gaussian L. Another notable example of causal CMA processes is the so-called Brownian semistationary process of Barndorff-Nielsen and Schmiegel (2008a), where the kernel function is assumed to be a gamma kernel, i.e., for $\nu > 1/2$ and $\lambda < 0$,

$$g(t) = t^{\nu-1}e^{\lambda t}\mathbf{1}_{(0,\infty)}(t), \quad t \in \mathbb{R}. \tag{II.iii}$$

A causal CMA process equipped with the kernel (II.iii) has an autocorrelation function of the Whittle-Matérn family (see e.g. Guttorp and Gneiting (2005)). The spectral density, that is the inverse Fourier transform of the autocorrelation function, of such a process decays as $\omega^{-2\nu}$ as ω tends to infinity. Power-law spectral densities are often observed, and they have a role of prime importance in turbulence, where Kolmogorov 5/3 law predicts $\nu = 5/6$. Therefore, such spectral densities have widely been employed in turbulence modelling, see e.g. von Kármán (1948) and the international standard IEC 61400-1 (1999).

III. CARMA processes

In this thesis a great deal of attention will be directed to CARMA processes driven by a second order zero-mean weak Lévy process L with $E[L_1] = 0$ and $E[L_1^2] = \sigma^2$. They represent a very tractable and flexible subclass of the CMA processes class, defined in the previous section. The process is defined as follows.

For non-negative integers p and q such that $q < p$, a CARMA(p, q) process $Y = \{Y_t\}_{t\in\mathbb{R}}$, with coefficients $a_1, \ldots, a_p$, $b_0, \ldots, b_q \in \mathbb{R}$, and driving Lévy process L, is defined to be the strictly stationary solution of the suitably interpreted formal equation,

$$a(D)Y_t = b(D)DL_t, \quad t \in \mathbb{R}, \tag{III.i}$$

where D denotes differentiation with respect to t, $a(\cdot)$ and $b(\cdot)$ are the polynomials,

$$a(z) := z^p + a_1 z^{p-1} + \cdots + a_p \quad \text{and} \quad b(z) := b_0 + b_1 z + \cdots + b_{p-1} z^{p-1},$$

and the coefficients b_j satisfy $b_q = 1$ and $b_j = 0$ for $q < j < p$. Throughout this thesis we shall denote by λ_i, $i = 1, \ldots, p$, and $-\mu_i$, $i = 1, \ldots, q$, the roots of $a(\cdot)$ and $b(\cdot)$ respectively, such that these polynomials can be written as $a(z) = \prod_{i=1}^{p}(z - \lambda_i)$ and $b(z) = \prod_{i=1}^{q}(z + \mu_i)$. Throughout this thesis we will further assume, to avoid non-interesting cases, that $a(\cdot)$ and $b(\cdot)$ have no common zeroes. For a study of the general case we refer to Brockwell and Lindner (2009).

Since the derivative DL_t does not exist in the usual sense, we interpret (III.i) as being equivalent to the observation and state equations

$$Y_t = \mathbf{b}^T \mathbf{X}_t\,, \tag{III.ii}$$

$$d\mathbf{X}_t = A\mathbf{X}_t dt + \mathbf{e}_p dL_t\,, \tag{III.iii}$$

where

$$\mathbf{X}_t = \begin{pmatrix} X(t) \\ X^{(1)}(t) \\ \vdots \\ X^{(p-2)}(t) \\ X^{(p-1)}(t) \end{pmatrix}, \quad \mathbf{b} = \begin{pmatrix} b_0 \\ b_1 \\ \vdots \\ b_{p-2} \\ b_{p-1} \end{pmatrix}, \quad \mathbf{e}_p = \begin{pmatrix} 0 \\ 0 \\ \vdots \\ 0 \\ 1 \end{pmatrix},$$

$$A = \begin{pmatrix} 0 & 1 & 0 & \ldots & 0 \\ 0 & 0 & 1 & \ldots & 0 \\ \vdots & \vdots & \vdots & \ddots & \vdots \\ 0 & 0 & 0 & \ldots & 1 \\ -a_p & -a_{p-1} & -a_{p-2} & \ldots & -a_1 \end{pmatrix} \quad \text{and } A = -a_1 \text{ for } p = 1.$$

It is easy to check that the eigenvalues of the matrix A, which we shall denote by $\lambda_1, \ldots, \lambda_p$, are the same as the zeroes of the autoregressive polynomial $a(\cdot)$.

If the roots of the polynomial $a(\cdot)$ lie in the left half-plane, it has been shown (Brockwell and Lindner (2009), Lemma 2.3) that these equations have the unique stationary solution

$$Y_t = \int_{-\infty}^{\infty} g(t-u)dL_u, \quad t \in \mathbb{R}, \tag{III.iv}$$

where

$$g(t) = \begin{cases} \frac{1}{2\pi i}\int_{\rho} \frac{b(z)}{a(z)} e^{tz} dz = \sum_{\lambda} Res_{z=\lambda}\left(e^{zt}\frac{b(z)}{a(z)}\right), & \text{if } t > 0, \\ 0, & \text{if } t \leq 0. \end{cases} \tag{III.v}$$

and ρ is any simple closed curve in the open left half of the complex plane encircling the zeroes of $a(\cdot)$. The integral in (III.iv) is again defined in L^2, as outlined in Section II. Therefore, the CARMA process is a causal, continuous-time moving average, whose kernel belongs to a specific parametric family, fully specified by the roots of $a(\cdot)$ and $b(\cdot)$.

We outline that the condition on the roots of $a(\cdot)$ to lie in the interior of the left half of the complex plane in order to have causality arises from Theorem V, p. 8, Paley and Wiener (1934), which is intrinsically connected with the Theorems in Titchmarsh (1948), pp. 125-129, on the Hilbert transform. A similar condition on the roots of $b(\cdot)$ will be needed in Chapters 2 and 3.

A more concise form for the kernel g is (Brockwell and Lindner (2009), equations (2.10) and (3.7))

$$g(t) = \mathbf{b}^{\top} e^{At} \mathbf{e}_p \mathbf{1}_{(0,\infty)}(t), \quad t \in \mathbb{R}. \tag{III.vi}$$

Gaussian CARMA processes, of which the Gaussian Ornstein-Uhlenbeck process is an early example, were first studied in detail by Doob (1944) (see also Doob (1990)). The state-space formulation, (III.ii) and (III.iii) (with $\mathbf{b}^{\top} = [1\ 0\ \cdots\ 0]$), was used by Jones (1981) to carry out inference for time-series with irregularly spaced observations. This formulation naturally leads to the definition of Lévy-driven and non-linear CARMA processes (see Brockwell and Lindner (2009) and the references therein).

IV. From continuous to discrete time: sampling schemes

In this thesis we will deal with the relationship between a continuous time process Y and the sampled process $Y^{\Delta} := \{Y_{n\in\Delta}\}_{n\in\mathbb{Z}}$ on a discrete grid, where $\Delta > 0$. The behaviour of the continuous-time process between two sequent observations at times $i\Delta$ and $(i+1)\Delta$ is of course unknown. A legitimate question is, whether it is possible to retrieve information about the continuous time process by using the sampled process when the sampling spacing Δ tends to zero. A recent reference on the subject is Jacod and Protter (2012). A classical result, bridging the continuous-time and the sampled spectral density, is the aliasing formula (Bloomfield (2000), p. 196, Eq. 9.17)

$$f_Y^{\Delta}(\omega) = \frac{1}{\Delta}\sum_{k\in\mathbb{Z}} f_Y\left(\frac{\omega + 2\pi k}{\Delta}\right), \quad -\pi \leq \omega \leq \pi.$$

As shown by the formula above, for a generic $\Delta > 0$, the discrete-time spectral density f_Y^Δ may bear little resemblance to the continuous-time spectral density f_Y. Most of the data available are discrete, therefore a numerous methods to estimate the discrete-time spectral density have been developed (see e.g. Priestley (1981), Brockwell and Davis (1991)). The problem of the convergence of the estimate of f_Y^Δ to the continuous time f_Y as $\Delta \downarrow 0$ for the class of CMA processes is discussed in Fasen (2012)

A classical time-series model for discrete-time data is the moving average (MA(∞)) process

$$Y_n^\Delta = \sum_{j=-\infty}^{n} \psi_{n-j}^\Delta Z_j^\Delta, \quad n \in \mathbb{Z}, \tag{IV.i}$$

where, for $\Delta > 0$, $\{\psi_j^\Delta\}_{j\in\mathbb{N}}$ is a deterministic, square-summable sequence with $\psi_0^\Delta = 1$; moreover, the process $Z^\Delta := \{Z_n^\Delta\}_{n\in\mathbb{Z}}$ is a discrete-time white noise process with variance σ_Δ^2. Similarly to the continuous-time setting, the Wold representation (Brockwell and Davis (1991), p. 187) states that a large class of discrete-time weakly stationary processes admits a MA(∞) representation. Moreover, under some technical conditions, the deterministic parameters of such a MA(∞) process can be directly computed from the discrete-time spectral density f_Y^Δ solving a spectral factorisation problem (see e.g. Sayed and Kailath (2001)). Notwithstanding, the parameters in (IV.i) depend in complicated fashion on the spacing $\Delta > 0$ and, therefore, via the aliasing formula, on the underlying continuous-time spectral density f_Y as well. The moving-average processes (IV.i) and (II.i) share a similar structure, where the kernel function g, respectively the coefficients $\{\psi_j^\Delta\}_{j\in\mathbb{N}}$, act as weight of the influence that the differential dL, respectively the white noise Z^Δ, has on the process Y, respectively Y^Δ. Moreover, in both discrete and continuous-time, a suitable stationary process can be represented as a moving average process. It is then natural to suppose that the framework of moving-average processes is the right setting to investigate the relationship between continuous-time and sampled processes.

The sampled sequence of a CARMA process satisfies the ARMA equation (see e.g. Brockwell and Brockwell (1999), Brockwell (1995), Brockwell and Lindner (2009))

$$\Phi_\Delta(B) Y_n^\Delta = \Theta_\Delta(B) Z_n^\Delta, \quad n \in \mathbb{Z}, \quad \Delta > 0, \tag{IV.ii}$$

where $\Phi_\Delta(\cdot) := \prod_{i=1}^{p} (1 - e^{\lambda_i \Delta} \cdot)$, $\Theta_\Delta(\cdot)$ is a polynomial of order less or equal to $p-1$ and B is the discrete-time back-shift operator, defined as $BX_n := X_{n-1}$. The white-noise Z^Δ in (IV.ii), under some technical condition, coincides with the one appearing in the MA(∞) (IV.i).

The ARMA processes, introduced by Whittle (1951) and popularised by Box et al. (1994), constitute a popular class of linear model for discrete-time data. An extensive review on the subject can be find in the classic Brockwell and Davis (1991).

Confronting (IV.ii) and (III.i), one can note that a CARMA process preserve a linear structure after sampling. In general the polynomial $\Theta_\Delta(\cdot)$ has a complicated dependence on $a(\cdot)$ and $b(\cdot)$ as $\Delta > 0$ and its order will be different from q. Results concerning the asymptotic behaviour of $\Theta_\Delta(\cdot)$, as Δ tends to zero, is given in Chapter 1.

In Chapter 2 and 3 we will investigate the relationship between the MA(∞) representation (IV.i) of the sampled sequence of a CARMA process and its CMA representation (II.i), once again as the spacing Δ tends to 0.

V. Outline of the thesis

As every of the following chapters of this thesis is based on a paper, they are basically self-contained and the notation is only unified within the individual chapters.

Chapter 1 We analyse the asymptotic behaviour of a CARMA process from the second order point of view, that is, we give asymptotic expression for the autocovariance function and the spectral density as Δ tends to zero. This Chapter is based on Brockwell, Ferrazzano and Klüppelberg (2012)

Chapter 2 We refine the results of Chapter 1, giving a asymptotic expression of the spectral density of higher order than the one given in Theorem 1.2.1. Moreover, we show that, under some assumptions, the coefficients in the Wold representation (IV.i) may be used to estimate the kernel g as the sampling spacing Δ tends to zero. This Chapter is based on Brockwell et al. (2013).

Chapter 3 We show that, under the same assumptions as in Chapter 2, the white noise Z^Δ in (3.2.1) approximates the increments of the driving process L, if properly rescaled. Moreover, we study the analogies between the representation (IV.i) of a CARMA process and the discretisation of (III.iv). This Chapter is based on Ferrazzano and Fuchs (2013).

Chapter 4 We illustrate the best practices to collect and to process the velocity samples of a turbulent flow. Due to the liquid status of a fluid, the velocity of a flow is hard to measure directly. Therefore a tiny electronically device is immersed in the flow, and the velocity of the flow itself is inferred from the electric signal of the device, which undergoes a complicated manipulation procedure. This Chapter is based on Ferrazzano (2010).

Chapter 5 We employ the results of Chapter 2 and 3 to estimate the kernel and the driving process of a CMA model from the Brookhaven data. Firstly, we fully characterise the CMA model from the physical point of view. Then we propose parametric models for the kernel and the driving noise, which are able to reproduce the stylised features

of turbulence. After fitting the model, we simulate thereupon, and we compare the obtained simulation with the original data. This Chapter is based on the working paper Ferrazzano, Klüppelberg and Ueltzhöfer (2012), due in March 2013.

1. High-frequency sampling of a continuous-time ARMA process

Continuous-time autoregressive moving average (CARMA) processes have recently been used widely in the modelling of non-uniformly spaced data and as a tool for dealing with high-frequency data of the form $Y_{n\Delta}, n = 0, 1, 2, \ldots$, where Δ is small and positive. Such data occur in many fields of application, particularly in finance and the study of turbulence. This Chapter is concerned with the characteristics of the process $\{Y_{n\Delta}\}_{n\in\mathbb{Z}}$, when Δ is small and the underlying continuous-time process $\{Y_t\}_{t\in\mathbb{R}}$ is a specified CARMA process.

This Chapter is organised as follows. In Section 1.1 we derive an expression for the spectral density of the sampled sequence $Y^\Delta := \{Y_{n\Delta}\}_{n\in\mathbb{Z}}$. It is known that the filtered process $\{\Phi_\Delta(B)Y_n^\Delta\}_{n\in\mathbb{Z}}$, where $\Phi_\Delta(B)$ is the filter defined in (3.1), is a moving average of order at most $p-1$. In Section 1.2, we determine the asymptotic behaviour of the spectral density and autocovariance function of $\{\Phi_\Delta(B)Y_n^\Delta\}_{n\in\mathbb{Z}}$ as $\Delta \downarrow 0$ and the asymptotic moving average coefficients and white noise variance in the cases $p-q = 1, 2$ and 3. In general we show that for small enough Δ the order of the moving average $\{\Phi_\Delta(B)Y_n^\Delta\}_{n\in\mathbb{Z}}$ is $p-1$.

1.1. The spectral density of $Y^\Delta := \{Y_{n\Delta}\}_{n\in\mathbb{Z}}$

From (III.v) we immediately see, since $g(t) = 0$ for $t < 0$, that the Fourier transform of g is

$$\mathcal{F}\{g(\cdot)\}(\omega) := \int_{\mathbb{R}} g(t)e^{i\omega t}dt = -\frac{1}{2\pi i}\int_\rho \frac{b(z)}{a(z)}\frac{1}{z+i\omega}dz = \frac{b(-i\omega)}{a(-i\omega)}, \quad \omega\in\mathbb{R}. \tag{1.1.1}$$

Since the autocovariance function $\gamma_Y(\cdot)$ is the convolution of $\sigma g(\cdot)$ and $\sigma g(-\cdot)$, its Fourier transform is given by

$$\mathcal{F}\{\gamma_Y(\cdot)\}(\omega) = \sigma^2\mathcal{F}\{g(\cdot)\}(\omega)\mathcal{F}\{g(\cdot)\}(-\omega) = \sigma^2\left|\frac{b(i\omega)}{a(i\omega)}\right|^2, \quad \omega\in\mathbb{R}.$$

The spectral density of Y is the inverse Fourier transform of γ_Y. Thus

$$f_Y(\omega) = \frac{1}{2\pi}\int_{\mathbb{R}} e^{-i\omega h}\gamma_Y(h)dh = \frac{1}{2\pi}\mathcal{F}\{\gamma_Y(\cdot)\}(-\omega) = \frac{\sigma^2}{2\pi}\left|\frac{b(i\omega)}{a(i\omega)}\right|^2, \quad \omega\in\mathbb{R}.$$

Substituting this expression into the relation

$$\gamma_Y(h) = \int_{\mathbb{R}} e^{i\omega h} f_Y(\omega) d\omega, \quad h \in \mathbb{R},$$

and changing the variable of integration from ω to $z = i\omega$ gives,

$$\gamma_Y(h) = \frac{\sigma^2}{2\pi i} \int_\rho \frac{b(z)b(-z)}{a(z)a(-z)} e^{|h|z} dz = \sigma^2 \sum_\lambda Res_{z=\lambda} \left(\frac{b(z)b(-z)}{a(z)a(-z)} e^{z|h|} \right), \tag{1.1.2}$$

where the sum is again over the distinct zeroes of $a(\cdot)$.

We can now compute the spectral density of the sampled sequence $Y^\Delta := (Y_{n\Delta})_{n\in\mathbb{Z}}$. This spectral density f_Δ will play a key role in the subsequent analysis. We have, from Corollary 4.3.2 in Brockwell and Davis (1991),

$$f_Y^\Delta(\omega) = \frac{1}{2\pi} \sum_{h=-\infty}^{\infty} \gamma_Y(h\Delta) e^{-ih\omega}, \quad -\pi \le \omega \le \pi,$$

and, substituting for γ_Y from (1.1.2),

$$f_\Delta(\omega) = \frac{-\sigma^2}{4\pi^2 i} \int_\rho \frac{b(z)b(-z)}{a(z)a(-z)} \frac{\sinh(\Delta z)}{\cosh(\Delta z) - \cos(\omega)} dz, \quad -\pi \le \omega \le \pi. \tag{1.1.3}$$

1.2. The filtered sequence $\{\Phi_\Delta(B)Y_n^\Delta\}_{n\in\mathbb{Z}}$

If $\lambda_1, \ldots, \lambda_p$ are the (not necessarily distinct) zeroes of $a(\cdot)$, then we know from Brockwell and Lindner (2009), Lemma 2.1, that if we apply the filter

$$\Phi_\Delta(B) := \prod_{j=1}^{p} (1 - e^{\lambda_j \Delta} B) \tag{1.2.1}$$

to the sampled sequence, Y^Δ, we obtain a strictly stationary sequence which is $(p-1)$-correlated and is hence, by Lemma 3.2.1 of Brockwell and Davis (1991), a moving average process of order $p-1$ or less.

Our goal in this Section is to study the asymptotic properties, as $\Delta \downarrow 0$, of the moving average $\Theta_\Delta(B)Z_n^\Delta$ in the ARMA representation,

$$\Phi_\Delta(B)Y_n^\Delta = \Theta_\Delta(B)Z_n^\Delta, \quad n \in \mathbb{Z}, \tag{1.2.2}$$

of the high-frequency sequence Y^Δ. Here B denotes the backward shift operator and $(Z_n^\Delta)_{n\in\mathbb{Z}}$ is an uncorrelated sequence of zero-mean random variables with constant variance which we shall denote by σ_Δ^2.

We shall denote by f_{MA}^Δ the spectral density of $\{\Theta_\Delta(B)Z_n^\Delta\}_{n\in\mathbb{Z}}$. Then, observing that the power transfer function of the filter (1.2.1) is

$$\psi(\omega) = |\prod_{j=1}^{p}(1-e^{\lambda_j\Delta+i\omega})|^2 = 2^p e^{-a_1\Delta}\prod_{i=1}^{p}(\cosh(\lambda_i\Delta)-\cos(\omega)), \quad -\pi\le\omega\le\pi, \quad (1.2.3)$$

we have

$$f_{\mathrm{MA}}^\Delta(\omega) = \psi(\omega)f_Y^\Delta(\omega), \quad -\pi\le\omega\le\pi, \quad (1.2.4)$$

where $\psi(\omega)$ and $f_Y^\Delta(\omega)$ are given by (1.2.3) and (1.1.3) respectively.

In principle the expression (1.2.4) determines the second order properties of the moving average process $\{\Theta_\Delta(B)Z_n^\Delta\}_{n\in\mathbb{Z}}$ and in particular the autocovariances $\gamma_{\mathrm{MA}}^\Delta(h)$ for $h = 0,\dots,p-1$. Ideally we would like to use these autocovariances to find the coefficients $\theta_1,\dots,\theta_{p-1}$ and white noise variance σ_Δ^2, all of which are uniquely determined by the autocovariances, if we impose the condition that $\theta(\cdot)$ has no zeros in the interior of the unit circle. Determination of these quantities is equivalent to finding the corresponding factorisation of the spectral density f_{MA}^Δ (see Sayed and Kailath (2001) for a recent paper on spectral factorisation).

From (1.1.3), (1.2.3) and (1.2.4) we can calculate the spectral density $f_{\mathrm{MA}}^\Delta(\omega)$ as $-\sigma^2\psi(\omega)/(2\pi)$ times the sum of the residues in the left half plane of the integrand in (1.1.3) , i.e.

$$f_{\mathrm{MA}}^\Delta(\omega) = -\frac{\sigma^2}{2\pi}\psi(\omega)\sum_\lambda D_z^{m(\lambda)-1}\left(\frac{\sinh(\Delta z)b(z)b(-z)}{(\cosh(\lambda\Delta)-\cos(\omega))a(-z)\prod_{\mu\neq\lambda}(z-\mu)^{m(\mu)}}\right)_{z=\lambda} \quad (1,2.5)$$

where the sum is over the distinct zeroes λ of $a(\cdot)$ and the product in the denominator is over the distinct zeroes μ of $a(\cdot)$, which are different from λ. The multiplicities of the zeroes λ and μ are denoted by $m(\lambda)$ and $m(\mu)$ respectively. When the zeroes $\lambda_1,\dots,\lambda_p$ each have multiplicity 1, the expression for $f_{\mathrm{MA}}^\Delta(\omega)$ simplifies to

$$f_{\mathrm{MA}}^\Delta(\omega) = \frac{(-2)^p e^{-a_1\Delta}\sigma^2}{2\pi}\sum_{i=1}^{p}\frac{b(\lambda_i)b(-\lambda_i)}{a'(\lambda_i)a(-\lambda_i)}\sinh(\lambda_i\Delta)\prod_{j\neq i}(\cos\omega-\cosh(\lambda_j\Delta)), \quad -\pi\le\omega\le\pi.$$

Although in principle the corresponding autocovariances $\gamma_{\mathrm{MA}}^\Delta(j)$ could be derived from f_{MA}^Δ, we derive a more direct explicit expression later as Proposition 1.2.6. The asymptotic behaviour of f_{MA}^Δ as $\Delta\downarrow 0$ is derived in the following theorem by expanding (1.1.3) in powers of Δ and evaluating the corresponding coefficients. Here and in all that follows we shall use the notation, $a(\Delta)\sim b(\Delta)$, to mean that $\lim_{\Delta\downarrow 0} a(\Delta)/b(\Delta) = 1$.

Theorem 1.2.1. *The spectral density f_{MA}^Δ of $\{\Theta_\Delta(B)Z_n^\Delta\}_{n\in\mathbb{Z}}$ in the ARMA representation* (1.2.2) *of the sampled process Y^Δ has the asymptotic form, as $\Delta\downarrow 0$,*

$$f_{\mathrm{MA}}^\Delta(\omega) \sim \frac{\sigma^2}{2\pi}(-1)^{p-q-1}\Delta^{2(p-q)-1}c_{p-q-1}(\omega)2^{p-1}(1-\cos\omega)^p, \quad -\pi\le\omega\le\pi, \quad (1.2.6)$$

where $c_k(\omega)$ is the coefficient of x^{2k+1} in the power series expansion

$$\frac{\sinh x}{\cosh x - \cos\omega} = \sum_{k=0}^{\infty} c_k(\omega)x^{2k+1}. \tag{1.2.7}$$

In particular, $c_0(\omega) = \frac{1}{1-\cos\omega}$, $c_1(\omega) = -\frac{2+\cos\omega}{6(1-\cos\omega)^2}$, $c_2(\omega) = \frac{33+26\cos\omega+\cos(2\omega)}{240(1-\cos\omega)^3}$, ...

Proof. The integrand in (1.1.3) can be expanded as a power series in Δ using (1.2.7). The integral can then be evaluated term by term using the identities, (see Example 3.1.2.3. of Mitrinović and Kečkić (1984))

$$\frac{1}{2\pi i}\int_\rho z^{2k+1}\frac{b(z)b(-z)}{a(z)a(-z)}dz = -\frac{1}{2}Res_{z=\infty}\left(\frac{z^{2k+1}b(z)b(-z)}{a(z)a(-z)}\right), \quad k\in\{0,1,2,\ldots\},$$

from which we obtain, in particular,

$$\frac{1}{2\pi i}\int_\rho z^{2k+1}\frac{b(z)b(-z)}{a(z)a(-z)}dz = \begin{cases} 0 & \text{if } 0\le k < p-q-1, \\ \frac{(-1)^{p-q}}{2} & \text{if } k = p-q-1. \end{cases}$$

Substituting the resulting expansion of the integral (1.1.3) and the asymptotic expression $\psi(\omega)\sim 2^p(1-\cos\omega)^p$ into (1.2.4) and retaining only the dominant power of Δ as $\Delta\downarrow 0$, we arrive at (1.2.6). □

Corollary 1.2.2. *The following special cases are of particular interest.*

$$p-q=1: \quad f_{\mathrm{MA}}^\Delta(\omega)\sim\frac{\sigma^2\Delta}{2\pi}2^q(1-\cos\omega)^q. \tag{1.2.8}$$

$$p-q=2: \quad f_{\mathrm{MA}}^\Delta(\omega)\sim\frac{\sigma^2\Delta^3}{2\pi}\left(\frac{2}{3}+\frac{\cos\omega}{3}\right)2^q(1-\cos\omega)^q. \tag{1.2.9}$$

$$p-q=3: \quad f_{\mathrm{MA}}^\Delta(\omega)\sim\frac{\sigma^2\Delta^5}{2\pi}\left(\frac{11}{20}+\frac{13\cos\omega}{30}+\frac{\cos(2\omega)}{60}\right)2^q(1-\cos\omega)^q. \tag{1.2.10}$$

Proof. These expressions are obtained from (1.2.6) using the values of $c_0(\omega), c_1(\omega)$ and $c_2(\omega)$ given in the statement of the theorem. □

Remark 1.2.3. (i) The right-hand side of (1.2.8) is the spectral density of a q-times differenced white noise with variance $\sigma^2\Delta$. It follows that, if $q=p-1$, then the moving average polynomial $\Theta_\Delta(B)$ in (1.2.2) is asymptotically $(1-B)^q$ and the white noise variance σ_Δ^2 is asymptotically $\sigma^2\Delta$ as $\Delta\downarrow 0$. This result is stated with the corresponding results for $p-q=2$ and $p-q=3$ in the following corollary.

(ii) By Proposition 3.32 of Marquardt and Stelzer (2007) a CARMA(p,q)-process has sample paths which are $(p-q-1)$-times differentiable. Consequently to represent processes

with non-differentiable sample-paths it is necessary to restrict attention to the case $p-q=1$. It is widely believed that sample-paths with more than two derivatives are too smooth to represent the processes observed empirically in finance and turbulence (see e.g. Jacod and Todorov (2010), Jacod et al. (2010)) so we are not concerned with the cases when $p-q>3$. □

Corollary 1.2.4. *The moving average process* $X_n^\Delta := \Theta_\Delta(B)Z_n^\Delta$ *in* (1.2.2) *has for* $\Delta \downarrow 0$ *the following asymptotic form.*

(a) If $p-q=1$, *then*

$$X_n^\Delta = (1-B)^q Z_n^\Delta, \quad n\in\mathbb{Z},$$

where $\sigma_\Delta^2 := Var(Z_n^\Delta) = \sigma^2\Delta$.

(b) If $p-q=2$, *then*

$$X_n^\Delta = (1+\theta B)(1-B)^q Z_n^\Delta, \quad n\in\mathbb{Z},$$

where $\theta = 2-\sqrt{3}$ *and* $\sigma_\Delta^2 := Var(Z_n^\Delta) = \sigma^2\Delta^3(2+\sqrt{3})/6$.

(c) If $p-q=3$, *then*

$$X_n^\Delta = (1+\theta_1 B+\theta_2 B^2)(1-B)^q Z_n^\Delta, \quad n\in\mathbb{Z},$$

where $\theta_2 = 2\left(8+\sqrt{30}\right) - \sqrt{375+64\sqrt{30}}$, $\theta_1 = 26\theta_2/(1+\theta_2) = 13-\sqrt{135+4\sqrt{30}}$ *and* $\sigma_\Delta^2 = \left(2\left(8+\sqrt{30}\right)+\sqrt{375+64\sqrt{30}}\right)\Delta^5\sigma^2/120$.

Proof. (a) follows immediately from Theorem 4.4.2 of Brockwell and Davis (1991).

To establish (b) we observe from (1.2.9) that the required moving average is the q times differenced MA(1) process with autocovariances at lags zero and one, $\gamma(0) = 2\sigma^2\Delta^3/3$ and $\gamma(1) = \sigma^2\Delta^3/6$. Expressing these covariances in terms of θ and σ_Δ^2 gives the equations,

$$(1+\theta^2)\sigma_\Delta^2 = 2\sigma^2\Delta^3/3,$$

$$\theta\sigma_\Delta^2 = \sigma^2\Delta^3/6,$$

from which we obtain a quadratic equation for θ. Choosing the unique solution which makes the MA(1) process invertible gives the required result.

The proof of (c) is analogous. The corresponding argument yields a quartic equation for θ_2. The particular solution given in the statement of (b) is the one which satisfies the condition that $\theta(z)$ is nonzero for all complex z such that $|z|<1$. □

Although the absence of the moving-average coefficients, b_j, from Corollary 3.4 suggests that they cannot be estimated from very closely-spaced observations, the coefficients do appear if the expansions are taken to higher order in Δ. An higher order expansion will

be shown in Chapter 2. The apparent weak dependence of the sampled sequence on the moving-average coefficients as $\Delta \downarrow 0$ is compensated by the increasing number of available observations.

In principle the autocovariance function $\gamma_{\mathrm{MA}}^\Delta$ can be calculated, as indicated earlier, from the corresponding spectral density f_{MA}^Δ given by (1.2.4) and (1.1.1). Below we derive a more direct representation of $\gamma_{\mathrm{MA}}^\Delta$ and use it to prove Theorem 1.2.7, which is the time-domain analogue of Theorem 1.2.1.

Define $B_\Delta g(t) = g(t-\Delta)$ for $t \in \mathbb{R}$. We show that $\Phi_\Delta(B_\Delta)g(\cdot) \equiv 0$ for $t > p\Delta$.

Lemma 1.2.5. *Let Y be the* CARMA(p,q) *process* (III.iv) *and $\Delta > 0$. Define $\Phi_\Delta(B)$ as in* (1.2.1)*. Then*

$$\Phi_\Delta(B_\Delta)g(t) := \prod_{j=1}^{p}(1 - e^{\lambda_j \Delta}B_\Delta)g(t) = 0, \quad t > p\Delta. \tag{1.2.11}$$

Proof. Rewriting the product in (1.2.11) as a sum we find $\Phi_\Delta(B_\Delta)g(t) = \sum_{j=0}^{p} A_j^p g(t - j\Delta)$, which has Fourier transform (invoking the shift property and the right hand side of (1.1.1))

$$\prod_\lambda (1 - e^{\Delta(\lambda+i\omega)})^{m(\lambda)} \frac{b(-i\omega)}{a(-i\omega)}, \quad \omega \in \mathbb{R},$$

where the product is taken over the distinct zeroes of $a(\cdot)$ having multiplicity $m(\lambda)$. Using the fact that the product of Fourier transforms corresponds to the convolution of functions, we obtain from (III.v)

$$\begin{aligned}\Phi_\Delta(B_\Delta)g(t) &= -\frac{1}{2\pi i}\int_\rho \prod_\lambda (1 - e^{\Delta(\lambda - z)})^{m(\lambda)} \frac{b(z)}{a(z)} e^{tz} dz \\ &= -\sum_\lambda Res_{z=\lambda}\left(e^{zt} b(z) \prod_\lambda \frac{(1 - e^{\Delta(\lambda - z)})^{m(\lambda)}}{(z-\lambda)^{m(\lambda)}} \right).\end{aligned}$$

Now note that, for every of the distinct zeroes λ_j,

$$\lim_{z\to\lambda_i} \frac{(1 - e^{\Delta(\lambda_j - z)})^{m(\lambda_j)}}{(z-\lambda_j)^{m(\lambda_j)}} = \Delta^{m(\lambda_j)}.$$

The singularities at $z = \lambda_j$ are removable and, therefore, using Cauchy residue theorem, Theorem 1 of Section 3.1.1, p. 25, and Theorem 2 of Section 2.1.2, p. 7, of Mitrinović and Kečkić (1984), the filtered kernel is zero for every $t \in \mathbb{R}$. □

Proposition 1.2.6. *Let Y be the* CARMA(p,q) *process* (III.iv) *and $\Delta > 0$. The autocovariance at lag n of $(\Phi_\Delta(B)Y_j^\Delta)_{j\in\mathbb{Z}}$ is, for $n = 0, 1, \ldots, p-1$,*

$$\gamma_{\mathrm{MA}}^\Delta(n) = \sigma^2 \sum_{i=1}^{p-n} \sum_{k=0}^{n+i-1} \sum_{h=0}^{i-1} A_k^p A_h^p \int_{(i-1)\Delta}^{i\Delta} g(s - h\Delta) g(s - (k-n)\Delta) ds, \tag{1.2.12}$$

with

$$A_k^p = (-1)^k \sum_{\{i_1,\ldots,i_k\}\in C_k^p} e^{\Delta(\lambda_{i_1}+\cdots+\lambda_{i_k})}, \quad k = 1,\ldots,p. \tag{1.2.13}$$

The sum in (1.2.13) *is taken over the* $\binom{p}{k}$ *subsets of size* k *of* $\{1,2,\ldots,p\}$.

Proof. We note that $\gamma_{\mathrm{MA}}^\Delta(n)$ is the same as $\mathbb{E}[(\Phi_\Delta(B_\Delta)Y)_t(\Phi_\Delta(B_\Delta)Y)_{t+\Delta n}]$ and use the same expansion as in the proof of Lemma 1.2.5, i.e.

$$\Phi_\Delta(B_\Delta) = \prod_{j=1}^p (1 - e^{\lambda_j\Delta}B_\Delta) = \sum_{k=0}^p A_k^p B_\Delta^k, \tag{1.2.14}$$

which we apply to Y. Observe that for $t \in \mathbb{R}$, setting $t_k := t - k\Delta$ for $k = 0,\ldots,p$, and $t_{p+1} := -\infty$,

$$B_\Delta^k Y_t = B_\Delta^k \int_{-\infty}^t g(t-u)dL_u = \int_{-\infty}^{t_k} g(t_k-u)dL_u = \sum_{i=k}^p \int_{t_{i+1}}^{t_i} g(t_k-u)dL_u. \tag{1.2.15}$$

Applying the operator (1.2.14) to Y_t, using (1.2.15) and interchanging the order of summation gives

$$(\Phi_\Delta(B_\Delta)Y)_t = \sum_{m=0}^p \int_{t_{m+1}}^{t_m} \sum_{k=0}^m A_k^p g(t_k-u)dL_u. \tag{1.2.16}$$

From Lemma 1.2.5 we know that the contribution from the term corresponding to $m = p$ is zero. By stationarity, the autocovariance function is independent of t, hence we can choose $t = \Delta n$. Then we obtain

$$\begin{aligned}(\Phi_\Delta(B_\Delta)Y)_{n\Delta} &= \sum_{j=0}^{p-1} \int_{\Delta(n-j-1)}^{\Delta(n-j)} \sum_{k=0}^j A_k^p g((n-k)\Delta-u)dL_u \\ &= \sum_{j=1}^{p} \int_{\Delta(n-j)}^{\Delta(n-j+1)} \sum_{k=0}^{j-1} A_k^p g((n-k)\Delta-u)dL_u.\end{aligned}$$

For $t = 0$, we obtain analogously

$$(\Phi_\Delta(B_\Delta)Y)_0 = \sum_{i=1}^p \int_{-\Delta i}^{-\Delta(i-1)} \sum_{h=0}^{i-1} A_h^p g(-\Delta h-u)dL_u.$$

For the autocovariance function we obtain for $n = 0,\ldots,p-1$ by using the fact that L has orthogonal increments,

$$\begin{aligned}\gamma_{\mathrm{MA}}^\Delta(n) &= \mathbb{E}[(\Phi_\Delta(B_\Delta)Y)_0(\Phi_\Delta(B_\Delta)Y)_{n\Delta}] \\ &= \sigma^2 \sum_{i=1}^{p-n} \sum_{k=0}^{i+n-1} \sum_{h=0}^{i-1} A_k^p A_h^p \int_{-i\Delta}^{-(i-1)\Delta} g((n-k)\Delta-u)g(-\Delta h-u)du.\end{aligned}$$

Finally, (1.2.12) is obtained by changing the variable of integration from u to $s = -u$. □

Theorem 1.2.7. *The autocovariance function $\gamma_{\mathrm{MA}}^\Delta(n)$ for $n = 1, \ldots, p-1$ has for $\Delta \downarrow 0$ the asymptotic form*

$$\gamma_{\mathrm{MA}}^\Delta(n) \sim \frac{\sigma^2\Delta^{2(p-q)-1}}{((p-q-1)!)^2}\sum_{i=1}^{p-n}\sum_{k=0}^{n+i-1}\sum_{h=0}^{i-1}(-1)^{h+k}\binom{p}{k}\binom{p}{h}C(h,k,i,n;p-q-1), \quad (1.2.17)$$

where for $N \in \mathbb{N}_0$

$$C(h,k,i,n;N) \;:=\; \int_0^1 (s+i-1-h)^N(s+i-1-k+n)^N ds.$$

Proof. The kernel g can also be expressed (Brockwell and Lindner (2009), equations (2.10) and (3.7)) as

$$g(t) = \mathbf{b}^\top e^{At}\mathbf{e}_p \mathbf{1}_{(0,\infty)}(t). \quad (1.2.18)$$

From this equation we see at once that g is infinitely differentiable on $(0,\infty)$ with k^{th} derivative,

$$g^{(k)}(t) = \mathbf{b}^\top e^{At}A^k\mathbf{e}_p, \; 0 < t < \infty.$$

Since $b_q = 1$ and $b_j = 0$ for $j > q$, the right derivatives $g^{(k)}(0+)$ satisfy

$$g^{(k)}(0+) = \mathbf{b}^\top A^k\mathbf{e}_p = \begin{cases} 0 & \text{if } k < p-q-1, \\ 1 & \text{if } k = p-q-1, \end{cases} \quad (1.2.19)$$

and in particular $g(0+) = 1$ if $p-q = 1$ and $g(0+) = 0$ if $p-q > 1$.

We can rewrite the integral in (1.2.12) as

$$\Delta\int_0^1 g((s+i-1-h)\Delta)g((s+i-1-k+n)\Delta)ds. \quad (1.2.20)$$

Since g is infinitely differentiable on $(0,\infty)$ and the right derivatives at 0 exist, the integrand has one-sided Taylor expansions of all orders $M \in \mathbb{N}$,

$$\begin{aligned}&\sum_{l=0}^{M}\frac{d^l\left[g((s+i-1-h)\Delta)g((s+i-1-k+n)\Delta)\right]}{d\Delta^l}\bigg|_{\Delta=0^+}\frac{\Delta^l}{l!} + o\left(\Delta^M\right)\\ &= \sum_{l=0}^{M}\sum_{m=0}^{l}\binom{l}{m}(s+i-1-h)^{l-m}(s+i-1-k+n)^m g^{(l-m)}(0+)g^{(m)}(0+)\frac{\Delta^l}{l!} + o\left(\Delta^M\right),\end{aligned}$$

as $\Delta \downarrow 0$. Choose $M = 2(p-q-1)$. Then by (1.2.19) there is only one term in the double sum which does not vanish, namely the term for which $m = p-q-1 = l-m$. Setting $N := p-q-1$ (so that $M = 2N$) the sum reduces to

$$\binom{2N}{N}(s+i-1-h)^N(s+i-1-k+n)^N\frac{1}{(2N)!}\Delta^{2N} + o\left(\Delta^{2N}\right).$$

Since $\binom{2N}{N}/(2N)! = (N!)^{-2}$, the integral in (1.2.20) is for $\Delta \downarrow 0$ asymptotically equal to

$$\frac{\Delta^{2N+1}}{(N!)^2}\int_0^1 (s+i-1-h)^N(s+i-1-k+n)^N ds + o(\Delta^{2N+1}), \tag{1.2.21}$$

and, since

$$\lim_{\Delta\downarrow 0}\sum_{\{i_1,\dots,i_h\}\in C_h^p} e^{\Delta(\lambda_{i_1}+\cdots+\lambda_{i_h})} = \binom{p}{h},$$

we also have

$$A_k^p A_h^p = (-1)^{h+k}\binom{p}{k}\binom{p}{h} + o(1) \quad \text{as } \Delta\downarrow 0. \tag{1.2.22}$$

Combining (1.2.21) and (1.2.22), we obtain (1.2.17). □

Remark 1.2.8. (i) For computations the following expansion may be useful (as usual we set $0^0 = 1$)

$$\begin{aligned} C(h,k,i,n;N) &:= \int_0^1 (s+i-1-h)^N(s+i-1-k+n)^N ds \\ &= \sum_{l_1,l_2=0}^N \binom{N}{l_1}\binom{N}{l_2}(i-1-h)^{N-l_1}(i-1-k+n)^{N-l_2}\int_0^1 s^{l_1+l_2}ds \\ &= \sum_{l_1,l_2=0}^N \binom{N}{l_1}\binom{N}{l_2}\frac{1}{l_1+l_2+1}(i-1-h)^{N-l_1}(i-1-k+n)^{N-l_2}. \end{aligned}$$

Furthermore, we observe that C depends on p and q only through $p-q$.
(ii) Note that the right hand sides of (1.2.5) and (1.2.6) are the discrete Fourier transforms of (1.2.12) and (1.2.17), respectively. Note also the symmetry between (1.2.5) and (1.2.12) in the dependence on Δ and $p-q-1$. □

So far we know that the moving average process $X_n^\Delta = \Theta_\Delta(B)Z_n^\Delta$ from (1.2.2) is of order not greater than $p-1$ but possibly lower. Our next result presents an asymptotic formula for $\gamma_{\mathrm{MA}}^\Delta(p-1)$, which shows clearly that this term is not 0.

Corollary 1.2.9. *For lag $n = p-1$ the autocovariance formula* (1.2.17) *reduces to*

$$\gamma_{\mathrm{MA}}^\Delta(p-1) \sim (-1)^q\frac{\sigma^2\Delta^{2(p-q)-1}}{(2(p-q-1))!} \tag{1.2.23}$$

and $\gamma_{\mathrm{MA}}^\Delta(p-1)$ is therefore non-zero for all sufficiently small $\Delta > 0$.

Proof. From the expansion (1.2.17) we find

$$\gamma_{\mathrm{MA}}^{\Delta}(p-1) \sim \frac{\sigma^2\Delta^{2(p-q)-1}}{((p-q-1)!)^2}\sum_{k=0}^{p-1}(-1)^k\binom{p}{k}C(0,k,1,p-1;p-q-1). \tag{1.2.24}$$

Set $d := p-q \geq 1$, then

$$C(0,k,1,p-1;d-1) = \int_0^1 s^{d-1}(s-k+p-1)^{d-1}ds,$$

and, from Remark 1.2.8, this is a polynomial of order $d-1$. In order to apply known results on the difference operator, we define the polynomial $f(x) = \int_0^1 s^{d-1}(x+s+p-1)^{d-1}ds$. Then, using Eq. (5.40), p. 188, and the last formula on p. 189 in Graham et al. (1994), the sum in (1.2.24) can be written as

$$\begin{aligned}
&\sum_{k=0}^{p-1}(-1)^k\binom{p}{k}C(0,k,1,p-1;d-1)\\
=\ &\sum_{k=0}^{p}(-1)^k\binom{p}{k}f(x-k)|_{x=0} - (-1)^p\binom{p}{p}C(0,k,1,p-1;d-1)\\
=\ &0+(-1)^{p+1}\int_0^1 s^{d-1}(s-1)^{d-1}ds \;=\; (-1)^{p+d}\int_0^1 s^{d-1}(1-s)^{d-1}ds, \qquad (1.2.25)
\end{aligned}$$

where we have used the fact that $d-1 = p-q-1 < p$. To obtain Eq. (1.2.23) it suffices to note that $(-1)^{p+d} = (-1)^{2p-q} = (-1)^q$ and that the integral in (1.2.25) is a beta function. Hence

$$\int_0^1 s^{d-1}(1-s)^{d-1}ds = \frac{(\Gamma(d))^2}{\Gamma(2d)} = \frac{((d-1)!)^2}{(2d-1)!} > 0, \quad d\in\mathbb{N}.$$

□

Remark 1.2.10. If Y is a CARMA(p,q) process, then, from Theorem 1.2.1, the spectral density of $(1-B)^{p-q}Y^\Delta$ is asymptotically, as $\Delta\downarrow 0$,

$$\frac{\sigma^2}{2\pi}\Delta(-2\Delta^2)^{p-q-1}c_{p-q-1}(\omega)(1-\cos\omega)^{p-q}, \quad \pi\leq\omega\leq\pi.$$

If $p-q = 1$, 2 or 3 this reduces to the corresponding spectral densities in Corollary 3.2, each divided by $2^q(1-\cos\omega)^q$. The corresponding moving average representations are as in Corollary 3.4 without the factors $(1-B)^q$.

In particular, for the CAR(1) process, $(1-B)Y^\Delta$ has a spectral density which is asymptotically $\sigma^2\Delta/(2\pi)$ so that, in the Gaussian case, the increments of Y^Δ for small Δ approximate those of Brownian motion with variance $\sigma^2 t$. □

$p-q$	1	2	3	4
$\gamma_{\mathrm{MA}}^{\Delta}(p-1)$	$\Delta(-1)^{p-1}\sigma^2$	$6^{-1}\Delta^3(-1)^{p-2}\sigma^2$	$120^{-1}\Delta^5(-1)^{p-3}\sigma^2$	$5040^{-1}\Delta^7(-1)^{p-4}\sigma^2$

Table 1.1.: Values of $\gamma_{\mathrm{MA}}^{\Delta}(p-1)$ for $p-q=1,\ldots,4$.

In this Chapter we have considered only second order properties of Y^{Δ}. It is possible (see Brockwell (2001), Theorem 2.2) to express the joint characteristic functions, $\mathbb{E}\exp(i\sum_{k=1}^{m}\theta_k Y_k^{\Delta})$, for $m\in\mathbb{N}$, in terms of the coefficients a_j and b_j and the function $\xi(\cdot)$, where $\xi(\theta)$, for $\theta\in\mathbb{R}$, is the exponent in the characteristic function, $\mathbb{E}e^{i\theta L_1}=e^{\xi(\theta)}$, of L_1. In particular the marginal characteristic function is given by $\mathbb{E}\exp(i\theta Y_k^{\Delta}) = \exp\int_0^{\infty}\xi(\theta\mathbf{b}'e^{Au}\mathbf{e})du$, where $\mathbf{b}$, A and $\mathbf{e}$ are defined as in (III.ii)-(III.iii).

These expressions are awkward to use in practice, however Brockwell et al. (2011) have found that least squares estimation (which depends only on second order properties) for closely and uniformly spaced observations of a CARMA(2,1) process on a fixed interval $[0,T]$ gives good results. They find in simulations that for large T the empirically-determined sample covariance matrix of the estimators of a_1, a_2 and b_0 is close to the matrix calculated from the asymptotic (as $T\to\infty$) covariance matrix of the maximum likelihood estimators based on continuous observation on $[0,T]$ of the corresponding Gaussian CARMA process.

1.3. Conclusions

When a CARMA(p,q) process Y is sampled at times $n\Delta$ for $n\in\mathbb{Z}$, it is well-known that the sampled process Y^{Δ} satisfies discrete-time ARMA equations of the form (1.2.2). The determination of the moving average coefficients and white noise variance for given grid size Δ, however, is a non-trivial procedure. In this Chapter we have focussed on *high frequency sampling* of Y. We have determined the relevant second order quantities, the spectral density f_{MA}^{Δ} of the moving average on the right-hand side of (1.2.2) and its asymptotic representation as $\Delta\downarrow 0$. This includes the moving average coefficients as well as the variance of the innovations. We also derived an explicit expression for the autocovariance function $\gamma_{\mathrm{MA}}^{\Delta}$ and its asymptotic representation as $\Delta\downarrow 0$. This shows, in particular, that the moving average is of order $p-1$ for Δ sufficiently small.

2. High-frequency sampling and kernel estimation for continuous-time moving average processes

Interest in continuous-time processes has increased rapidly in recent years, largely because of high-frequency data available in many applications. We develop a method for estimating the kernel function g of a second-order stationary Lévy-driven continuous-time moving average (CMA) process Y based on observations of the discrete-time process Y^Δ obtained by sampling Y at $\Delta, 2\Delta, \ldots, n\Delta$ for small Δ. We approximate g by g^Δ based on the Wold representation and prove its pointwise convergence to g as $\Delta \downarrow 0$ for CARMA(p, q) processes. Two non-parametric estimators of g^Δ, based on the innovations algorithm and the Durbin-Levinson algorithm, are proposed to estimate g. For a Gaussian CARMA process we give conditions on the sample size n and the grid-spacing $\Delta(n)$ under which the innovations estimator is consistent and asymptotically normal as $n \to \infty$. The estimators can be calculated from sampled observations of *any* CMA process and simulations suggest that they perform well even outside the class of CARMA processes. We illustrate their performance for simulated data and apply them to the Brookhaven turbulent wind speed data. Finally we extend results of Chapter 1 for sampled CARMA processes to a much wider class of CMA processes.

This Chapter is organised as follows: in Section 2.1 we derive higher-order asymptotics for Y^Δ which apply (unlike those of Chapter 1) to *all* CARMA(p, q) processes. In Section 2.3 we generalise the first order asymptotic results of Chapter 1 in a different direction by deriving analogous results for a broader class of CMA processes with strictly positive spectral density. In Section 2.2 we use the results of Section 2.1 to establish the pointwise convergence of a family of functions g^Δ, defined in terms of the Wold representation of Y^Δ, to g as $\Delta \downarrow 0$. In Section 2.4, we show under some conditions the consistency and asymptotic normality of the innovation algorithm as $n \to \infty$ and $\Delta \downarrow 0$. Moreover, these results are confirmed by a small simulation study. The algorithm is applied to a turbulent

velocity time-series in Section 2.5. The outcome of a more detailed statistical analysis for turbulence data is presented in Chapter 5.

We use the following notation throughout: $\Re(z)$ denotes the real part of the complex number z; B denotes the backward shift operator, $BY_n^\Delta := Y_{n-1}^\Delta$ for $n \in \mathbb{Z}$; $a(\Delta) \sim b(\Delta)$ means $\lim_{\Delta \downarrow 0} a(\Delta)/b(\Delta) = 1$. As g can have a singularity in 0, the spectral densities of Y or Y^Δ may have a singularity in 0 as well, and we may have to restrict the range of frequencies for their spectral densities to $\Omega_c := \mathbb{R}\backslash\{0\}$ and $\Omega_d := [-\pi, \pi]\backslash\{0\}$.

2.1. Asymptotic behaviour of Y^Δ as $\Delta \downarrow 0$

In Chapter 2 and 3 we need some more precise hypothesis on the nature of the roots of $a(\cdot)$ and $b(\cdot)$.

Assumption 1. *(i) The zeroes of the polynomial $a(\cdot)$ satisfy $\Re(\lambda_j) < 0$ for every $j = 1, \ldots, p$,*

(ii) the zeros of $b(\cdot)$ have non-vanishing real part, i.e. $\Re(\mu_j) \neq 0$ for all $j = 1, \ldots, q$.

The part (i) is the assumption under which a CARMA process is causal, and part (ii) is a technical assumption.

In analogy to the discrete-time case, we establish the notion of invertibility for the continuous-time ARMA process.

Definition 2.1.1. *A* CARMA(p, q) *process is said to be invertible if the roots of the moving average polynomial $b(\cdot)$ have negative real parts, i.e. $\Re(\mu_i) > 0$ for all $i = 1, \ldots, q$.*

The CMA process Y defined by (II.i) has autocovariance function

$$\gamma_Y(h) = \sigma^2 \int_{-\infty}^{\infty} g(x)g(x+h)dx, \quad h \in \mathbb{R},$$

and spectral density

$$f_Y(\omega) = \frac{1}{2\pi} \int_{-\infty}^{\infty} e^{-i\omega h}\gamma(h)dh = \frac{\sigma^2}{2\pi}|\mathcal{F}\{g(\cdot)\}|^2(\omega), \quad \omega \in \Omega_c, \tag{2.1.1}$$

where

$$\mathcal{F}\{g(\cdot)\}(\omega) := \int_{-\infty}^{\infty} g(x)e^{i\omega x}dx.$$

The spectral density of the sampled process, $Y^\Delta := (Y_{n\Delta})_{n\in\mathbb{Z}}$ is (Bloomfield (2000), p. 196, Eq. 9.17)

$$f_Y^\Delta(\omega) = \frac{1}{\Delta} \sum_{k=-\infty}^{\infty} f_Y\Big(\frac{\omega + 2k\pi}{\Delta}\Big), \quad \omega \in \Omega_d. \tag{2.1.2}$$

For the causal, finite variance Lévy-driven CARMA(p,q) process, autoregressive polynomial $a(z)$ and moving average polynomial $b(z)$, the spectral density is

$$f_Y(\omega) = \frac{\sigma^2}{2\pi}\left|\frac{b(i\omega)}{a(i\omega)}\right|^2, \quad -\pi \le \omega \le \pi, \tag{2.1.3}$$

where $a(z) = z^p + a_1 z^{p-1} + \cdots + a_p$, $b(z) = b_0 + b_1 z + \cdots + b_q z^{p-1}$, $p > q$, $b_q = 1$, and the zeros of $a(z)$ all have strictly negative real parts. Without loss of generality we can also assume that $a(z)$ and $b(z)$ have no common zeros (see Brockwell and Lindner (2009), Theorem 4.1). The kernel is

$$g(t) = \frac{1}{2\pi i}\int_\rho \frac{b(z)}{a(z)} e^{tz} dz \; \mathbf{1}_{(0,\infty)}(t) = \sum_\lambda \mathrm{Res}_{z=\lambda}\left(e^z \frac{b(z)}{a(z)}\right)\mathbf{1}_{(0,\infty)}(t), \tag{2.1.4}$$

where the integration is anticlockwise around any simple closed curve ρ in the interior of the left half of the complex plane, encircling the distinct zeroes λ of $a(z)$, and $\mathrm{Res}_{z=\lambda}(f(z))$ denotes the residue of the function f at λ. For such processes it was shown in Chapter 1, Section 2, that the spectral density f_Y^Δ of the sampled process Y^Δ is

$$f_\Delta(\omega) = \frac{-\sigma^2}{4\pi^2 i}\int_\rho \frac{b(z)b(-z)}{a(z)a(-z)}\frac{\sinh(\Delta z)}{\cosh(\Delta z) - \cos(\omega)} dz, \; -\pi \le \omega \le \pi, \tag{2.1.5}$$

where the integral, as in (2.1.4), is anticlockwise around any simple closed contour ρ in the interior of the left half of the complex plane, enclosing the zeroes of $a(z)$. It is known that the sampled process Y^Δ satisfies the ARMA equations,

$$\Phi_\Delta(B) Y_n^\Delta = \Theta_\Delta(B) Z_n^\Delta, \quad n \in \mathbb{Z}, \quad \{Z_n^\Delta\}_{n\in\mathbb{Z}} \sim \mathrm{WN}(0, \sigma_\Delta^2) \tag{2.1.6}$$

where B is the backward shift operator, $\Theta_\Delta(z)$ is a polynomial of degree less than p, $(Z_n^\Delta)_{n\in\mathbb{Z}}$ is an uncorrelated sequence of zero-mean random variables with variance, which we denote by σ_Δ^2,

$$\Phi_\Delta(z) = \prod_{j=1}^p (1 - e^{\lambda_j \Delta} z), \quad z \in \mathbb{C},$$

and $\lambda_1, \ldots, \lambda_p$ are the zeroes of the polynomial $a(z)$. Since the polynomial $\Phi_\Delta(z)$ is known precisely for any given CARMA process, the second order properties of the sampled process Y^Δ for small Δ can be determined by studying the properties of the moving average term, $X_n^\Delta := \Theta_\Delta(B) Z_n^\Delta$ in (2.1.6), as $\Delta \downarrow 0$. Denoting by f_{MA}^Δ the spectral density of X, we find from (2.1.6) that

$$f_{\mathrm{MA}}^\Delta(\omega) = 2^p e^{-a_1\Delta} f_Y^\Delta(\omega) \prod_{j=1}^p (\cosh(\lambda_j \Delta) - \cos(\omega)), \quad -\pi \le \omega \le \pi. \tag{2.1.7}$$

Chapter 1 determined the leading terms in the expansions of f_Y^Δ and f_{MA}^Δ in powers of Δ. These terms determine the local second order behaviour of the corresponding processes. In Section 4 we extend these results to a more general class of CMA processes.

In the following Section we introduce a small-Δ approximation g^Δ to the kernel g of Y based on the Wold representation of the sampled process Y^Δ. In order to show the convergence of g^Δ to g as $\Delta \downarrow 0$ for CARMA(p,q) processes, we need to consider higher order expansions of the spectral densities f_Y^Δ and f_{MA}^Δ than were considered in Chapter 1. We conclude this Section by deriving the required expansions.

From (2.1.5) it follows at once that the spectral density $f_Y^\Delta(\omega)$ is $-\sigma^2/(2\pi)$ times the sum of the residues at the singularities of the integrand in the left half-plane, or more simply $\sigma^2/(4\pi)$ times the residue of the integrand at ∞, which is much simpler to calculate. Thus,

$$f_Y^\Delta(\omega) = \frac{\sigma^2}{4\pi}\mathrm{Res}_{z=\infty}\left[\frac{b(z)b(-z)}{a(z)a(-z)}\frac{\sinh(\Delta z)}{\cosh(\Delta z)-\cos(\omega)}\right], \quad -\pi \le \omega \le \pi.$$

The spectral density can also be expressed as a power series,

$$f_Y^\Delta(\omega) = \frac{\sigma^2}{4\pi}\sum_{j=0}^{\infty}\sigma^2\Delta^{2j+1}r_j c_j(\omega), \quad -\pi \le \omega \le \pi, \tag{2.1.8}$$

where $c_k(\omega)$ is the coefficient of z^{2k+1} in

$$\sum_{k=0}^{\infty} c_k(\omega)z^{2k+1} = \frac{\sinh z}{\cosh z - \cos\omega}, \quad -\pi \le \omega \le \pi,$$

and

$$r_j := \mathrm{Res}_{z=\infty}\left[z^{2j+1}\frac{b(z)b(-z)}{a(z)a(-z)}\right],$$

i.e. the coefficient of z^{2j} in the power series expansion,

$$\sum_{j=0}^{\infty} r_j z^{2j} = (-z^2)^{p-q-1}\frac{\prod_{i=1}^{q}(1-\mu_i^2 z^2)}{\prod_{i=1}^{p}(1-\lambda_i^2 z^2)}, \tag{2.1.9}$$

where $a(z) = \prod_{i=1}^{p}(z-\lambda_i)$ and $b(z) = \prod_{i=1}^{q}(z+\mu_i)$. The power series (2.1.8) is the required expansion for f_Y^Δ. The expansion for f_{MA}^Δ is obtained from (2.1.7) and (2.1.8) as

$$f_{\mathrm{MA}}^\Delta(\omega) = \frac{2^p\sigma^2 e^{-a_1\Delta}}{4\pi}\prod_{i=1}^{p}\Big(1-\cos\omega+\sum_{j=1}^{\infty}\frac{(\lambda_i\Delta)^{2j}}{(2j)!}\Big)\sum_{k=0}^{\infty} r_k c_k(\omega)\Delta^{2k+1}, \quad -\pi \le \omega \le \pi.$$

This can be simplified by re-expressing it in terms of $x := 1-\cos\omega$. Thus

$$f_{\mathrm{MA}}^\Delta(\omega) = \frac{2^p\sigma^2 e^{-a_1\Delta}}{4\pi}\prod_{i=1}^{p}\Big(x+\sum_{j=1}^{\infty}\frac{(\lambda_i\Delta)^{2j}}{(2j)!}\Big)\sum_{k=0}^{\infty} r_k \alpha_k(x)\Delta^{2k+1}, \tag{2.1.10}$$

where $\alpha_k(x)$ is the coefficient of z^{2k+1} in the expansion,

$$\sum_{k=0}^{\infty} \alpha_k(x) z^{2k+1} = \frac{\sinh z}{\cosh z - 1 + x}.$$

In particular $\alpha_0(x) = 1/x, \alpha_1(x) = (x-3)/(3!x^2)$ and $\alpha_2(x) = (x^2 - 15x + 30)/(5!x^3)$. More generally, $\alpha_k(x)$ has the form.

$$\alpha_k(x) = \frac{1}{(2k+1)!x^{k+1}} \prod_{i=1}^{k} (x - \xi_{k,i}), \tag{2.1.11}$$

where

$$\prod_{i=1}^{k} \xi_{k,i} = (2k+1)!\, 2^{-k}, \tag{2.1.12}$$

and the product, when $k = 0$, is defined to be 1. Since $\alpha_{p-q-1}(x)$ plays a particularly important role in what follows, we shall denote its zeroes more simply as

$$\xi_i := \xi_{p-q-1,i}, \quad i = 1, \ldots, p-q-1.$$

From (2.1.10), with the aid of (2.1.9) and (2.1.11), we can now derive the required higher-order approximation to $f^\Delta_{\mathrm{MA}}(\omega)$. Observe first that the expression on the right of (2.1.10), in spite of its forbidding appearance, is in fact a polynomial in x of degree less than p. We therefore collect together the coefficients of $x^{p-1}, x^{p-2}, \ldots, x^0$. This gives (using the identity (2.1.12) and defining $y := \Delta^2$) the asymptotic expression as $\Delta \downarrow 0$,

$$f^\Delta_{\mathrm{MA}}(\omega) = \frac{2^p \sigma^2 e^{-a_1\Delta} \Delta^{2(p-q)-1}}{4\pi} \left[x^p r_{p-q-1} \alpha_{p-q-1}(x) + o(1) + \sum_{j=1}^{q} \rho_j x^{q-j} y^j \right], \tag{2.1.13}$$

with

$$\begin{aligned} \rho_j &= (-2)^{-(p-q-1+j)} \left[r_{p-q-1+j} - r_{p-q-2+j} \sum_{i=1}^{p} \lambda_i^2 \right] + o(1) \\ &= 2^{-(p-q-1+j)} \sum \mu_{i_1}^2 \ldots \mu_{i_j}^2 + o(1), \end{aligned}$$

where the second line follows from (2.1.9) and the sum on the second line is over all subsets of size j of the q zeroes of the polynomial $b(z)$.

Finally, replacing r_{p-q-1} in (2.1.13) by $(-1)^{p-q-1}$, substituting for $\alpha_{p-q-1}(x)$ from (2.1.11) and using the continuity of the zeroes of a polynomial as functions of its coefficients, we can rewrite (2.1.13) (recalling that $x := 1 - \cos\omega$ and $\xi_i, i = 1, \ldots, p-q-1$ are the zeroes of $\alpha_{p-q-1}(x)$) as

$$f^\Delta_{\mathrm{MA}}(\omega) = \frac{\Delta(-\Delta^2)^{p-q-1} 2^p \sigma^2 e^{-a_1\Delta}}{[2(p-q)-1]!4\pi} \prod_{i=1}^{p-1-q} [x - \xi_i(1+o(1))] \prod_{k=1}^{q} \left[x + \frac{\mu_k^2 \Delta^2}{2}(1+o(1)) \right]. \tag{2.1.14}$$

Observe now that we can write

$$x + \frac{\mu_k^2 \Delta^2}{2}(1 + o(1)) = \frac{1}{2\zeta_k}(1 - \zeta_k e^{-i\omega})(1 - \zeta_j e^{i\omega}), \quad -\pi \leq \omega \leq \pi,$$

where

$$\zeta_k = 1 \pm \mu_k \Delta + o(\Delta), \tag{2.1.15}$$

and the sign is chosen so that $|\zeta_k| = 1 \pm 2\Re(\mu_k) + |\mu_k|^2 \Delta^2 < 1$ for sufficiently small Δ. For each $k = 1, \ldots, q$, we would then choose the plus if $\Re(\mu_k) < 0$, or the minus if $\Re(\mu_k) > 0$. The Assumption 1 (ii) excludes the case $\Re(\mu_k) = 0$, since either signs gives a root greater than 1.

Similarly we can write

$$x - \xi_i(1 + o(1)) = -\frac{1}{2\eta(\xi_i)}(1 + \eta(\xi_i)e^{-i\omega})(1 + \eta(\xi_i)e^{i\omega}),$$

where

$$\eta(\xi_i) = \xi_i - 1 \pm \sqrt{(\xi_i - 1)^2 - 1} + o(1), \tag{2.1.16}$$

and the sign is chosen so that $\lim_{\Delta \downarrow 0} |\eta(\xi_i)| \leq 1$. If the zero ξ_i of $\alpha_{p-q-1}(x)$ is such that both choices of sign cause the limit to be 1, then either choice will do provided the same choice is made for $\eta(\overline{\xi}_i)$, where $\overline{\xi}_i$ denotes the complex conjugate of ξ_i. A more precise characterisation of the roots ξ_i, $i = 1, \ldots, p - q - 1$, will be given in Chapter 3.

These factorisations allow us to give the following asymptotic representation of the moving average process $X_n^\Delta = \Theta_\Delta(B) Z_n^\Delta$ appearing in (2.1.6).

Theorem 2.1.2. *The moving average process $\{X_n^\Delta\}_{n \in \mathbb{Z}}$ with spectral density f_{MA}^Δ has the asymptotic representation, as $\Delta \downarrow 0$,*

$$X_n^\Delta = \prod_{i=1}^{p-1-q} (1 + \eta(\xi_i)B) \prod_{k=1}^{q} (1 - \zeta_k B) Z_n^\Delta, \quad \{Z_n^\Delta\}_{n \in \mathbb{Z}} \sim \mathrm{WN}(0, \sigma_\Delta^2), \tag{2.1.17}$$

where

$$\sigma_\Delta^2 = \frac{\Delta^{2(p-q)-1} e^{-a_1 \Delta} \sigma^2}{[2(p-q)-1]! \prod_{i=1}^{p-q-1} \eta(\xi_i) \prod_{k=1}^{q} \zeta_k}, \tag{2.1.18}$$

with ζ_k and $\eta(\xi_i)$ as in (2.1.15) and (2.1.16).

Proof. The result follows at once from (2.1.14), (2.1.15) and (2.1.16). □

Remark 2.1.3. (i) The parameters $\eta(\xi_i)$ and ζ_k may be complex but the moving average operator will have real coefficients because of the existence of corresponding complex conjugate parameters in the product.

(ii) The representation in Theorem 2.1.2 is a substantial generalisation of the one in Corollary 2 of Chapter 1, since it is not only of higher-order in Δ, but it applies to all CARMA(p, q) processes, not only to those with $p - q \leq 3$. □

2.2. The Wold approximation to the CARMA(p, q) kernel

In this Section we introduce an approximation g^Δ to the kernel g of the CMA process Y, which depends only on the Wold representation,

$$Y_n^\Delta = \sum_{j=0}^{\infty} \psi_j^\Delta Z_{n-j}^\Delta, \quad n \in \mathbb{Z}, \quad \{Z_n^\Delta\}_{n\in\mathbb{Z}} \sim \mathrm{WN}(0, \sigma_\Delta^2), \tag{2.2.1}$$

of the sampled process Y^Δ. The approximation is

$$g^\Delta(x) := \sum_{j=0}^{\infty} \frac{\sigma_\Delta}{\sqrt{\Delta}} \psi_j^\Delta \mathbf{1}_{[j\Delta,(j+1)\Delta)}(x). \tag{2.2.2}$$

Using Theorem 2.1.2, we shall show that, for all CARMA(p, q) processes, as $\Delta \downarrow 0$, g^Δ converges pointwise to σg, or to g if L is standardised so that $E[L_1^2] = 1$. We first illustrate the convergence in the simplest case, namely when Y is a CARMA(1,0) (or stationary Ornstein-Uhlenbeck) process, for which the quantities ψ_j^Δ and σ_Δ can easily be found explicitly. The example also illustrates the role of the scale factor $\sigma_\Delta/\sqrt{\Delta}$ which multiplies the Wold coefficients, ψ_j^Δ in (2.2.2).

Example 2.2.1. [The CARMA(1,0) process] This a special case of (II.i) with kernel

$$g(x) = e^{\lambda x}\mathbf{1}_{(0,\infty)}(x) \text{ where } \lambda < 0.$$

The sampled process Y^Δ is the discrete-time AR(1) process satisfying

$$Y_n^\Delta = e^{\lambda\Delta} Y_{n-1}^\Delta + Z_n^\Delta, \quad n \in \mathbb{Z},$$

where $Z^\Delta = \left\{Z_n^\Delta\right\}_{n\in\mathbb{Z}}$ is the independent and identically distributed sequence defined by

$$Z_n^\Delta = \int_{(n-1)\Delta}^{n\Delta} e^{\lambda(n\Delta-u)} dL_u, \quad n \in \mathbb{Z}.$$

In this case it is easy to write down the coefficients ψ_j^Δ and the white noise variance σ_Δ^2 in the Wold representation of Y^Δ. From well-known properties of discrete-time AR(1) processes, they are $\psi_j^\Delta = e^{j\lambda\Delta}, j = 0, 1, 2, \ldots$, and $\sigma_\Delta^2 = \frac{\sigma^2}{2\lambda}(e^{2\lambda\Delta} - 1)$. Substituting these values in the definition (2.2.2) we find that

$$g^\Delta(x) = \sum_{j=0}^{\infty} \sigma \sqrt{\frac{e^{2\lambda\Delta} - 1}{2\lambda\Delta}} e^{j\lambda\Delta} \mathbf{1}_{[j\Delta,(j+1)\Delta)}(x),$$

which converges pointwise to σg as $\Delta \downarrow 0$. □

The approximation (2.2.2) is well defined for all processes (II.i) and there are standard methods for estimating the coefficients and white noise variance appearing in the definition from observations of Y^Δ. Example 3.1 shows that g^Δ converges pointwise to σg for CAR(1) processes. Our aim now is to establish this convergence for all CARMA(p,q) processes. We give the proof under the assumption that the zeroes $\lambda_1,\dots,\lambda_p$ of the autoregressive polynomial $a(z)$ all have multiplicity one. Multiple roots can be handled by supposing them to be separated and letting the separation(s) converge to zero.

The kernel (2.1.4) of a causal CARMA(p,q) process Y whose autoregressive roots each have multiplicity one reduces (see e.g. Brockwell and Lindner (2009)) to

$$g(x)=\sum_{j=1}^{p}\frac{b(\lambda_i)}{a'(\lambda_i)}e^{\lambda_i x}\mathbf{1}_{(0,\infty)}(x), \tag{2.2.3}$$

where $a(z)=\prod_{i=1}^{p}(z-\lambda_i)$ and $b(z)=\prod_{i=1}^{q}(z+\mu_i)$ are the autoregressive and moving average polynomials respectively and a' denotes the derivative of the function a. We now establish the convergence, as $\Delta\downarrow 0$, of g^Δ as defined in (2.2.2) to σg. Theorem 2.1.2 is used to determine the parameters of the Wold representation appearing in the definition of g^Δ.

Theorem 2.2.2. *If Y is the* CARMA(p,q) *process with kernel (2.2.3),*

(i) the Wold coefficients and white noise variance of the sampled process Y^Δ are

$$\psi_j^\Delta=\sum_{r=1}^{p}\frac{\prod_{i=1}^{p-1-q}(1+\eta(\xi_i)e^{-\lambda_r\Delta})\prod_{k=1}^{q}(1-\zeta_k e^{-\lambda_r\Delta})}{\prod_{m\neq r}(1-e^{(\lambda_m-\lambda_r)\Delta})}e^{j\lambda_r\Delta}, \tag{2.2.4}$$

and

$$\sigma_\Delta^2=\frac{\Delta^{2(p-q)-1}e^{-a_1\Delta}\sigma^2}{[2(p-q)-1]!\prod_{i=1}^{p-q-1}\eta(\xi_i)\prod_{k=1}^{q}\zeta_j}, \tag{2.2.5}$$

with ζ_k and $\eta(\xi_i)$ as in (2.1.15) and (2.1.16) and

(ii) the approximation g^Δ defined by (2.2.2) with ψ_j^Δ and σ_Δ^2 as in (2.2.4) and (2.2.5) converges pointwise to σg with g as in (2.2.3), if and only the CARMA process is invertible. That is, if $\Re(\mu_i)>0$ for every $i=1,\dots,q$.

Proof. (i) The expression for σ_Δ^2 was found already as part of Theorem 2.1.2. The coefficient ψ_j^Δ is the coefficient of z^j in the power series expansion,

$$\sum_{j=0}^{\infty}\psi_j^\Delta z^j=\frac{\prod_{i=1}^{p-1-q}(1+\eta(\xi_i)z)\prod_{k=1}^{q}(1-\zeta_k z)}{\prod_{m=1}^{p}(1-e^{\lambda_m\Delta}z)},$$

which can be seen, by partial fraction expansion, to be equal to (2.2.4).

(ii) We start noticing that, as $\Delta \downarrow 0$

$$\prod_{k=1}^{q}(1-\zeta_k e^{-\lambda_r \Delta}) = \Delta^q \prod_{k=1}^{q}(\lambda_r \mp \mu_k) + o(\Delta^q),$$

where the sign is taken to be the same as $\Re(\mu_k)$, for each $k = 1, \ldots, q$, as in (2.1.15). It easy to see that the product above is asymptotically equal to $\Delta^q b(\lambda_r)$ if and only if the process is invertible, that is, $\Re(\mu_k) > 0$.

Under this assumptions, the convergence of g^Δ to (2.2.3) follows by substituting for ψ_j^Δ and σ_Δ^2 from (2.2.4) and (2.2.5) into (2.2.2), substituting for ζ_k from (2.1.15), letting $\Delta \downarrow 0$ and using the identities

$$a'(\lambda_r) = \prod_{m \neq r}(\lambda_r - \lambda_m)$$

and

$$\prod_{i=1}^{p-q-1} \frac{(1+\eta(\xi_i))^2}{\eta(\xi_i)} = \prod_{i=1}^{p-q-1} \frac{\xi_i}{2} = [2(p-q)-1]!,$$

the last equality following from (2.1.12).

□

Remark 2.2.3. Although we have established the convergence of g^Δ only for CARMA processes, the non-parametric nature of g^Δ strongly suggests that the result is true for all processes defined as in (II.i). In practice we have found that estimation of σg by estimation of g^Δ with Δ small works extremely well for simulated processes with non-rational spectral densities also. The assumption on the roots of b will appear in Chapter 3 to be the continuous-time analogue of the invertibility condition for the discrete-time ARMA processes. □

2.3. Asymptotics for a class of sampled CMA processes as $\Delta \downarrow 0$

Brockwell et al. (2012) derived first-order asymptotic expressions, as $\Delta \downarrow 0$, for the spectral density f_Y^Δ when Y is a CARMA(p, q) process with $p - q \leq 3$. Although, as pointed out in Section 2, these asymptotic expressions are not sufficiently precise to establish the convergence of g^Δ to g, they do reveal the *local second order behaviour* of the process Y. For example, if Y is a CARMA$(p, p-1)$ process driven by a Lévy process L with $\mathrm{Var}(L_1) = \sigma^2$ then equations (15) and (19) of Brockwell et al. (2012) give, as $\Delta \downarrow 0$,

$$f_Y^\Delta(\omega) \sim \frac{\sigma^2 \Delta}{4\pi(1-\cos\omega)}, \quad -\pi \leq \omega \leq \pi,$$

showing that the spectral density of the *normalised differenced* sequence $\{(Y_{n\Delta} - Y_{(n-1)\Delta})/\sqrt{\Delta}\}_{n\in\mathbb{Z}}$ converges to that of white noise with variance σ^2 as $\Delta \downarrow 0$. In other words, for any fixed positive integer k, the sequence of observations $Y_{n\Delta}/\sqrt{\Delta}$, $n = 1, \ldots, k$, from a second order point of view, behaves as $\Delta \downarrow 0$ like a sequence of observations of integrated white noise with white-noise variance σ^2.

In this Section we derive analogous asymptotic approximations for the spectral densities of more general CMA processes and the implications for their local second order behaviour. Since we allow in this Section for spectral densities with a singularity at zero we recall the definition of the spectral domains,

$$\Omega_d := [-\pi, \pi]\backslash\{0\} \text{ and } \Omega_c := (-\infty, \infty)\backslash\{0\}.$$

We require the CMA processes to have spectral density satisfying a weak regularity condition at infinity. To formulate this condition we first need a definition.

Definition 2.3.1 (Regularly varying function (cf. Bingham et al. (1987))**.** *Let f be a positive, measurable function defined on $(0, \infty)$. If there exists $\rho \in \mathbb{R}$ such that*

$$\lim_{x\to\infty} \frac{f(\lambda x)}{f(x)} = \lambda^\rho, \quad \text{for all } \lambda > 0,$$

holds, f is called a regularly varying function of index ρ at ∞*. The convergence is then automatically locally uniform in λ. We shall denote this class of functions by $\mathcal{R}_\rho(\infty)$. Furthermore we shall say that $f(\cdot) \in \mathcal{R}_\rho(0+)$ if and only if $f(1/\cdot) \in \mathcal{R}_{-\rho}(\infty)$.*

The characterisation theorem for regularly varying functions (Theorem 1.4.1. in Bingham et al. (1987)) tells us that $f \in \mathcal{R}_\rho(\infty)$ if and only if $f(x) = x^\rho L(x)$, where $L \in \mathcal{R}_0(\infty)$.

Theorem 2.3.2. *Let Y be the* CMA *process with strictly positive spectral density f_Y such that $f_Y \in \mathcal{R}_{-\alpha}(\infty)$, where $\alpha > 1$, i.e., for $L \in \mathcal{R}_0(\infty)$,*

$$f_Y(\omega) = |\omega|^{-\alpha} L(|\omega|), \quad \omega \in \Omega_c. \tag{2.3.1}$$

Then the following assertions hold.

(a) The spectral density of the sampled process Y^Δ has for $\Delta \downarrow 0$ the asymptotic representation

$$f_Y^\Delta(\omega) \sim L(\Delta^{-1})\Delta^{\alpha-1}\left[|\omega|^{-\alpha} + (2\pi)^{-\alpha}\zeta\left(\alpha, 1 - \frac{\omega}{2\pi}\right) + (2\pi)^{-\alpha}\zeta\left(\alpha, 1 + \frac{\omega}{2\pi}\right)\right], \quad \omega \in \Omega_d, \tag{2.3.2}$$

where $\zeta(s, r)$ is the Hurwitz zeta function, defined as

$$\zeta(s, r) := \sum_{k=0}^{\infty} \frac{1}{(r+k)^s}, \quad \Re(s) > 1, \quad r \neq 0, -1, -2, \ldots.$$

(b) The right hand side of (2.3.2) *is not integrable for any* $\Delta > 0$*. However, the corresponding asymptotic spectral density of the differenced sequence* $(1-B)^{\alpha/2}Y^{\Delta}$ *is integrable for each fixed* $\Delta > 0$ *and the spectral density of*

$$\frac{(1-B)^{\alpha/2}}{L(\Delta^{-1})^{1/2}\Delta^{(\alpha-1)/2}}Y^{\Delta} \tag{2.3.3}$$

converges as $\Delta \downarrow 0$ *to that of a short-memory stationary process, i.e. a stationary process with spectral density bounded in a neighbourhood of the origin.*

(c) The variance of the innovations $\{Z_n^{\Delta}\}_{n\in\mathbb{Z}}$ *in the Wold representation (2.2.1) of* Y^{Δ} *satisfies*

$$\sigma_{\Delta}^2 \sim 2\pi C_{\alpha} L\left(\Delta^{-1}\right)\Delta^{\alpha-1}, \quad \Delta \downarrow 0,$$

where

$$C_{\alpha} = \exp\left\{\frac{1}{2\pi}\int_{-\pi}^{\pi}\log\left[|\omega|^{-\alpha} + (2\pi)^{-\alpha}\zeta\left(\alpha, 1-\frac{\omega}{2\pi}\right) + (2\pi)^{-\alpha}\zeta\left(\alpha, 1+\frac{\omega}{2\pi}\right)\right]d\omega\right\}. \tag{2.3.4}$$

Proof. (a) Since f_Y is positive, Eq. (2.1.2) can be rewritten as

$$f_Y^{\Delta}(\omega) = \Delta^{-1}f_Y(\Delta^{-1})\sum_{k=-\infty}^{\infty}\frac{f_Y(|\omega+2\pi k|\Delta^{-1})}{f_Y(\Delta^{-1})}, \quad \omega \in \Omega_d. \tag{2.3.5}$$

Each of the summands converges by regular variation to $|\omega+2\pi k|^{-\alpha}$. It remains to show that we can interchange the infinite sum with this limit. Invoking the Potter bounds (Theorem 1.5.6 (iii) of Bingham et al. (1987)), for every $\epsilon > 0$ there exists a Δ_{ϵ}, such that for all $\Delta \leq \Delta_{\epsilon}$ and $|2\pi k + \omega| > 0$

$$(1-\epsilon)|2\pi k+\omega|^{-\alpha-\epsilon} < \frac{f_Y(|\omega+2\pi k|\Delta^{-1})}{f_Y(\Delta^{-1})} < (1+\epsilon)|2\pi k+\omega|^{-\alpha+\epsilon}. \tag{2.3.6}$$

We take $\epsilon > 0$ such that $\alpha - \epsilon > 1$. Then, using (2.3.6), we can bound (2.3.5) as follows:

$$(1-\epsilon)\frac{f_Y(\Delta^{-1})}{\Delta}\sum_{k=-\infty}^{\infty}|2\pi k+\omega|^{-\alpha-\epsilon} < f_Y^{\Delta}(\omega) < (1+\epsilon)\frac{f_Y(\Delta^{-1})}{\Delta}\sum_{k=-\infty}^{\infty}|2\pi k+\omega|^{-\alpha+\epsilon}, \quad \omega \in \Omega_d. \tag{2.3.7}$$

Since ϵ can be chosen arbitrarily small, we conclude that as $\Delta \downarrow 0$

$$f_Y^{\Delta}(\omega) \sim \frac{f_Y(\Delta^{-1})}{\Delta}\sum_{k=-\infty}^{\infty}|\omega+2k\pi|^{-\alpha}, \quad \omega \in \Omega_d.$$

We can rewrite the sum above as

$$\sum_{k=-\infty}^{\infty} |\omega + 2k\pi|^{-\alpha} = (2\pi)^{-\alpha} \sum_{k=-\infty}^{\infty} \left|\frac{\omega}{2\pi} + k\right|^{-\alpha}$$
$$= |\omega|^{-\alpha} + (2\pi)^{-\alpha} \sum_{k=0}^{\infty} \left[\left(k + 1 - \frac{\omega}{2\pi}\right)^{-\alpha} + \left(k + 1 + \frac{\omega}{2\pi}\right)^{-\alpha}\right], \quad \omega \in \Omega_d. \tag{2.3.8}$$

From this and the definition of ζ we obtain (2.3.2).

(b) We first note that the Hurwitz zeta function $\zeta(-\alpha, 1 \pm \omega/2\pi)$ is bounded and strictly positive for all $\omega \in \Omega_d$, therefore, its integral over $[-\pi, \pi]$ is positive and finite. On the other hand, since $\alpha > 1$, the term $\omega^{-\alpha}$ is not integrable over $[-\pi, \pi]$. However, the differenced sequence $(1 - B)^{\alpha/2} Y^{\Delta}$, has spectral density

$$h^{\Delta}(\omega) = 2^{\alpha/2}(1 - \cos\omega)^{\alpha/2} f_Y^{\Delta}(\omega), \quad \omega \in \Omega_d. \tag{2.3.9}$$

As $\Delta \downarrow 0$ we can write, for $\omega \in \Omega_d$, by (2.3.2)

$$\begin{aligned} h^{\Delta}(\omega) \;\sim\; & 2^{\alpha/2}(1 - \cos\omega)^{\alpha/2} L(\Delta^{-1})\Delta^{\alpha-1} \times \\ & \left[|\omega|^{-\alpha} + (2\pi)^{-\alpha}\zeta\left(\alpha, 1 - \frac{\omega}{2\pi}\right) + (2\pi)^{-\alpha}\zeta\left(\alpha, 1 + \frac{\omega}{2\pi}\right)\right]. \end{aligned}$$

The right hand side is integrable over $[-\pi, \pi]$ and bounded in a neighbourhood of the origin, since $2^{\alpha/2}(1 - \cos\omega)^{\alpha/2}\omega^{-\alpha} \to 1$ as $\omega \to 0$. Thus we conclude that the spectral density of the rescaled differenced sequence (2.3.3) converges to that of a short-memory stationary process.

(c) It is easy to check that the sampled CMA process has a Wold representation of the form (2.2.1) and that its one-step prediction mean-squared error based on the infinite past is σ_{Δ}^2. Kolmogorov formula (see, e.g., Theorem 5.8.1 of Brockwell and Davis (1991)) states that the one-step prediction mean-squared error for a discrete-time stationary process with spectral density f is

$$\tau^2 = 2\pi \exp\left\{\frac{1}{2\pi}\int_{-\pi}^{\pi} \log f(\omega) d\omega\right\} \tag{2.3.10}$$

Applying it to the *differenced* process we find that its one-step prediction mean-squared error is

$$\begin{aligned} & 2\pi \exp\left\{\frac{1}{2\pi}\int_{-\pi}^{\pi} \log h^{\Delta}(\omega) d\omega\right\} \\ &= 2\pi \exp\left\{\frac{\alpha}{4\pi}\int_{-\pi}^{\pi} \log(2 - 2\cos\omega) d\omega\right\} \times \exp\left\{\frac{1}{2\pi}\int_{-\pi}^{\pi} \log f_Y^{\Delta}(\omega) d\omega\right\} \;=\; \sigma_{\Delta}^2. \end{aligned}$$

Hence the differenced sequence has the same one-step prediction mean-squared error as Y^Δ itself. Since from (2.3.7), as $\Delta \downarrow 0$,

$$\log f_Y^\Delta(\omega) - \log(L(\Delta^{-1})\Delta^{\alpha-1}) - \log\Big[\sum_{-\infty}^{\infty} |2\pi k + \omega|^{-\alpha}\Big] \to 0$$

pointwise on Ω_d, and since the left side is dominated by an integrable function on Ω_d, we conclude from the dominated convergence theorem that, as $\Delta \downarrow 0$,

$$\frac{1}{L(\Delta^{-1})\Delta^{\alpha-1}} \exp\left\{\frac{1}{2\pi}\int_{-\pi}^{\pi} \log f_Y^\Delta(\omega) d\omega\right\} \to \exp\left\{\frac{1}{2\pi}\int_{-\pi}^{\pi} \log\left[\sum_{-\infty}^{\infty} |2\pi k + \omega|^{-\alpha} d\omega\right]\right\},$$

which, with (2.3.8) and (2.3.10), shows that as $\Delta \downarrow 0$,

$$\sigma_\Delta^2 \sim 2\pi C_\alpha L\left(\Delta^{-1}\right)\Delta^{\alpha-1}. \tag{2.3.11}$$

□

Remark 2.3.3. (i) Theorem 2.3.2(b) means that, from a second order point of view, a sample $\{Y_n^\Delta, n = 1, \ldots, k\}$ with k fixed and Δ small resembles a sample from an $(\alpha/2)$-times integrated short-memory stationary sequence. If in (b) we replace $(1-B)^{\alpha/2}$ by $(1-B)^\gamma$ where $\gamma > (\alpha-1)/2$, then the conclusion holds for the over-differenced process. If, for example, we difference at order $\gamma = \lfloor(\alpha+1)/2\rfloor$ (the smallest integer greater than $(\alpha-1)/2$) we get a stationary process. In particular, if $1 < \alpha < 3$, then $\lfloor(\alpha+1)/2\rfloor = 1$ and, by (2.3.2) and (2.3.9), the differenced sequence $(1-B)Y^\Delta$ has the asymptotic spectral density, as $\Delta \downarrow 0$,

$$L(\Delta^{-1})\Delta^{\alpha-1} 2(1-\cos\omega)\left[|\omega|^{-\alpha} + (2\pi)^{-\alpha}\zeta\left(\alpha, 1-\frac{\omega}{2\pi}\right) + (2\pi)^{-\alpha}\zeta\left(\alpha, 1+\frac{\omega}{2\pi}\right)\right], \quad \omega \in \Omega_d.$$

This is the spectral density of the increment process of a self-similar process with self-similarity parameter $H = (\alpha-1)/2$ (see Beran (1992), eq. (2)). Moreover, for a generic $\alpha > 1$ the asymptotic autocorrelation function of the filtered sequence has unbounded support. The only notable exception is when α is even, where the asymptotic autocorrelation sequence is the one of a moving-average process with order $\alpha/2$, as in Brockwell et al. (2012) or in Example 2.3.7.

(ii) The constant C_α of (2.3.4) is shown as a function of α in Figure 1. The values, when α is an even positive integer, can be derived from (2.2.5) since CARMA processes constitute a subclass of the processes covered by the theorem (see Example 2.3.7). It is clear from (2.3.4) that C_α is exponentially bounded as $\alpha \to \infty$. □

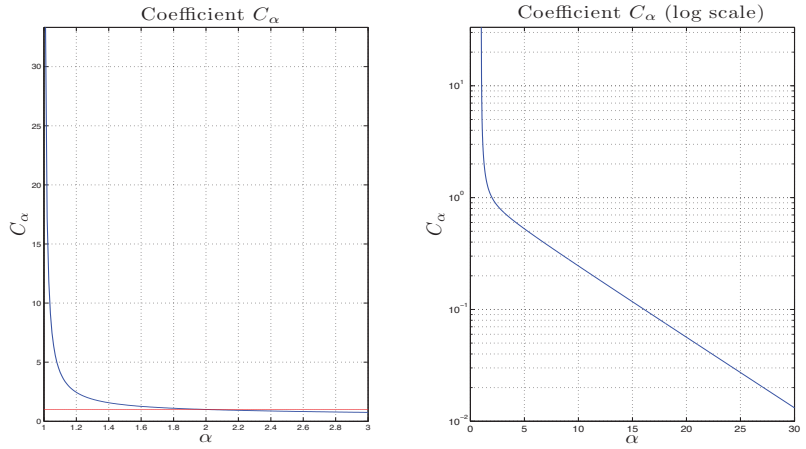

Figure 2.1.: The constant C_α, as a function of the index of regular variation α, is shown on the left using a linear scale and on the right using a logarithmic scale. From Corollary 3.4 (a) of Brockwell et al. (2012) we know that $C_2 = 1$. The horizontal line indicates the value 1.

Corollary 2.3.4. *Let Y be a CMA process satisfying the assumptions of Theorem 2.3.2 with $1 < \alpha < 2p + 1$. Then for $\Delta \downarrow 0$,*

$$\mathbb{E}[((1-B)^p Y_n^\Delta)^2] \sim 2^p S_{p,\alpha} L(\Delta^{-1}) \Delta^{\alpha-1},$$

where

$$S_{p,\alpha} = \int_{-\pi}^{\pi} (1-\cos\omega)^p \left[|\omega|^{-\alpha} + (2\pi)^{-\alpha} \zeta\left(\alpha, 1 - \frac{\omega}{2\pi}\right) + (2\pi)^{-\alpha} \zeta\left(\alpha, 1 + \frac{\omega}{2\pi}\right) \right] d\omega.$$

Proof. By stationarity we have $\mathbb{E}[(1-B)^p Y_n^\Delta] = 0$ and, hence $\mathbb{E}[((1-B)^p Y_n^\Delta)^2]$ is the variance, of $((1-B)^p Y_n^\Delta)$ which can be calculated as the integral of its spectral density. Thus

$$\mathbb{E}[((1-B)^p Y_n^\Delta)^2] = 2^p \int_{-\pi}^{\pi} (1-\cos\omega)^p f_Y^\Delta(\omega) d\omega.$$

Using the inequalities (2.3.7) and Lebesgue dominated convergence theorem, we find that as $\Delta \downarrow 0$,

$$\frac{1}{L(\Delta^{-1})\Delta^{\alpha-1}} \int_{-\pi}^{\pi} (1-\cos\omega)^p f_Y^\Delta(\omega) d\omega \to \int_{-\pi}^{\pi} (1-\cos\omega)^p \sum_{k=-\infty}^{\infty} |2k\pi + \omega|^{-\alpha} d\omega,$$

which, with the previous equation and (2.3.8), gives the result. □

The kernel of the CMA process and its spectral density are linked by formula (2.1.1). Moreover, it has long been known that local properties of a function imply global properties of its Fourier transform (see e.g. Titchmarsh (1948), Theorems 85 and 86).

An Abelian theorem of Cline (1991) allows us to show, under the conditions of the following proposition, that CMA processes with regularly varying kernels at the origin have regularly varying spectral densities at infinity.

Proposition 2.3.5. *Let Y be a CMA process with kernel $g \in \mathcal{R}_{\nu-1}(0+)$ for $\nu > 1/2$. Assume that the derivatives in 0 satisfy the assumptions*

(A1) $g^{(\lfloor \nu \rfloor)}(0+) \neq 0$;
(A2) $g^{(\lfloor \nu - 1 \rfloor)} \in \mathcal{R}_\alpha(0+)$ *for* $\alpha \in [0,1)$ *(with* $g^{(-1)} := \int_0^t g(s)ds$*);*
(A3) *For some* $x_0 > 0$,

$$q(u) := \sup_{x \leq x_0} \sup_{0 \leq w \leq v \leq 1} \left| \frac{g^{(\lfloor \nu-1 \rfloor)}((u+v+w)x) - g^{(\lfloor \nu-1 \rfloor)}((u+v)x) - g^{(\lfloor \nu-1 \rfloor)}((u+w)x) + g^{(\lfloor \nu-1 \rfloor)}(ux)}{g^{(\lfloor \nu-1 \rfloor)}(x)} \right|,$$

is bounded and integrable on $[1, \infty)$.

Then

$$f_Y(|\cdot|) \in \mathcal{R}_{-2\nu}(\infty).$$

Proof. Under conditions ***(A1)***-***(A3)*** we can apply Theorem 2 of Cline (1991), which yields

$$F(g)(|\omega|) \sim \Gamma(\nu+1) e^{\pm i\nu\pi/2} \int_0^{1/|\omega|} g(s)ds, \quad \omega \to \pm\infty. \tag{2.3.12}$$

Moreover, Karamata theorem (Theorem 1.5.11(ii) in Bingham et al. (1987)) gives

$$\int_0^{1/|\omega|} g(s)ds = \int_{|\omega|}^{\infty} s^{-2} g(1/s)ds \sim |\omega|^{-1} g(1/|\omega|)/\nu, \quad \omega \to \pm\infty,$$

where we used the fact $g(\cdot) \in \mathcal{R}_{\nu-1}(0+)$ means $g(1/\cdot) \in \mathcal{R}_{-\nu+1}(\infty)$.

Substituting (2.3.12) into (2.1.1) and recalling that $\Gamma(\nu+1) = \nu\Gamma(\nu)$, we obtain

$$f_Y(|\omega|) = \frac{1}{2\pi} |F(g)|^2(\omega) \sim \frac{\Gamma^2(\nu)}{2\pi} |\omega|^{-2} g^2(1/|\omega|), \quad \omega \to \pm\infty,$$

which gives the desired result. □

Remark 2.3.6. Condition (***A2***) can be replaced by a monotonicity condition on the derivative $g^{(\lfloor \nu \rfloor)}(\cdot)$ near the origin, so that the monotone density theorem (Bingham et al. (1987), Theorem 1.7.2) can be applied. □

Example 2.3.7. [CARMA(p,q) process]
The CARMA(p,q) process Y has spectral density (2.1.3), which clearly has the form

$$f_Y(\omega) = |\omega|^{-\alpha} L(|\omega|), \quad \omega \in \mathbb{R},$$

where $\alpha = 2(p-q)$ and $\lim_{\omega\to\infty} L(|\omega|) = \sigma^2/(2\pi)$. Hence, by Theorem 2.3.2(c), the white noise variance in the Wold representation of Y^Δ satisfies as $\Delta \downarrow 0$,

$$\sigma_\Delta^2 \sim \sigma^2 C_{2(p-q)} \Delta^{2(p-q)-1}, \tag{2.3.13}$$

where $C_{2(p-q)}$ can be calculated from (2.3.4). However $C_{2(p-q)}$ can also be calculated from (2.2.5) as $C_{2(p-q)} = [(2(p-q)-1)! \prod_{i=1}^{p-q-1} \lim_{\Delta\downarrow 0} \eta(\xi_i)]^{-1}$, where $\eta(\xi_i)$ was defined in (2.1.16). Theorem 2.3.2(b) implies that the spectral density of $\Delta^{q-p+1/2}(1-B)^{p-q}Y^\Delta$ converges to that of a short memory stationary process. From Theorem 2.1.2 we get the more precise result that the spectral density of $C_{2(p-q)}^{1/2}\Delta^{q-p+1/2}(1-B)^{p-q}\prod_{i=1}^{q}(1+\eta(\xi_i)B)^{-1}Y^\Delta$ converges to that of white noise with variance σ^2. □

Example 2.3.8. [FICARMA(p,d,q) process, Brockwell and Marquardt (2005)]
The fractionally integrated causal CARMA(p,d,q) process has spectral density

$$f_Y(\omega) = \frac{\sigma^2}{2\pi}\frac{1}{|\omega|^{2d}}\left|\frac{b(i\omega)}{a(i\omega)}\right|^2, \quad \omega \in \Omega_c, \tag{2.3.14}$$

with $a(\cdot)$ and $b(\cdot)$ as in (2.1.3) and $0 < d < 0.5$. Hence

$$f_Y(\omega) = |\omega|^{-\alpha} L(|\omega|), \quad \omega \in \Omega_c,$$

where $\alpha = 2(p+d-q)$ and $\lim_{\omega\to\infty} L(|\omega|) = \sigma^2/(2\pi)$. The spectral density (2.3.14) has a singularity at frequency 0 which gives rise to the slowly decaying autocorrelation function associated with long memory. Applying Theorem 2.3.2(c) as in Example 2.3.7, the white noise variance in the Wold representation of Y^Δ satisfies as $\Delta \downarrow 0$

$$\sigma_\Delta^2 \sim \sigma^2 C_{2(p+d-q)} \Delta^{2(p+d-q)-1}, \tag{2.3.15}$$

where $C_{2(p+d-q)}$ can be calculated from (2.3.4). As $\Delta \downarrow 0$, the asymptotic spectral density f_Y^Δ of Y^Δ is given by (2.3.2) with $\alpha = 2(p+d-q) > 1$ and is therefore not integrable for any $\Delta > 0$. However Theorem 2.3.2(b) implies that the spectral density of $\Delta^{q-p-d+1/2}(1-B)^{p+d-q}Y^\Delta$ converges to that of a short memory stationary process. □

Our next two examples are widely used in the modelling of turbulence. Kolmogorov famous 5/3 law (see Frisch (1996) Section 6.3.1, Pope (2000) Section 6.1.3) suggests a regularly varying spectral density model for turbulent flows.

Example 2.3.9. [Two turbulence models]
Denote by $\overline{U}$ the mean flow velocity, with ℓ the integral scale parameter and define $\overline{\ell} = \ell/\overline{U}$.

(i) The von Kármán (1948) spectrum models the isotropic energy spectrum. Its spectral density is, for C and c_ℓ positive, given by

$$f_Y(\omega) = C\overline{U}^{-2/3}|\omega|^{-5/3}\left(\frac{\omega^2}{\omega^2 + c_\ell/\overline{\ell}^2}\right)^{17/6}, \quad \omega \in \Omega_c.$$

Moreover, $f_Y \in \mathcal{R}_{-5/3}$, so it has a representation (2.3.1) and the conclusions of Theorem 2.3.2 hold with $\alpha = 5/3$.

(ii) The Kaimal spectrum for the longitudinal component of the energy spectrum is the current standard of the International Electrotechnical Commission; cf. IEC 61400-1 (1999). The spectral density is given by

$$f_Y(\omega) = v\frac{4\overline{\ell}}{(1 + 6\overline{\ell}\omega)^{5/3}}, \quad \omega \in \Omega_c, \tag{2.3.16}$$

where v is the variance of Y. Moreover, $f_Y \in \mathcal{R}_{-5/3}$, so it has a representation (2.3.1) and the conclusions of Theorem 2.3.2 hold with $\alpha = 5/3$. □

Example 2.3.10. [Gamma kernels and Whittle-Matérn autocorrelations]
The CMA process (II.i) with gamma kernel,

$$g(t) = t^{\nu-1}e^{-\lambda t}\mathbf{1}_{(0,\infty)}(t),\ \lambda > 0,\ \nu > 1/2, \tag{2.3.17}$$

has variance

$$\gamma_Y(0) = \sigma^2(2\lambda)^{1-2\nu}\Gamma(2\nu - 1)$$

and autocorrelation function

$$\rho_Y(h) = \frac{2^{3/2-\nu}}{\Gamma(\nu - 1/2)}|\lambda h|^{\nu-1/2}K_{\nu-1/2}(|\lambda h|), \tag{2.3.18}$$

which is the Whittle-Matérn autocorrelation function (see Guttorp and Gneiting (2005)) with parameter $\nu - 1/2$, evaluated at λh. The function $K_{\nu-1/2}$ in (2.3.18) is the modified Bessel function of the second kind with index $\nu - 1/2$ (Abramowitz and Stegun (1974), Section 9.6).

Note that $g \in \mathcal{R}_{\nu-1}(0+)$ and that it satisfies the assumptions of Proposition 2.3.5. From (2.1.1) with $\mathcal{F}\{g(\cdot)\}(\omega) = \Gamma(\nu)(\lambda - i\omega)^{-\nu}$, we obtain the spectral density

$$f_Y(\omega) = \frac{\sigma^2}{2\pi}|\mathcal{F}\{g(\cdot)\}|^2(\omega) = \frac{\sigma^2}{2\pi}\frac{\Gamma^2(\nu)}{(\lambda^2 + \omega^2)^\nu} = \omega^{-2\nu}\frac{\sigma^2\Gamma^2(\nu)}{2\pi\left((\lambda/\omega)^2 + 1\right)^\nu}, \quad \omega \in \Omega_c.$$

which belongs to $\mathcal{R}_{-2\nu}(\infty)$ and slowly varying function L such that $\lim_{\omega\to\infty} L(\omega) = \sigma^2\Gamma^2(\nu)/2\pi$.

Note that if $\nu = 5/6$, then f_Y, like the von Kármán spectral density of Example 4.9 (i), decays as $\omega^{-5/3}$ for $\omega \to \infty$, in accordance with Kolmogorov 5/3 law.

Theorem 2.3.2 gives the asymptotic form of the spectral density of the sequence $\{(1-B)^\nu Y_n^\Delta\}_{n\in\mathbb{Z}}$ as $\Delta \downarrow 0$,

$$h^\Delta(\omega) \sim \sigma^2\Gamma^2(\nu)(2\pi)^{-1}2^\nu\Delta^{2\nu-1}(1-\cos\omega)^\nu \times \left[|\omega|^{-2\nu} + (2\pi)^{-2\nu}\zeta\left(2\nu, 1-\frac{\omega}{2\pi}\right) + (2\pi)^{-2\nu}\zeta\left(2\nu, 1+\frac{\omega}{2\pi}\right)\right], \quad \omega \in \Omega_d.$$

The second order structure function, $S_2(\Delta) := \mathbb{E}[(Y_\Delta - Y_0)^2]$, plays an important role in the physics of turbulence. For the kernel (2.3.17) with $1/2 < \nu < 3/2$ its asymptotic behaviour as $\Delta \downarrow 0$ is given by

$$S_2(\Delta) = 2\gamma_Y(0)(1-\rho_Y(\Delta)), \quad \Delta > 0,$$

which, by the asymptotic behaviour as $\Delta \downarrow 0$ of $K_{\nu-1/2}(\Delta)$ (see Abramowitz and Stegun (1974), Section 9.6), gives the asymptotic formulae,

$$\frac{S_2(\Delta)}{2\gamma_Y(0)} = \begin{cases} 2^{1-2\nu}\dfrac{\Gamma(3/2-\nu)}{\Gamma(\nu+1/2)}(\lambda\Delta)^{2\nu-1} + O(\Delta^2), & 1/2 < \nu < 3/2, \\ \frac{1}{2}(\lambda\Delta)^2|\log\Delta| + O(\Delta^3), & \nu = 3/2, \\ \dfrac{1}{4(\nu-3/2)}(\lambda\Delta)^2 + O(\Delta^{2\nu-1}), & \nu > 3/2, \end{cases}$$

which can be found in Pope (2000), Appendix G, and Barndorff-Nielsen et al. (2011). The first of these formulae can also be obtained as a special case of Corollary 2.3.4 with $p = 1$. □

2.4. Estimation of g^Δ

Given observations of Y^Δ with Δ small, we estimate the kernel g by estimating the approximation g^Δ defined in (2.2.2) which, as shown in the preceding section, converges pointwise to σg as $\Delta \downarrow 0$ for all CARMA(p,q) processes. If the driving Lévy process is standardized so that Var(L_1)=1, then g^Δ converges pointwise to g. From now on we make this assumption since without it g is identifiable only to within multiplication by a constant.

To estimate g^Δ it suffices to estimate the coefficients and white noise variance in the Wold representation (2.2.1) of Y^Δ, for which standard non-parametric methods are available. Being non-parametric they require no *a priori* knowledge of the order of the underlying CARMA process and moreover they can be applied to the sampled observations

of any CMA of the form (5.1.2). The most direct estimator of the Wold parameters of a causal invertible ARMA process is based on the innovations algorithm (see Brockwell and Davis (1991), Section 8.3). Noting that the definition (2.2.2) is equivalent to

$$g^\Delta(t) = \frac{\sigma_\Delta}{\sqrt{\Delta}} \psi^\Delta_{\lfloor t/\Delta \rfloor}, \tag{2.4.1}$$

where $\lfloor t/\Delta \rfloor$ denotes the integer part of t/Δ, we obtain the following asymptotic result for the estimation of $g^\Delta(t)$ for fixed Δ as $n \to \infty$ in the important cases when Y is either a Gaussian CARMA process of arbitrary order or a CARMA(1,0) process with arbitrary second-order driving Lévy process. It follows directly from Theorem 2.1 of Brockwell and Davis (1988).

Theorem 2.4.1. *Suppose that Y is a Gaussian* CARMA(p,q) *process or a general Lévy-driven* CARMA$(1,0)$ *process observed at times $k\Delta$, $k = 1, \ldots, n$. For any fixed $t \geq 0$ and $\Delta > 0$, let $r = \lfloor t/\Delta \rfloor$. Then the innovations estimators $\hat{\theta}_{m,r}$ and $\hat{v}_m$ of $\psi^\Delta_{\lfloor t/\Delta \rfloor}$ and σ^2_Δ, respectively, have the following asymptotic properties. For any sequence of positive integers $\{m(n), n = 1, 2, \ldots\}$ such that $m < n$, $m \to \infty$ and $m = o(n^{1/3})$ as $n \to \infty$, $\hat{\theta}_{m(n),r}$ is consistent for $\psi^\Delta_{\lfloor t/\Delta \rfloor}$ and asymptotically normal. More specifically,*

$$\sqrt{n}(\hat{\theta}_{m(n),r} - \psi^\Delta_{\lfloor t/\Delta \rfloor}) \Rightarrow \mathrm{N}(0, a_\Delta), \tag{2.4.2}$$

where $a_\Delta := \sum_{j=0}^{r-1} (\psi^\Delta_j)^2$, *and*

$$\hat{v}_{m(n)} \xrightarrow{P} \sigma^2_\Delta. \tag{2.4.3}$$

Remark 2.4.2. (i) The restriction to either Gaussian or CARMA(1,0) processes stems from the fact that in these cases the driving noise sequence $\{Z^\Delta_n\}_{n\in\mathbb{Z}}$ is i.i.d. as required by Theorem 2.1 of Brockwell and Davis (1988). By Lemma 2.1 of Brockwell and Lindner (2009) the driving noise sequence is in general uncorrelated but not i.i.d. For general Lévy-driven CARMA processes, Ferrazzano and Fuchs (2013) show that the sequence Z^Δ, with appropriate normalisation, is a consistent estimator, as $\Delta \downarrow 0$, of the increments of the driving Lévy process, suggesting that the sequence $\{Z^\Delta_n\}_{n\in\mathbb{Z}}$ is approximately i.i.d. for small Δ even in the general case.

(ii) In the following corollaries and in Theorem 2.4.6 we retain the assumptions on Y and the sequence $\{m(n)\}$ made in the statement of Theorem 2.4.1. □

Corollary 2.4.3. *In the notation of Theorem 2.4.1, the estimator,*

$$\widehat{g}^\Delta(t) := \frac{\sqrt{\hat{v}_{m(n)}}}{\sqrt{\Delta}} \hat{\theta}_{m(n),r}, \tag{2.4.4}$$

of $g(t)$ has error,

$$\widehat{g}^\Delta(t) - g(t) = g^\Delta(t) - g(t) + \epsilon_n(t), \tag{2.4.5}$$

where $\epsilon_n(t)$ is asymptotically normal as $n \to \infty$, with asymptotic mean and variance, 0 and $a_\Delta \sigma_\Delta^2/(n\Delta)$, respectively.

Proof. Using (2.4.1), (2.4.3) and (2.4.4) we deduce from (2.4.2) that, as $n \to \infty$,

$$\frac{\sqrt{n\Delta}}{\sigma_\Delta}\epsilon_n(t) = \frac{\sqrt{n\Delta}}{\sigma_\Delta}(\widehat{g}^\Delta(t) - g^\Delta(t)) \Rightarrow \mathrm{N}(0, a_\Delta), \tag{2.4.6}$$

which is equivalent to the statement of the corollary. □

Example 2.4.4. [The CARMA(1,0) process] Application of Corollary 4.2 to the CARMA$(1,0)$ process using the results of Example 2.2.1 (with $\sigma^2 = 1$) immediately yields the representation

$$\widehat{g}^\Delta(t) - g(t) = \epsilon_n(t) + \left(\sqrt{\frac{e^{2\lambda\Delta} - 1}{2\lambda\Delta}} - 1\right) e^{\lambda t}, \tag{2.4.7}$$

where, as $n \to \infty$, $\epsilon_n(t)$ is asymptotically normal with mean 0 and variance $(e^{2\lambda t} - 1)/(2\lambda n\Delta)$. The last term in (2.4.7) tends to zero as $\Delta \downarrow 0$ and $\epsilon_n(t)$ converges in probability to 0 if we allow Δ to depend on n in such a way that $\Delta(n) \to 0$ and $n\Delta(n) \to \infty$ as $n \to \infty$. □

In the following we shall suppose, as in Example 2.4.4, that Δ depends on n in such a way that $\Delta(n) \to 0$ and $n\Delta(n) \to \infty$ as $n \to \infty$ and study the asymptotic behaviour of $\widehat{g}^\Delta(t)$ as $n \to \infty$.

Corollary 2.4.5. *If $\Delta(n) \to 0$ and $n \to \infty$ in such a way that $n\Delta(n) \to \infty$ (i.e. such that the time interval over which the observations are made goes to ∞) then $\widehat{g}^\Delta(t)$ is consistent for $g(t)$ for each fixed t.*

Proof. Under the conditions stated, the random variables $\epsilon_n(t)$ in (2.4.5) converge in probability to zero by Corollary 2.4.3 and the fact that $a_\Delta \sigma_\Delta^2 \leq \mathrm{Var}(Y(t))$. The deterministic component of (2.4.5), $g^\Delta(t) - g(t)$, converges to zero by Theorem 2.2.2. □

If we impose an additional condition on the rate at which $\Delta(n)$ converges to zero we obtain the following central limit theorem for our estimator $\widehat{g}^\Delta(t)$. Its proof is given in the Appendix.

Theorem 2.4.6. *Suppose that Y is a Gaussian* CARMA(p,q) *process or a general Lévy-driven CARMA(1,0) process observed at times $k\Delta(n)$, $k = 1, \ldots n$. If $\Delta(n) \to 0$, $n\Delta(n) \to \infty$ and $n(\Delta(n))^3 \to 0$ as $n \to \infty$, then, for fixed $t \geq 0$,*

$$\sqrt{n\Delta}(\widehat{g}^\Delta(t) - g(t)) \Rightarrow \mathrm{N}(0, \int_0^t g^2(u)du) \text{ as } n \to \infty.$$

Proof. Without loss of generality, we assume that $\Delta < 1$. We assume also, as in Section 4, that $\sigma^2 = 1$. Then the error of the innovations estimator, given by Corollary 2.4.3, is

$$\widehat{g}^\Delta(t) - g(t) = g^\Delta(t) - g(t) + \epsilon_n(t).$$

We multiply both sides by $\sqrt{n\Delta}$, obtaining

$$\sqrt{n\Delta}(\widehat{g}^\Delta(t) - g(t)) = \sqrt{n\Delta}(g^\Delta(t) - g(t)) + \sqrt{n\Delta}\epsilon_n(t). \tag{2.4.8}$$

In order to prove our result, we need to ensure that, as $n \to \infty$ with $\Delta(n)$ satisfying the conditions specified in the statement of the theorem, (i) the first term on the right of (2.4.8) converges to zero and (ii) the last term converges in distribution to a normal random variable with variance $\int_0^t g^2(u)du$. The proofs follow.

(i) Note first that

$$g^\Delta(t) - g(t) = \sum_{r=1}^{p} \left[C(r,\Delta) - \frac{b(\lambda_r)}{a'(\lambda_r)} \right] e^{\lambda_r t}, \tag{2.4.9}$$

where $C(r,\Delta)$ is the coefficient obtained plugging (2.2.4) and (2.2.5) into (2.4.1). The function $C(r,\Delta)$ is a rational bounded function, whose parameters depend continuously on Δ. Therefore we can write the series expansion

$$C(r,\Delta) = \sum_{k=0}^{\infty} \bar{c}_k(r)\Delta^k \tag{2.4.10}$$

where, from Theorem 2.2.2(ii), $\bar{c}_0(r) = b(\lambda_r)/a'(\lambda_r)$. This implies that

$$C(r,1) = \bar{c}_0(r) + \sum_{k=1}^{\infty} \bar{c}_k(r) < \infty, \quad 1 \le r \le p.$$

Then the deterministic part of (2.4.8) can be written as

$$\begin{aligned}\sqrt{n\Delta}\left|g^\Delta(t) - g(t)\right| &= \left| \sum_{r=1}^{p} \left(\sqrt{n} \sum_{k=1}^{\infty} \bar{c}_k(r)\Delta^{k+1/2} \right) e^{\lambda_r t} \right| . \\ &\le \sum_{r=1}^{p} \left| \sqrt{n} \sum_{k=1}^{\infty} \bar{c}_k(r)\Delta^{k+1/2} \right| \left| e^{\lambda_r t} \right| .\end{aligned}$$

Since $\Delta < 1$, for $k \ge 1$

$$0 < \sqrt{n}\Delta^{k+1/2} = \Delta^{k-1}\sqrt{n}\Delta^{3/2} \le \sqrt{n}\Delta^{3/2}.$$

Therefore,

$$0 < \sqrt{n\Delta}|g^\Delta(t) - g(t)| \le \Delta^{3/2}\sqrt{n} \sum_{r=1}^{p} \left| \sum_{k=1}^{\infty} \bar{c}_k(r) \right| \left| e^{\lambda_r t} \right| \to 0$$

if $n(\Delta(n))^3 \to 0$ as $n \to \infty$.

(ii) For fixed $\Delta > 0$ Corollary 2.4.3 implies that $\sqrt{n\Delta}\epsilon_n(t) \Rightarrow N(0, a_\Delta \sigma_\Delta^2)$ as $n \to \infty$. We shall show now that $\lim_{\Delta\to 0} a_\Delta \sigma_\Delta^2 = \int_0^t g^2(u)du$. Then it follows that if Δ depends on n in such a way that $\Delta(n) \to 0$ and $n\Delta(n) \to \infty$ as $n \to \infty$, we have the convergence in distribution,

$$\sqrt{n\Delta(n)}\epsilon_n(t) \Rightarrow N(0, \int_0^t g^2(u)du), \quad \text{as } n \to \infty,$$

which, with (i), completes the proof of the theorem.

Now $a_\Delta \sigma_\Delta^2$ is the mean squared error of the best linear predictor of $Y_{\Delta\lfloor t/\Delta\rfloor}$ based on $Y_{k\Delta}, k = 0, -1, -2, \ldots$, and $\int_0^{\Delta\lfloor t/\Delta\rfloor} g^2(u)du$ is the mean squared error of the best linear predictor of $Y_{\Delta\lfloor t/\Delta\rfloor}$ based on $Y_t, t \in (-\infty, 0]$. The mean-square continuity of Y means that the difference converges to zero as $\Delta \to 0$, which in turn implies that

$$a_\Delta \sigma_\Delta^2 - \int_0^t g^2(u)du \to 0 \quad \text{as } \Delta \to 0.$$

□

Remark 2.4.7. We shall refer to the estimator (2.4.4) as the *innovations estimator* of $g(t)$. Instead of using the innovations estimates of $\psi^\Delta_{\lfloor t/\Delta\rfloor}$ and σ^Δ as in (2.4.4), we could also use the coefficients and white-noise standard deviation obtained by using the Durbin-Levinson algorithm to fit a high-order causal AR process with white-noise variance τ^2 to the observed values of $Y_k^\Delta, k = 1, \ldots n$, and numerically inverting the fitted autoregressive polynomial $\phi(z) = 1 - \phi_1 z - \ldots - \phi_p z^p$ to obtain the moving average representation

$$Y_n^\Delta = \sum_{j=0}^{\infty} \beta_j Z_{n-j}, \quad \{Z_n\}_{n\in\mathbb{Z}} \sim \text{WN}(0, \tau^2).$$

where $\beta(z) := \sum_{j=0}^\infty \beta_j z^j = 1/\phi(z), \ |z| \le 1$. Substituting the estimators τ^2 for v_m and β_r for $\theta_{m(n),r}$ gives the *Durbin-Levinson estimator* (of order p) for $g^\Delta(t)$. Both of these estimators will be used in the examples which follow. In practice it has been found that the Durbin-Levinson algorithm gives better results except when the fitted autoregressive polynomial has zeroes very close to the unit circle. □

Example 2.4.8. [Simulation results] We now illustrate the performance of the estimators by applying them to realizations of the Gaussian CMA process Y defined by (5.1.2) with gamma kernel function, Example 2.3.10

$$g(t) = t^{\nu-1}e^{-\lambda t}\mathbf{1}_{(0,\infty)}(t), \quad \lambda > 0, \ \nu > 1/2, \tag{2.4.11}$$

with standard Brownian motion as the driving Lévy process.

The simulations were carried out with $\lambda = 1$ and two values of ν, namely $\nu = 1.05$ and $\nu = 2$. The kernel with $\nu = 2$ is actually the kernel of the CARMA$(2,0)$ process (3.1.1) with $a(z) = (z+\lambda)^2$, $b(z) = 1$ and $\sigma^2 = 1$. The gamma kernel with $\nu = 1.05$ however is the kernel of a CMA process but not of any CARMA process.

We first estimated $\widehat{g}^{\Delta}$ by applying both the Durbin-Levinson and innovations algorithms to the *true* autocovariance functions which are known for the simulated processes. The purpose was to assess the effect of the sampling error when the *sample* autocovariances of the data are used. The estimated kernel functions are shown in the upper rows of Figures 1-4.

The continuous-time sample-paths of Y were simulated at the very finely-spaced times $k\Delta$ with $\Delta = 10^{-6}$. The sequences Y^{Δ} used to estimate g were then sampled from these values using two different spacings, $\Delta = 0.25$ and $\Delta = 0.0625$ We then estimated the kernel function $g(\cdot)$ up to time $T = 8$, and plotted $\widehat{g}^{\Delta}((j+\frac{1}{2})\Delta)$ for $j = 0, \ldots, N = 32$ and for $j = 0, \ldots, N = 128$, respectively. In the case of the innovations algorithm, we used (for the true as well as for the estimated autocovariances) values of the discrete autocovariance functions up to $3N$, i.e. we chose m in (2.4.4) to be $3N$. We could equally well have plotted $\widehat{g}^{\Delta}((j+h)\Delta)$ for any $h \in [0,1)$, where the bias depends on h. However the variation becomes negligible as $\Delta \downarrow 0$. Some partial results regarding the optimal choice of h are given in Chapter 3.

The results are shown in the bottom rows of Figures 1-4, where the squares denote the estimates from the innovations algorithm, and the circles denote those from the Durbin-Levinson algorithm. For reference the true kernel function is plotted with a solid line. Comparing the top and bottom rows of Figures 1-4 we find for the estimated autocovariance function an intrinsic finite-sample error, which influences the kernel estimation. We notice that in all cases considered, the Durbin-Levinson algorithm gives better estimates. Furthermore, as expected, the estimates for both algorithms improve with decreasing grid spacing. The Durbin-Levinson algorithm provides estimates which are in good agreement with the original kernel function even for the coarse grid with $\Delta = 0.25$. □

2.5. An application to real data: mean flow turbulent velocities

We now apply the Durbin-Levinson algorithm of Section 2.4 to the Brookhaven turbulent wind-speed data, which consists of 20×10^6 measurements taken at 5000Hz (i.e. 5000 data points per second). The series thus covers a total time interval of approximately 67 minutes and the sampling interval Δ is 2×10^{-4} seconds. This dataset displays a rather high Reynolds number (about 17000), typical of turbulent phenomena. A more detailed presentation of turbulence phenomena and an application of the CMA model

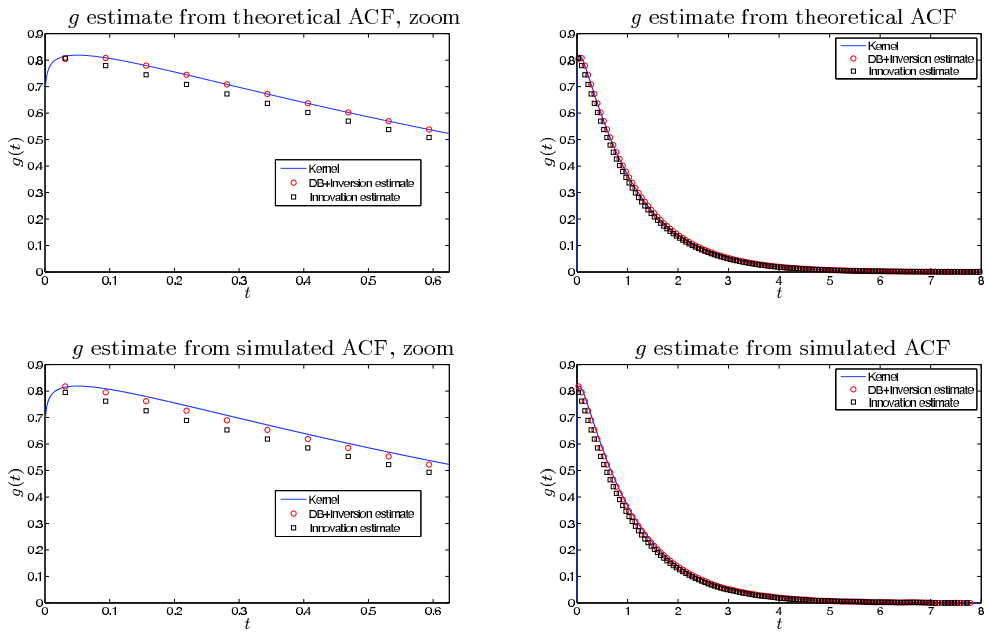

Figure 2.2.: Estimation of the gamma kernel for $\nu = 1.05$ and $\Delta = 2^{-2}$.

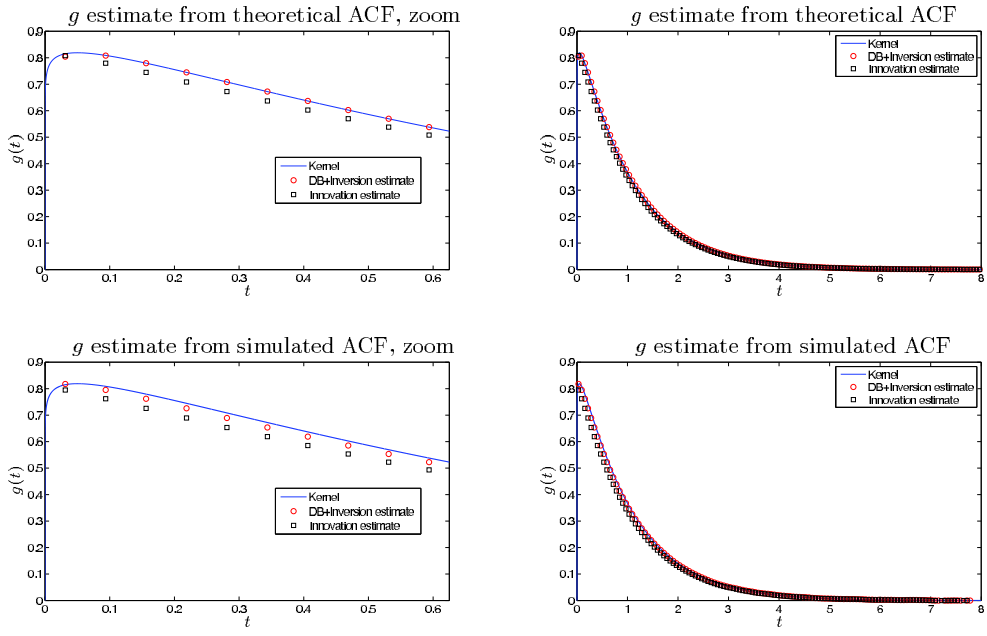

Figure 2.3.: Estimation of the gamma kernel for $\nu = 1.05$ and $\Delta = 2^{-4}$.

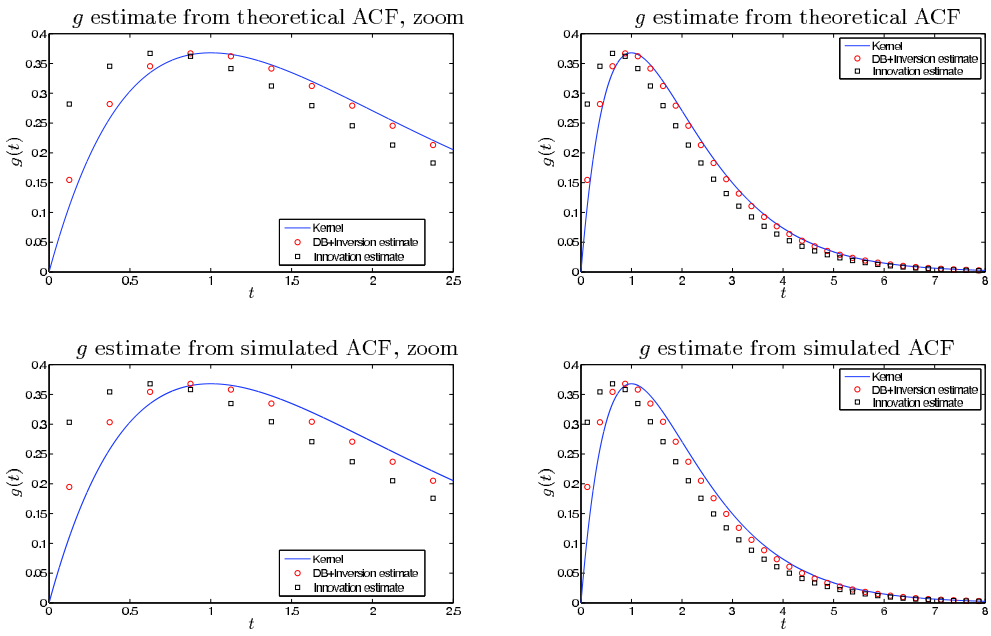

Figure 2.4.: Estimation of the gamma kernel for $\nu = 2$ (CAR(2) process) and $\Delta = 2^{-2}$.

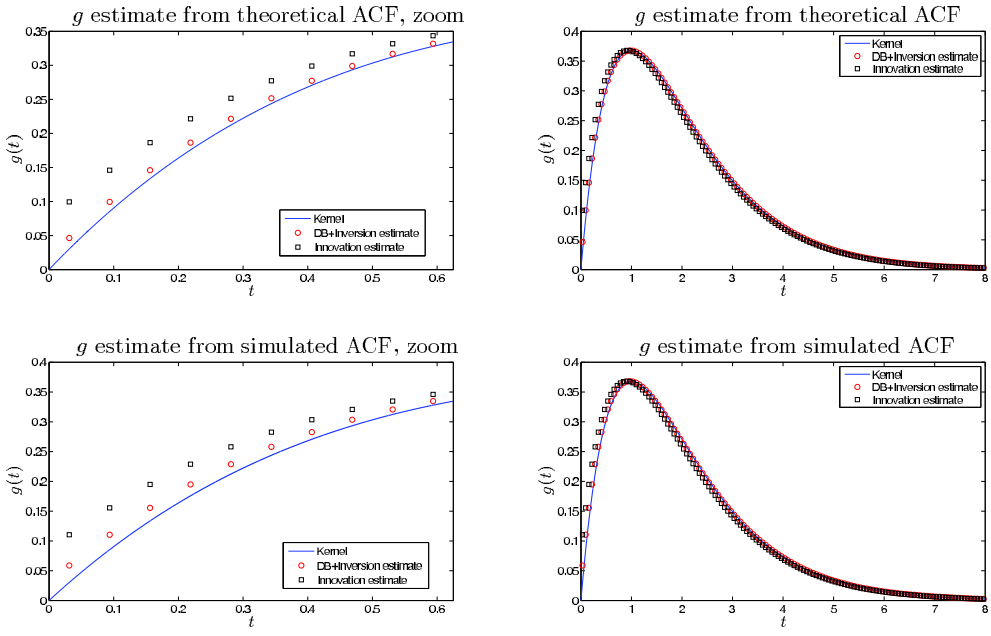

Figure 2.5.: Estimation of the gamma kernel for $\nu = 2$ (CAR(2) process) and $\Delta = 2^{-4}$.

(5.1.2) in the context of turbulence modelling is given in Chapter 5; moreover we refer to Drhuva (2000), Ferrazzano (2010) for a precise description of the data, and to Pope (2000), Frisch (1996) for a comprehensive review of turbulence theory. A CMA model (5.1.2) with a gamma kernel as in Example 2.3.10 has been suggested as a parametric model in Barndorff-Nielsen and Schmiegel (2009).

Figure 2.6 a) shows the sample autocorrelation function up to 120 seconds, which appears to be exponentially decreasing. In general, the data are not significantly correlated after a lag of 100 seconds.

The estimated spectral density $\widehat{f_Y}$ of Y^Δ is shown in Figure 2.6 b), plotted against the frequency φ, measured in cycles per second (Hz). The estimates marked by circles were estimated by Welch's method (Welch (1967)) with segments of 2^{22} data points (circa 14 minutes), windowed with a Hamming window and using an overlapping factor of 50%. This method allows a significant reduction of the variance of the estimate, sacrificing some resolution in frequency. In order to have a better resolution near frequency zero, we estimated the spectral density for $\varphi \leq 10^{-3}$ Hz with the raw periodogram (Brockwell and Davis (1991), p. 322), which provides a better resolution in frequency at cost of a larger variance. The results are plotted in the leftmost part of Figure 2.6 b) with diamonds, and the two ranges of estimation are indicated by a vertical solid line. The spectral density is plotted on a log-log scale, so that any power-law relationship will be reflected by linearity of the graph. The spectral density in the neighborhood of zero appears to be essentially constant, as is compatible with an exponentially decreasing autocorrelation function (such as the gamma kernel function of Example 2.3.10).

For frequencies φ between 10^{-2} and 200Hz, $\log \widehat{f_Y}$ decreases linearly with $\log \varphi$ with a slope of approximately $-5/3$, in accordance with Kolmogorov's 5/3-law. For comparison, the solid line corresponds to a spectral density proportional to $\varphi^{-5/3}$. For φ larger than 200Hz, the spectral density deviates from the 5/3-law, decaying with a steeper slope. We note that a spectral density decaying as prescribed by Kolmogorov's law in the neighborhood of ∞ would require a kernel behaving like $t^{-1/6}$ near to the origin, according to Proposition 2.3.5 (see below).

The estimated kernel function $\widehat{g}^\Delta(t)$ is plotted in Figure 2.6 c) on a log-linear scale in order to highlight the behaviour of the kernel estimate at both very large and very small values of t. The estimated $g(t)$ decays rapidly with t, with small oscillations around zero for $t > 100$ seconds. As t decreases from this value to roughly 10^{-3} seconds, the estimated kernel increases in accordance with Kolmogorov's 5/3-law, dropping off to zero as t decreases further, matching the steeper decay of the spectral density at high frequencies evident in Figures 5 b) and 5 d).

Figure 6 d) shows the spectral density computed directly from the estimated kernel function $\widehat{g}^\Delta$. Its close resemblance to the spectral density calculated by Welch's method provides justification for our estimator of g even when there is no underlying parametric model.

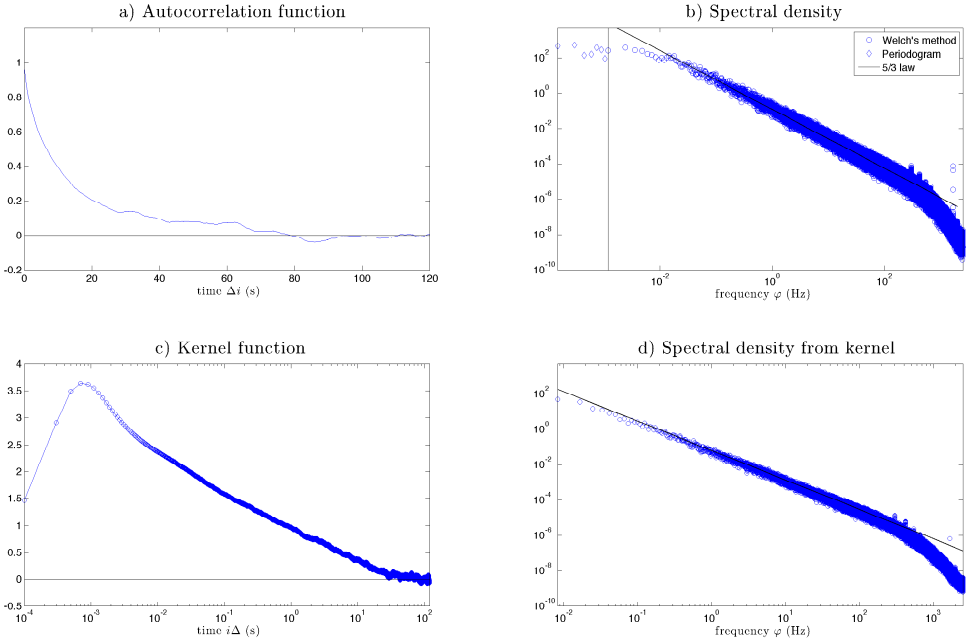

Figure 2.6.: Estimates for the Brookhaven dataset: a) autocorrelation function b) spectral density (Welch estimator and periodogram) c) kernel function (linear-log scale) d) spectral density computed using the estimated kernel.

3. Noise recovery for Lévy-driven CARMA processes and high-frequency behaviour of approximating Riemann sums

We consider high-frequency sampled continuous-time autoregressive moving average (CARMA) models driven by finite-variance zero-mean Lévy processes. An L^2-consistent estimator for the increments of the driving Lévy process without order selection in advance is proposed if the CARMA model is invertible. In the second part we analyse the high-frequency behaviour of approximating Riemann sum processes, which represent a natural way to simulate continuous-time moving average processes on a discrete grid. We shall compare their autocovariance structure with the one of sampled CARMA processes, where the rule of integration plays a crucial role. Moreover, new insight into the kernel estimation procedure of Chapter 2 is given.

The outline of the Chapter is as follows. In Section 3.1 we are going to recall the definition of finite-variance CARMA models and summarise important properties of high-frequency sampled CARMA processes. In particular, we fix a global assumption that guarantees causality and invertibility for the sampled sequence. In the third Section we then derive an L^2-consistent estimator for the increments of the driving Lévy process starting from the Wold representation of the sampled process. It will turn out that *invertibility* of the original continuous-time process is sufficient and necessary for the recovery result to hold. Section 3.2 is completed by an illustrating example for CAR(2) and CARMA$(2,1)$ processes. Thereafter, the high-frequency behaviour of approximating Riemann sum processes is studied in Section 3.3. First, an ARMA representation for the Riemann sum approximation is established in general and then the role of the rule of integration is analysed by matching the asymptotic autocovariance structure of sampled CARMA processes and their Riemann sum approximations in the cases where the autoregressive order is less or equal to 3. The connection between the Wold representation and the approximating Riemann sum yields a deeper insight into the kernel estimation procedure introduced in Chapter 2. A short conclusion can be found in Section 3.4 and some auxiliary results are

established in the Section 3.5.

3.1. Preliminaries

3.1.1. Finite-variance CARMA processes

Throughout this Chapter we shall be concerned with a CARMA process driven by a second order zero-mean Lévy process $L = \{L_t\}_{t\in\mathbb{R}}$ with $E[L_1] = 0$ and $E[L_1^2] = 1$. It is defined as follows.

For non-negative integers p and q such that $q < p$, a CARMA(p, q) process $Y = (Y_t)_{t\in\mathbb{R}}$ with coefficients $a_1, \ldots, a_p$, $b_0, \ldots, b_q \in \mathbb{R}$ and driving Lévy process L is defined to be a strictly stationary solution of the suitably interpreted formal equation

$$a(D)Y_t = \sigma b(D)DL_t, \quad t \in \mathbb{R}, \tag{3.1.1}$$

where D denotes differentiation with respect to t, $a(\cdot)$ and $b(\cdot)$ are the characteristic polynomials,

$$a(z) := z^p + a_1 z^{p-1} + \cdots + a_p \quad \text{and} \quad b(z) := b_0 + b_1 z + \cdots + b_{p-1} z^{p-1},$$

the coefficients b_j satisfy $b_q = 1$ and $b_j = 0$ for $q < j < p$, and $\sigma > 0$ is a constant. The polynomials $a(\cdot)$ and $b(\cdot)$ are assumed to have no common zeroes.

Since the derivative DL_t does not exist in the usual sense, we interpret (3.1.1) as being equivalent to the observation and state equations

$$Y_t = \mathbf{b}^T \mathbf{X}_t\,, \tag{3.1.2}$$

$$d\mathbf{X}_t = A\mathbf{X}_t dt + \mathbf{e}_p dL_t\,, \tag{3.1.3}$$

where

$$\mathbf{X}_t = \begin{pmatrix} X(t) \\ X^{(1)}(t) \\ \vdots \\ X^{(p-2)}(t) \\ X^{(p-1)}(t) \end{pmatrix}, \quad \mathbf{b} = \begin{pmatrix} b_0 \\ b_1 \\ \vdots \\ b_{p-2} \\ b_{p-1} \end{pmatrix}, \quad \mathbf{e}_p = \begin{pmatrix} 0 \\ 0 \\ \vdots \\ 0 \\ 1 \end{pmatrix},$$

$$A = \begin{pmatrix} 0 & 1 & 0 & \ldots & 0 \\ 0 & 0 & 1 & \ldots & 0 \\ \vdots & \vdots & \vdots & \ddots & \vdots \\ 0 & 0 & 0 & \ldots & 1 \\ -a_p & -a_{p-1} & -a_{p-2} & \ldots & -a_1 \end{pmatrix} \quad \text{and } A = -a_1 \text{ for } p = 1.$$

It is easy to check that the eigenvalues of the matrix A are the same as the zeroes of the autoregressive polynomial $a(\cdot)$.

Under Assumption 1 (i) it has been shown in (Brockwell and Lindner (2009), Theorem 3.3) that Eqs. (3.1.2)-(3.1.3) have the unique strictly stationary solution,

$$Y_t = \int_{-\infty}^{\infty} g(t-u)dL_u, \quad t \in \mathbb{R}, \tag{3.1.4}$$

where

$$g(t) = \begin{cases} \frac{\sigma}{2\pi i}\int_\rho \frac{b(z)}{a(z)}e^{tz}dz = \sigma\sum_\lambda Res_{z=\lambda}\left(e^{zt}\frac{b(z)}{a(z)}\right), & \text{if } t>0, \\ 0, & \text{if } t \leq 0, \end{cases} \tag{3.1.5}$$

and ρ is any simple closed curve in the open left half of the complex plane encircling the zeroes of $a(\cdot)$. The sum is over the distinct zeroes λ of $a(\cdot)$ and $\mathrm{Res}_{z=\lambda}(\cdot)$ denotes the residue at λ of the function in brackets. The kernel g can also be expressed (Brockwell and Lindner (2009), equations (2.10) and (3.7)) as

$$g(t) = \sigma \mathbf{b}^\top e^{At}\mathbf{e}_p \mathbf{1}_{(0,\infty)}(t), \quad t \in \mathbb{R}, \tag{3.1.6}$$

and its Fourier transform is

$$\mathcal{F}\{g(\cdot)\}(\omega) := \int_{\mathbb{R}} g(s)e^{i\omega s}ds = \sigma\frac{b(-i\omega)}{a(-i\omega)}, \quad \omega \in \mathbb{R}. \tag{3.1.7}$$

In the light of Eqs. (3.1.4)-(3.1.7), we can interpret a CARMA process as a continuous-time filtered white noise, whose transfer function has a finite number of poles and zeros. We outline that the request on the roots of $a(\cdot)$ to lie in the interior of the left half of the complex plane in order to have causality arises from Theorem V, p. 8, Paley and Wiener (1934), which is intrinsically connected with the Theorems in Titchmarsh (1948), pp. 125-129, on the Hilbert transform. A similar request on the roots of $b(\cdot)$ will turn out to be necessary for recovering the driving Lévy process.

3.1.2. Properties of high-frequency sampled CARMA processes

We now recall some properties of the sampled process $Y^\Delta := \{Y_{n\Delta}\}_{n\in\mathbb{Z}}$ of a CARMA(p,q) process where $\Delta > 0$; cf. Brockwell et al. (2013, 2012) and references therein. It is known that the sampled process Y^Δ satisfies the ARMA$(p, p-1)$ equations

$$\Phi_\Delta(B)Y_n^\Delta = \Theta_\Delta(B)Z_n^\Delta, \quad n \in \mathbb{Z}, \quad \{Z_n^\Delta\} \sim \mathrm{WN}(0,\sigma_\Delta^2), \tag{3.1.8}$$

with the AR part $\Phi_\Delta(B) := \prod_{i=1}^p (1 - e^{\Delta\lambda_i}B)$, where B is the discrete-time backshift operator, $BY_n^\Delta := Y_{n-1}^\Delta$. Finally, the MA part $\Theta_\Delta(\cdot)$ is a polynomial of order $p-1$, chosen in such a way that it has no roots inside the unit circle. For $p > 3$ and fixed $\Delta > 0$ there is no explicit expression for the coefficients of $\Theta_\Delta(\cdot)$ nor the white noise process

Z^{Δ}. Nonetheless, asymptotic expressions for $\Theta_{\Delta}(\cdot)$ and $\sigma_{\Delta}^2 = \mathrm{var}(Z_n^{\Delta})$ as $\Delta \downarrow 0$ were obtained in Brockwell et al. (2013, 2012). Namely we have that the polynomial $\Theta_{\Delta}(z)$ can be written as (see Theorem 2.1, Chapter 2)

$$\Theta_{\Delta}(z) = \prod_{i=1}^{p-q-1} (1 + \eta(\xi_i)z) \prod_{k=1}^{q} (1 - \zeta_k z), \quad z \in \mathbb{C}, \tag{3.1.9}$$

$$\sigma_{\Delta}^2 = \frac{\sigma^2 \Delta^{2(p-q)-1}}{(2(p-q)-1)! \prod_{i=1}^{p-q-1} \eta(\xi_i)} (1 + o(1)), \quad \text{as} \Delta \downarrow 0, \tag{3.1.10}$$

where, again as $\Delta \downarrow 0$,

$$\begin{aligned} \zeta_k &= 1 \pm \mu_k \Delta + o(\Delta), & k &= 1, \ldots, q, \\ \eta(\xi_i) &= \xi_i - 1 \pm \sqrt{(\xi_i - 1)^2 - 1} + o(1), & i &= 1, \ldots, p-q-1. \end{aligned} \tag{3.1.11}$$

The signs $\pm$ in (3.1.11) are chosen respectively such that, for sufficiently small Δ, the coefficients ζ_k and $\eta(\xi_i)$ are less than 1 in absolute value, to ensure that (3.1.8) is invertible. Moreover, ξ_i, $i = 1, \ldots, p-q-1$, are the zeros of $\alpha_{p-q-1}(\cdot)$, which is defined as the $(p-q-1)$-th coefficient in the series expansion

$$\frac{\sinh(z)}{\cosh(z) - 1 + x} = \sum_{k=0}^{\infty} \alpha_k(x) z^{2k+1}, \quad z \in \mathbb{C},\ x \in \mathbb{R}\backslash\{0\}, \tag{3.1.12}$$

where the L.H.S. of Eq. (3.1.12) is a power transfer function arising from the sampling procedure (cf. Brockwell et al. (2012), Eq. (11)). Therefore the coefficients $\eta(\xi_i)$, $i = 1, \ldots, p-q-1$, can be regarded as spurious, as they do not depend on the parameters of the underlying continuous-time process Y, but just on $p-q$.

Remark 3.1.1. *Our notion of sampled process is a weak one, since we only require that the sampled process has the same autocovariance structure as the continuous-time process, when observed on a discrete grid. We know that the filtered process on the LHS of* (3.1.8) *(Brockwell and Lindner (2009), Lemma 2.1) is a* $(p-1)$*-dependent discrete-time process. Therefore there exist* 2^{p-1} *possible representations for the RHS of* (3.1.8) *yielding the same autocovariance function of the filtered process, but only one having its roots outside the unit circle, which is called minimum-phase spectral factor (see Sayed and Kailath (2001) for a review on the topic). Since it is not possible to discriminate between them, we always take the minimum-phase spectral factor without any further question. This will be crucial in our main result.*

Moreover, the rationale behind Assumption 1 (ii) becomes clear now: if $\Re(\mu_k) = 0$ *for some* k*, then the corresponding* $|\zeta_k|^2$ *is equal to* $1 + \Delta^2 |\mu_k|^2 + o(\Delta^2)$*, for either sign choice. Then the* $\mathrm{MA}(p-1)$ *polynomial in* (3.1.9) *will never be invertible for small* Δ*.*

In order to ensure that the sampled CARMA process is invertible, we need to verify that $|\eta(\xi_i)|$ will be strictly less than 1 for all $i = 1, \ldots, p-q-1$ and sufficiently small Δ.

Proposition 3.1.2. *The coefficients $\eta(\xi_i)$ in Eq. (3.1.11) are uniquely determined by*

$$\eta(\xi_i) = \xi_i - 1 - \sqrt{(\xi_i - 1)^2 - 1} + o(1), \quad i = 1, \ldots, p-q-1,$$

and we have that $\xi_i - 1 - \sqrt{(\xi_i - 1)^2 - 1} \in (0, 1)$ for all $i = 1, \ldots, p-q-1$.

Proof. It follows from Proposition 3.5.1 that $\xi_i \in (2, \infty)$ for all $i = 1, \ldots, p-q-1$. This yields $\xi_i - 1 + \sqrt{(\xi_i - 1)^2 - 1} > 1$ for all i and hence, we have that

$$\eta(\xi_i) = \xi_i - 1 - \sqrt{(\xi_i - 1)^2 - 1} + o(1), \quad i = 1, \ldots, p-q-1.$$

Since the first-order term of $\eta(\xi_i)$ is positive and monotonously decreasing in ξ_i, the additional claim follows. □

3.2. Noise recovery

In this Section we are going to prove the first main statement of this Chapter, which is a recovery result for the driving Lévy process. We start with some motivation for our approach.

We know that the sampled CARMA process $Y^\Delta = \{Y_{n\Delta}\}_{n\in\mathbb{Z}}$ has the Wold representation (cf. Brockwell and Davis (1991), p. 187)

$$Y_n^\Delta = \sum_{j=0}^{\infty} \psi_j^\Delta Z_{n-j}^\Delta = \sum_{j=0}^{\infty} \left(\frac{\sigma_\Delta}{\sqrt{\Delta}} \psi_j^\Delta \right) \left(\frac{\sqrt{\Delta}}{\sigma_\Delta} Z_{n-j}^\Delta \right), \quad n \in \mathbb{Z}, \tag{3.2.1}$$

where $\sum_{j=0}^{\infty} (\psi_j^\Delta)^2 < \infty$. Moreover, Eq. (3.2.1) is the causal representation of Eq. (3.1.8), and it has been shown in Chapter 2 that for every causal and invertible CARMA(p, q) process, as $\Delta \downarrow 0$,

$$\frac{\sigma_\Delta}{\sqrt{\Delta}} \psi_{\lfloor t/\Delta \rfloor}^\Delta \to g(t), \quad t \geq 0, \tag{3.2.2}$$

where g is the kernel in the moving average representation (3.1.4). Given the availability of classical time-series methods to estimate $\{\psi_j^\Delta\}_{j\in\mathbb{N}}$ and σ_Δ^2, and the flexibility of CARMA processes, we argue that this result can be applied to more general continuous-time moving average processes.

Given Eqs. (3.2.1) and (3.2.2) it is natural to investigate, whether the quantity

$$\bar{L}_n^\Delta := \frac{\sqrt{\Delta}}{\sigma_\Delta} Z_n^\Delta, \quad n \in \mathbb{Z},$$

approximates the increments of the driving Lévy process in the sense that for every fixed $t \in (0, \infty)$,

$$\sum_{i=1}^{\lfloor t/\Delta \rfloor} \bar{L}_i^\Delta \xrightarrow{L^2} L_t, \quad \Delta \downarrow 0. \tag{3.2.3}$$

As usual, convergence in L^2 implies also convergence in probability and distribution.

The first results on retrieving the increments of L were given in Brockwell et al. (2011), and furthermore generalised to the multivariate case by Brockwell and Schlemm (2013). The essential limitation of this parametric method is that it might not be robust with respect to model misspecification. More precisely, the fact that a CARMA(p, q) process is $(p - q - 1)$-times differentiable (see Proposition 3.32 of Marquardt and Stelzer (2007)) is essential for the procedure to work (cf. Theorem 4.3 of Brockwell and Schlemm (2013)). However, if the underlying process is instead CARMA(p', q') with $p' - q' < p - q$, then some of the necessary derivatives do not longer exist. In contrast to the aforementioned procedure, in the method we propose there is no need to specify the autoregressive and the moving average orders p and q in advance.
Our main theorem is the following:

Theorem 3.2.1. *Let Y be a finite-variance* CARMA(p, q) *process and Z^Δ the noise on the RHS of the sampled Eq.* (3.1.8)*. Moreover, let Assumption 1 hold and define $\bar{L}^\Delta := \sqrt{\Delta}/\sigma_\Delta Z^\Delta$. Then, as $\Delta \downarrow 0$,*

$$\sum_{i=1}^{\lfloor t/\Delta \rfloor} \bar{L}_i^\Delta \xrightarrow{L^2} L_t, \quad t \in (0, \infty), \tag{3.2.4}$$

if and only if the roots of the moving average polynomial $b(\cdot)$ on the RHS of the CARMA *Eq.* (3.1.1) *have negative real parts, i.e. if and only if the* CARMA *process is invertible.*

Proof. Under Assumption 1 (ii) and using Proposition 3.1.2, the sampled ARMA equation (3.1.8) is invertible. The noise on the RHS of Eq. (3.1.8) is then obtained using the classical inversion formula

$$Z_n^\Delta = \frac{\Phi_\Delta(B)}{\Theta_\Delta(B)} Y_n^\Delta, \quad n \in \mathbb{Z},$$

where B is the usual backshift operator. Let us consider the stationary *continuous-time* process

$$\mathcal{Z}_t^\Delta := \frac{\Phi_\Delta(B_\Delta)}{\Theta_\Delta(B_\Delta)} Y_t = \sum_{i=0}^{\infty} a_i^\Delta \int_{-\infty}^{t-i\Delta} g(t - i\Delta - s) dL_s, \quad t \in \mathbb{R}, \tag{3.2.5}$$

where the continuous-time backshift operator B_Δ is defined such that $B_\Delta Y_t := Y_{t-\Delta}$ for every $t \in \mathbb{R}$ and the series in the RHS of (3.2.5) is the Laurent expansion of the rational function $\Phi_\Delta(\cdot)\Theta_\Delta^{-1}(\cdot)$. Moreover, $\mathcal{Z}_{n\Delta}^\Delta = Z_n^\Delta$ for every $n \in \mathbb{N}$; as a consequence, the random variables $\mathcal{Z}_s^\Delta, \mathcal{Z}_t^\Delta$ are uncorrelated for $|t - s| \geq \Delta$ and $\mathrm{var}(\mathcal{Z}_t^\Delta) = \mathrm{var}(Z_n^\Delta)$.

Exchanging the sum and the integral signs in (3.2.5), and the fact that $g(\cdot) = 0$ for negative arguments, we have that $\mathcal{Z}^\Delta$ is a continuous-time moving average process

$$\mathcal{Z}_t^\Delta = \int_{-\infty}^{t} g^\Delta(t-s)dL_s, \quad t \in \mathbb{R},$$

whose kernel function g^Δ has Fourier transform (cf. Eq. (3.1.7))

$$\mathcal{F}\{g^\Delta(\cdot)\}(\omega) = \frac{\Phi_\Delta(e^{i\omega\Delta})}{\Theta_\Delta(e^{i\omega\Delta})}\mathcal{F}\{g(\cdot)\}(\omega) = \sigma\frac{\Phi_\Delta(e^{i\omega\Delta})}{\Theta_\Delta(e^{i\omega\Delta})}\frac{b(-i\omega)}{a(-i\omega)}, \quad \omega \in \mathbb{R}, \quad \Delta > 0.$$

Since we can write $L_t - L_{t-\Delta} = \int_{-\infty}^{t} \mathbf{1}_{(0,\Delta)}(t-s)dL_s$, $t \in \mathbb{R}$, the sum of the differences between the rescaled sampled noise terms and the increments of the Lévy process is given by

$$\sum_{j=1}^{n} \bar{L}_j^\Delta - L_{n\Delta} = \int_{-\infty}^{n\Delta} \sum_{j=1}^{n} \left[\frac{\sqrt{\Delta}}{\sigma_\Delta} g^\Delta(j\Delta - s) - \mathbf{1}_{(0,\Delta)}(j\Delta - s)\right] dL_s = \int_{-\infty}^{n\Delta} h_n^\Delta(n\Delta - s)dL_s, \tag{3.2.6}$$

where, for every $n \in \mathbb{N}$,

$$h_n^\Delta(s) := \sum_{j=1}^{n} \left[\frac{\sqrt{\Delta}}{\sigma_\Delta} g^\Delta(s + (j-n)\Delta) - \mathbf{1}_{(0,\Delta)}(s + (j-n)\Delta)\right], \quad s \in \mathbb{R},$$

and the stochastic integral in Eq. (3.2.6) w.r.t. L is still in the L^2-sense. It is a standard result, cf. (Gikhman and Skorokhod 2004, Ch. IV, §4), that the variance of the moving average process in Eq. (3.2.6) is given by

$$\mathbb{E}\left[\sum_{j=1}^{n} \bar{L}_j^\Delta - L_{n\Delta}\right]^2 = \int_{-\infty}^{n\Delta} \left(h_n^\Delta(n\Delta - s)\right)^2 ds = \|h_n^\Delta(\cdot)\|_{L^2}^2, \tag{3.2.7}$$

where the latter equality is true since $h_n^\Delta(s) = 0$ for any $s \leq 0$.

Furthermore, the Fourier transform of $h_n^\Delta(\cdot)$ can be readily calculated, invoking the linearity and the shift property of the Fourier transform. We thus obtain

$$\begin{aligned}
\mathcal{F}\{h_n^\Delta(\cdot)\}(\omega) &= \left[\frac{\sqrt{\Delta}}{\sigma_\Delta}\mathcal{F}\{g^\Delta(\cdot)\}(\omega) - \mathcal{F}\{\mathbf{1}_{(0,\Delta)}(\cdot)\}(\omega)\right] \sum_{j=1}^{n} e^{i\omega(n-j)\Delta} \\
&= \left[\sigma\frac{\sqrt{\Delta}}{\sigma_\Delta}\frac{\prod_{j=1}^{p}(1 - e^{\Delta(\lambda_j + i\omega)})}{\Theta_\Delta(e^{i\omega\Delta})}\frac{b(-i\omega)}{a(-i\omega)} - \frac{e^{i\omega\Delta} - 1}{i\omega}\right] \frac{1 - e^{i\omega\Delta n}}{1 - e^{i\omega\Delta}} \\
&=: \left[h^{\Delta,1}(\omega) - h^{\Delta,2}(\omega)\right] \cdot h_n^{\Delta,3}(\omega), \quad \omega \in \mathbb{R}.
\end{aligned}$$

Due to Plancherel Theorem, we deduce

$$\begin{aligned}\operatorname{var}\left[\sum_{i=1}^{n}\bar{L}_j^{\Delta}-L_{n\Delta}\right] &= \|h_n^{\Delta}(\cdot)\|_{L^2}^2 = \frac{1}{2\pi}\int_{\mathbb{R}}|\mathcal{F}\{h_n^{\Delta}(\cdot)\}|^2(\omega)d\omega,\\ &= \frac{1}{2\pi}\int_{\mathbb{R}}\left[\left|h^{\Delta,1}\cdot h_n^{\Delta,3}(\omega)\right|^2+\left|h^{\Delta,2}\cdot h_n^{\Delta,3}(\omega)\right|^2-2\Re\left(h^{\Delta,1}\cdot\overline{h^{\Delta,2}}(\omega)\right)\left|h_n^{\Delta,3}(\omega)\right|^2\right]d\omega.\end{aligned} \tag{3.2.8}$$

It is easy to see that the first two integrals in Eq. (3.2.8) are, respectively, the variances of $\sum_{i=1}^{n}\bar{L}_j^{\Delta}$ and $L_{n\Delta}$, both equal to $n\Delta$. Setting $n:=\lfloor t/\Delta\rfloor$ yields for fixed positive t, as $\Delta\downarrow 0$,

$$\begin{aligned}\operatorname{var}\left[\sum_{i=1}^{\lfloor t/\Delta\rfloor}\bar{L}_j^{\Delta}-L_{\lfloor t/\Delta\rfloor\Delta}\right] &= 2\lfloor t/\Delta\rfloor\Delta-\frac{1}{\pi}\int_{\mathbb{R}}\Re\left(h^{\Delta,1}\cdot\overline{h^{\Delta,2}}(\omega)\right)\left|h^{\Delta,3}_{\lfloor t/\Delta\rfloor}(\omega)\right|^2d\omega\\ &= 2t(1+o(1))-\frac{1}{\pi}\int_{\mathbb{R}}\Re\left(h^{\Delta,1}\cdot\overline{h^{\Delta,2}}(\omega)\right)\left|h^{\Delta,3}_{\lfloor t/\Delta\rfloor}(\omega)\right|^2d\omega.\end{aligned}$$

Thus, in order to show Eq. (3.2.4), it remains to prove that

$$\frac{1}{\pi}\int_{\mathbb{R}}\Re\left(h^{\Delta,1}\cdot\overline{h^{\Delta,2}}(\omega)\right)\left|h^{\Delta,3}_{\lfloor t/\Delta\rfloor}(\omega)\right|^2d\omega=2t(1+o(1))\quad\text{as }\Delta\downarrow 0,$$

which in turn is equivalent to

$$\begin{aligned}\frac{1}{2\pi t}\int_{\mathbb{R}}\sigma\frac{\sqrt{\Delta}}{\sigma_\Delta}\frac{1-\cos(\omega\lfloor t/\Delta\rfloor\Delta)}{1-\cos(\omega\Delta)}\Bigg[&\frac{\sin(\omega\Delta)}{\omega}\Re\left(\frac{\prod_{j=1}^{p}(1-e^{\Delta(\lambda_j+i\omega)})}{\Theta_\Delta(e^{i\omega\Delta})}\frac{b(-i\omega)}{a(-i\omega)}\right)\\ &+\frac{1-\cos(\omega\Delta)}{\omega}\Im\left(\frac{\prod_{j=1}^{p}(1-e^{\Delta(\lambda_j+i\omega)})}{\Theta_\Delta(e^{i\omega\Delta})}\frac{b(-i\omega)}{a(-i\omega)}\right)\Bigg]d\omega=1+o(1)\quad\text{as }\Delta\downarrow 0.\end{aligned} \tag{3.2.9}$$

Now, Lemma 3.5.2 shows that the integrand in Eq. (3.2.9) converges pointwise, for every $\omega\in\mathbb{R}\backslash\{0\}$, to $2(1-\cos(\omega t))/\omega^2$ as $\Delta\downarrow 0$. Since, for sufficiently small Δ, the integrand is dominated by an integrable function (see Lemma 3.5.3), we can apply Lebesgue Dominated Convergence Theorem and deduce that the LHS of Eq. (3.2.9) converges, as $\Delta\downarrow 0$, to

$$\frac{1}{\pi t}\int_{\mathbb{R}}\frac{1-\cos(\omega t)}{\omega^2}d\omega=\frac{2}{\pi}\int_0^{\infty}\frac{1-\cos(\omega)}{\omega^2}d\omega=1.$$

This proves Eq. (3.2.9) and concludes the proof of the "if"-statement.

As to the "only if"-statement, let $J := \{j = 1, \dots, q : \ \Re(\mu_j) < 0\}$ and suppose that $|J| \geq 1$. Then we have, by (3.1.9) for $\Delta \downarrow 0$,

$$\begin{aligned}\frac{b(-i\omega)}{\Theta_\Delta(e^{i\omega\Delta})} &= \prod_{j=1}^{p-q-1} (1+\eta(\xi_j))^{-1} \prod_{j=1}^{q} \frac{\mu_j - i\omega}{1-\zeta_j\, e^{i\omega\Delta}} \\ &= \prod_{j=1}^{p-q-1} (1+\eta(\xi_j))^{-1}\, \Delta^{-q} \prod_{j\in J} \frac{\mu_j - i\omega}{-\mu_j - i\omega}(1+o(1)) \\ &= \prod_{j=1}^{p-q-1} (1+\eta(\xi_j))^{-1}\, \Delta^{-q}(1+D(\omega))(1+o(1)), \qquad \omega \in \mathbb{R}, \end{aligned} \tag{3.2.10}$$

where $D(\omega) := -1 + \prod_{j\in J}(\mu_j - i\omega)/(-\mu_j - i\omega)$. By virtue of Lemmata 3.5.2 and 3.5.3, we then obtain that the LHS of Eq. (3.2.9) converges, as $\Delta \downarrow 0$, to

$$\frac{1}{\pi t}\int_{\mathbb{R}} \frac{1-\cos(\omega t)}{\omega^2}\big(1+\Re(D(\omega))\big)\, d\omega = 1 + \frac{1}{\pi}\int_{\mathbb{R}} \frac{1-\cos(\omega)}{\omega^2}\Re(D(\omega/t))\, d\omega.$$

Since $|\prod_{j\in J}(\mu_j - i\omega)/(-\mu_j - i\omega)| = 1$, we further deduce that $\Re(D(\omega)) \leq 0$ for any $\omega \in \mathbb{R}$. Obviously, $\Re(D(\omega)) \not\equiv 0$ and hence,

$$\frac{1}{\pi t}\int_{\mathbb{R}} \frac{1-\cos(\omega t)}{\omega^2}\big(1+\Re(D(\omega))\big)\, d\omega < 1,$$

which, in turn, shows that the convergence result (3.2.4) cannot hold.

□

Remark 3.2.2. *(i) It is an easy consequence of the triangle and Hölder inequality that, if the recovery result* (3.2.4) *holds, then also*

$$\sum_{i=1}^{\lfloor t/\Delta\rfloor} \bar{L}_i^\Delta \sum_{j=\lfloor t/\Delta\rfloor+1}^{\lfloor s/\Delta\rfloor} \bar{L}_j^\Delta \xrightarrow{L^1} L_t(L_s - L_t), \quad t,s \in (0,\infty),\ t \leq s,$$

is valid.

(ii) Minor modifications of the proof above show that the recovery result in Eq. (3.2.4) *remains still valid if we drop the assumption of causality (i.e. Assumption 1 (i)) and suppose instead only $\Re(\lambda_j) \neq 0$ for every $j = 1, \dots, p$. Hence, invertibility of the* CARMA *process is necessary for the noise recovery result to hold, whereas causality is not. In the non-causal case, the obtained white noise process will not be the same as in the Wold representation* (3.2.1).

(iii) The necessity and sufficiency of the invertibility assumption descends directly from the fact that we always choose the minimum-phase spectral factor, as pointed out in Remark 3.1.1.

(iv) The proof suggests that this procedure should work in a much more general framework. Let $I^\Delta(\cdot)$ *denote the inversion filter in Eq.* (3.2.5) *and* $\psi^\Delta := \left\{\psi_i^\Delta\right\}_{i\in\mathbb{N}}$ *the coefficients in the Wold representation* (3.2.1)*. Then the proof of Theorem 3.2.1 essentially needs, apart from the rather technical Lemma 3.5.3, that, as* $\Delta \downarrow 0$*,*

$$I^\Delta(e^{i\omega\Delta})\mathcal{F}\{g(\cdot)\}(\omega) = \frac{\int_0^\infty g(s)e^{i\omega s}ds}{\sum_{k=0}^\infty \psi_k^\Delta e^{ik\omega\Delta}} \to 1, \quad \omega \in \mathbb{R}, \tag{3.2.11}$$

provided that the function $\sum_{k=0}^\infty \psi_k^\Delta z^k$ *does not have any zero inside the unit circle. In other words, we need that the discrete Fourier transform in the denominator of* (3.2.11) *converges to the Fourier transform in the numerator; this can be easily related to the kernel estimation result in* (3.2.2)*. Given the peculiar structure of* CARMA *processes, this relationship can be calculated explicitly, but the results should hold true for continuous-time moving average processes with more general kernels, too.*

We illustrate Theorem 3.2.1 and the necessity of the invertibility assumption by an example where the convergence result is established using a time domain approach. That gives an explicit result also when the invertibility assumption is violated.

Unfortunately this strategy is not viable for a general CARMA process, due to the complexity of calculations involved when $p > 2$.

Example 3.2.3 (CARMA$(2, q)$ process)**.** *The causal* CARMA$(2, q)$ *process is the strictly stationary solution to the formal stochastic differential equation*

$$\begin{aligned}(D-\lambda_2)(D-\lambda_1)Y_t &= \sigma DL_t, && q = 0,\\ (D-\lambda_2)(D-\lambda_1)Y_t &= \sigma(b+D)DL_t, && q = 1,\end{aligned}$$

and it can be represented as a continuous-time moving average process, as in (3.1.4)*, for* $\lambda_1, \lambda_2 < 0$*,* $\lambda_1 \neq \lambda_2$ *and* $b \in \mathbb{R}\backslash\{0\}$*, with kernel*

$$\begin{aligned}g(t) &= \sigma\frac{e^{t\lambda_1} - e^{t\lambda_2}}{\lambda_1 - \lambda_2}, && q = 0,\\ g(t) &= \sigma\frac{b+\lambda_1}{\lambda_1-\lambda_2}e^{t\lambda_1} + \sigma\frac{b+\lambda_2}{\lambda_2-\lambda_1}e^{t\lambda_2}, && q = 1,\end{aligned}$$

for $t > 0$ *and* 0 *elsewhere. The corresponding sampled process* $Y_n^\Delta = Y_{n\Delta}$*,* $n \in \mathbb{Z}$*, satisfies the causal and invertible* ARMA$(2, 1)$ *equations, as in* (3.1.8) *where, from* (1.2.15) *and for* $n \in \mathbb{Z}$*,*

$$\Phi_\Delta(B)Y_n^\Delta = \int_{(n-1)\Delta}^{n\Delta} g(n\Delta - u)dL_u + \int_{(n-2)\Delta}^{(n-1)\Delta} [g(n\Delta - u) - (e^{\lambda_1\Delta} + e^{\lambda_2\Delta})g((n-1)\Delta - u)]dL_u. \tag{3.2.12}$$

The corresponding MA(1) *polynomial in* (3.1.8) *is* $\Theta_\Delta(B) = 1 - \theta_\Delta B$*, with asymptotic parameters*

$$\begin{aligned} \theta_\Delta &= \sqrt{3} - 2 + o(1), \quad \sigma_\Delta^2 = \sigma^2\Delta^3(2+\sqrt{3})/6 + o(\Delta^3), && q = 0, \\ \theta_\Delta &= 1 - \operatorname{sgn}(b)\, b\, \Delta + o(\Delta), \quad \sigma_\Delta^2 = \sigma^2\Delta + o(\Delta), && q = 1. \end{aligned}$$

The inversion of (3.1.8) *and* (3.2.12) *gives, for every* $\Delta > 0$*,*

$$\begin{aligned} Z_n^\Delta =& \frac{\Phi_\Delta(B)}{\Theta_\Delta(B)} Y_n^\Delta = \sum_{i=0}^{\infty} (\theta_\Delta B)^i \prod_{i=1}^{2} (1 - e^{\lambda_i \Delta} B) Y_n^\Delta, \\ =& \int_{(n-1)\Delta}^{n\Delta} g(n\Delta - u) dL_u \\ &+ \sum_{i=0}^{\infty} \theta_\Delta^i \int_{(n-i-2)\Delta}^{(n-i-1)\Delta} [g((n-i)\Delta - u) - (e^{\lambda_1\Delta} + e^{\lambda_2\Delta} - \theta_\Delta) g((n-i-1)\Delta - u)] dL_u. \end{aligned}$$

Then $Z^\Delta := \{Z_n^\Delta\}_{n\in\mathbb{Z}}$ *is a weak white-noise process. Moreover, using that* $\Delta L_n = \int_{(n-1)\Delta}^{n\Delta} dL_s$*, we have*

$$\mathbb{E}[Z_n^\Delta\, \Delta L_{n-j}] = \begin{cases} 0, & j < 0, \\ \int_0^\Delta g(s) ds, & j = 0, \\ \theta_\Delta^{j-1} \int_0^\Delta [g(\Delta + s) - (e^{\lambda_1\Delta} + e^{\lambda_2\Delta} - \theta_\Delta) g(s)] ds, & j > 0. \end{cases} \tag{3.2.13}$$

For a fixed $t \in (0, \infty)$*, using the fact that* ΔL *and* $\bar{L}^\Delta$ *are both second order stationary white noises with variance* Δ*, we have that*

$$\begin{aligned} \mathbb{E}\left[\sum_{i=1}^{\lfloor t/\Delta \rfloor} (\bar{L}_i^\Delta - \Delta L_i)\right]^2 &= 2\lfloor t/\Delta \rfloor \Delta - 2 \sum_{i=1}^{\lfloor t/\Delta \rfloor} \mathbb{E}[\bar{L}_i^\Delta \Delta L_i] - 2 \sum_{i \neq j} \mathbb{E}[\bar{L}_i^\Delta \Delta L_j] \\ &= 2\lfloor t/\Delta \rfloor \Delta - \frac{2\sqrt{\Delta}}{\sigma_\Delta} \lfloor t/\Delta \rfloor \int_0^\Delta g(s) ds \\ &\quad - \frac{2\sqrt{\Delta}}{\sigma_\Delta} \int_0^\Delta [g(\Delta + s) - (e^{\lambda_1\Delta} + e^{\lambda_2\Delta} - \theta_\Delta) g(s)] ds \sum_{i=1}^{\lfloor t/\Delta \rfloor} \sum_{j=1}^{i-1} \theta_\Delta^{j-1} \end{aligned}$$

where the last equality is obtained using (3.2.13)*. Moreover, for every* $a \neq 1$*,*

$$\sum_{i=1}^{n} \sum_{j=1}^{i-1} a^{j-1} = \frac{a^n + (1-a)n - 1}{(1-a)^2}, \quad n \in \mathbb{N}.$$

Then the variance of the error can be explicitly calculated as

$$\mathbb{E}\left[\sum_{i=1}^{\lfloor t/\Delta\rfloor}(\bar{L}_i^\Delta - \Delta L_i)\right]^2 = 2\lfloor t/\Delta\rfloor\Delta - \frac{2\sqrt{\Delta}}{\sigma_\Delta}\lfloor t/\Delta\rfloor\int_0^\Delta g(s)ds$$
$$- \frac{2\sqrt{\Delta}}{\sigma_\Delta}\frac{\theta_\Delta{}^{\lfloor t/\Delta\rfloor} + \lfloor t/\Delta\rfloor(1-\theta_\Delta) - 1}{(1-\theta_\Delta)^2}\int_0^\Delta [g(\Delta+s) - (e^{\lambda_1\Delta} + e^{\lambda_2\Delta} - \theta_\Delta)g(s)]ds.$$

We now compute the asymptotic expansion for $\Delta \downarrow 0$ of the equation above. We obviously have that $2\lfloor t/\Delta\rfloor\Delta = 2t(1+o(1))$ and, using the explicit formulas for the kernel functions g,

	$q=0$	$q=1$
$\frac{2\sqrt{\Delta}}{\sigma_\Delta}\lfloor t/\Delta\rfloor\int_0^\Delta g(s)ds =$	$\left(3-\sqrt{3}\right)t + o(1),$	$2t + o(1),$
$\frac{2\sqrt{\Delta}}{\sigma_\Delta}\int_0^\Delta [g(\Delta+s) - (e^{\lambda_1\Delta} + e^{\lambda_2\Delta} - \theta_\Delta)g(s)]ds =$	$\left(4\sqrt{3}-6\right)\Delta(1+o(1)),$	$2(b - \operatorname{sgn}(b)\, b)\Delta^2 + o(\Delta^2),$
$(\theta_\Delta{}^{\lfloor t/\Delta\rfloor} + \lfloor t/\Delta\rfloor(1-\theta_\Delta) - 1)(1-\theta_\Delta)^{-2} =$	$\frac{1}{6}\left(3+\sqrt{3}\right)t/\Delta(1+o(1)),$	$(e^{-\operatorname{sgn}(b)bt} + \operatorname{sgn}(b)bt - 1)/(b\Delta)^2 + o(\Delta^{-2}).$

Hence, for a fixed $t \in (0,\infty)$ and $\Delta \downarrow 0$, we get

$$\mathbb{E}\left[\sum_{i=1}^{\lfloor t/\Delta\rfloor}(\bar{L}_i^\Delta - \Delta L_i)\right]^2 = \begin{cases} o(1), & q=0, \\ 2(e^{-\operatorname{sgn}(b)bt} + \operatorname{sgn}(b)bt - 1)(\operatorname{sgn}(b)-1)/b + o(1), & q=1, \end{cases}$$

i.e. (3.2.4) *holds always for $q=0$, whereas for $q=1$ if and only if $b>0$. If $b<0$, the error approximating the driving Lévy by inversion of the discretised process grows as $4t$ for large t.*

3.3. High-frequency behaviour of approximating Riemann sums

The fact that, in the sense of Eq. (3.2.3), $\bar{L}_n^\Delta \approx \Delta L_n = L_{n\Delta} - L_{(n-1)\Delta}$ for small Δ, along with Eq. (3.2.2), gives rise to the conjecture that the Wold representation Eq. (3.2.1) for Y^Δ behaves on a high-frequency time grid approximately like the MA(∞) process

$$\tilde{Y}_n^{\Delta,h} := \sum_{j=0}^{\infty} g(\Delta(j+h))\Delta L_{n-j}, \quad n \in \mathbb{Z}, \tag{3.3.1}$$

for some $h \in [0,1]$ and g is the kernel function as in (3.1.6). In other terms, we have for a CARMA process, under the assumption of invertibility and causality, that the discrete-time quantities appearing in the Wold representation approximate the quantities in Eq. (3.3.1) when $\Delta \downarrow 0$. The transfer function of Eq. (3.3.1) is then defined as

$$\psi_h^\Delta(\omega) := \sum_{j=0}^{\infty} g(\Delta(j+h))e^{-i\omega j}, \quad -\pi \le \omega \le \pi, \tag{3.3.2}$$

and its spectral density can be written as

$$\tilde{f}_h^{\Delta}(\omega) = \frac{1}{2\pi}|\psi_h^{\Delta}|^2(\omega), \quad -\pi \leq \omega \leq \pi.$$

It is well known that a CMA process can be defined (for a fixed time point t) as the L^2-limit of Eq. (3.3.1); this fact is naturally employed to easily simulate a CMA process, when all the relevant quantities are known a priori. Therefore we will name the process $\tilde{Y}^{\Delta,h}$ *approximating Riemann sum* of Eq. (3.1.4), and h is the so-called *rule* of the approximating sum; e.g. if $h = 1/2$, we have the popular *mid-point rule*.

In order to give an answer to our conjecture, we will investigate properties of the approximating Riemann sum $\tilde{Y}^{\Delta,h}$ of a CARMA process and compare its asymptotic autocovariance structure with the one of the sampled CARMA process Y^{Δ}. This will yield more insight into the role of h for the behaviour of $\tilde{Y}^{\Delta,h}$ as a process.

We start with a well known property of approximating sums.

Proposition 3.3.1. *Let g be in L^2 and Riemann-integrable. Then, for every $h \in [0,1]$, as $\Delta \downarrow 0$:*

(i) $\tilde{Y}_k^{\Delta,h} - Y_k^{\Delta} \xrightarrow{L^2} 0$, *for every* $k \in \mathbb{Z}$.

(ii) $\tilde{Y}_{\lfloor t/\Delta \rfloor}^{\Delta,h} \xrightarrow{L^2} Y_t$, *for every* $t \in \mathbb{R}$.

Proof. This follows immediately from the hypotheses made on g and the definition of L^2-integrals. □

This result essentially says only that approximating sums converge to Y_t for every fixed t. However, for a CARMA(p,q) process we have that the approximating Riemann sum process satisfies for every h and Δ an ARMA$(p,p-1)$ equation (see Proposition 3.3.2 below), meaning that there might exist a process, whose autocorrelation structure is the same as the one of the approximating sum. Given that the AR filter in this representation is the same as in Eq. (3.1.8), it is reasonable to investigate whether $\Phi_{\Delta}(B)Y^{\Delta}$ and $\Phi_{\Delta}(B)\tilde{Y}^{\Delta,h}$ have, as $\Delta \downarrow 0$, the same asymptotic autocovariance structure, which can be expected but is not granted by Proposition 3.3.1.

The following proposition gives the ARMA$(p,p-1)$ representation for the approximating Riemann sum.

Proposition 3.3.2. *Let Y be a* CARMA(p,q) *process, satisfying Assumption 1, and furthermore suppose that the roots of the autoregressive polynomial $a(\cdot)$ are distinct. Then the approximating Riemann sum process $\tilde{Y}^{\Delta,h}$ of Y defined by Eq.* (3.3.1) *satisfies, for every $h \in [0,1]$, the* ARMA$(p,p-1)$ *equation*

$$\Phi_{\Delta}(B)\tilde{Y}_n^{\Delta,h} = \sigma\tilde{\Theta}_{\Delta,h}(B)\Delta L_n, \quad n \in \mathbb{Z}, \tag{3.3.3}$$

where

$$\tilde{\Theta}_{\Delta,h}(z) := \tilde{\theta}_0^{\Delta,h} - \tilde{\theta}_1^{\Delta,h} z + - \ldots + (-1)^{p-1} \tilde{\theta}_{p-1}^{\Delta,h} z^{p-1} \tag{3.3.4}$$

and

$$\tilde{\theta}_k^{\Delta,h} := \sum_{l=1}^{p} \frac{b(\lambda_l)}{a'(\lambda_l)} e^{h\Delta\lambda_l} \sum e^{\Delta(\lambda_{j_1}+\lambda_{j_2}+\ldots+\lambda_{j_k})}, \quad k = 0, \ldots, p-1,$$

where the right-hand sum is defined to be 1 *for* $k = 0$ *and it is evaluated over all possible subsets* $\{j_1, \ldots, j_k\}$ *of* $\{1, \ldots, p\} \backslash \{l\}$*, having cardinality* k*, for* $k > 0$*.*

Proof. Write $\Phi_\Delta(z) = \prod_{j=1}^{p}(1 - e^{\Delta\lambda_j} z) = -\sum_{j=0}^{p} \phi_j^\Delta z^j$ and observe that

$$\begin{aligned}
\Phi_\Delta(B)\tilde{Y}_n^{\Delta,h} &= -\sum_{j=0}^{p} \phi_j^\Delta Y_{n-j}^{\Delta,h} \\
&= -\sigma \mathbf{b}^\top \sum_{k=0}^{p-1} \left(\sum_{j=0}^{k} \phi_j^\Delta e^{A(k-j)\Delta} \right) e^{Ah\Delta} \mathbf{e}_p \cdot \Delta L_{n-k} \\
&\qquad -\sigma \mathbf{b}^\top \sum_{j=0}^{p} \sum_{k=p-j}^{\infty} \phi_j^\Delta e^{A(h+k)\Delta} \mathbf{e}_p \cdot \Delta L_{n-j-k} \\
&= -\sigma \mathbf{b}^\top \sum_{k=0}^{p-1} \left(\sum_{j=0}^{k} \phi_j^\Delta e^{A(k-j)\Delta} \right) e^{Ah\Delta} \mathbf{e}_p \cdot \Delta L_{n-k} \\
&\qquad -\sigma \mathbf{b}^\top \sum_{k=p}^{\infty} \left(-\sum_{j=0}^{p} \phi_j^\Delta e^{-Aj\Delta} \right) e^{A(h+k)\Delta} \mathbf{e}_p \cdot \Delta L_{n-k}.
\end{aligned}$$

By virtue of the Cayley-Hamilton theorem (cf. also (Brockwell and Lindner 2009, proof of Lemma 2.1)), we have that

$$-\sum_{j=0}^{p} \phi_j^\Delta e^{-Aj\Delta} = 0,$$

and hence, $\Phi_\Delta(B)\tilde{Y}_n^{\Delta,h} = -\sigma \mathbf{b}^\top \sum_{k=0}^{p-1} \left(\sum_{j=0}^{k} \phi_j^\Delta e^{A(k-j)\Delta} \right) e^{Ah\Delta} \mathbf{e}_p \cdot \Delta L_{n-k}$. We conclude with (Fasen and Fuchs 2013, Lemma 2.1(i) and Eq. (4.4)). □

Remark 3.3.3. *(i) The approximating Riemann sum of a causal* CARMA *process is automatically a causal* ARMA *process. On the other hand, even if the* CARMA *process is invertible in the sense of Definition 2.1.1, the roots of* $\tilde{\Theta}_{\Delta,h}(\cdot)$ *may lie inside the unit circle, causing* $\tilde{Y}^{\Delta,h}$ *to be non-invertible.*

(ii) It is easy to see that $\tilde{\theta}_0^{\Delta,h} = g(h\Delta)$*. Then for* $p - q \geq 2$*, if* $h = 0$*, we have that* $\tilde{\theta}_0^{\Delta,0} = 0$*, giving that* $\tilde{\Theta}_{\Delta,0}(0) = 0$*. This is never the case for* $\Theta_\Delta(\cdot)$*, as one can*

see from (3.1.9) *and Proposition 3.1.2. Moreover, it is possible to show that for* $h = 1$ *and* $p - q \geq 2$*, the coefficient* $\tilde{\theta}_{p-1}^{\Delta,1}$ *is* 0*, implying that Eq.* (3.3.3) *is actually an* ARMA$(p, p-2)$ *equation. For those values of* h*, the* ARMA *equations solved by the approximating Riemann sums will never have the same asymptotic form as Eq.* (3.1.8)*: therefore we shall restrict ourselves to the case* $h \in (0,1)$ *from now on.*

(iii) The assumption of distinct autoregressive roots might seem restrictive, but the omitted cases can be obtained by letting distinct roots tend to each other. This would, of course, change the coefficients of the MA polynomial in Eq. (3.3.4)*. Moreover, as shown in Brockwell et al. (2013, 2012), the multiplicity of the zeroes does not matter when* L^2*-asymptotic relationships as* $\Delta \downarrow 0$ *are considered.*

Due to the complexity of retrieving the roots of a polynomial of arbitrary order from its coefficients, finding the asymptotic expression of $\tilde{\Theta}_{\Delta,h}(\cdot)$ for arbitrary p is a daunting task. Nonetheless, using Proposition 3.3.2, it is not difficult to give an answer for processes with $p \leq 3$, which are the most used in practice.

Proposition 3.3.4. *Let* $\tilde{Y}^{\Delta,h}$ *be the approximating Riemann sum for a* CARMA(p,q) *process, with* $p \leq 3$*, let Assumption 1 hold and the roots of* $a(\cdot)$ *be distinct.*

If $p = 1$*, the process* $\tilde{Y}^{\Delta,h}$ *is an* AR(1) *process driven by* $Z_n^{\Delta} = \sigma e^{\Delta h \lambda_1} \Delta L_n$*, for every* $\Delta > 0$*.*
If $p = 2, 3$*, we have*

$$\Phi_\Delta(B)\tilde{Y}_n^{\Delta,h} = \prod_{i=1}^{q}(1 - (1 - \Delta\mu_i + o(\Delta))B) \prod_{i=1}^{p-q-1}(1 - \chi_{p-q,i}(h)B)\left(\sigma\frac{(h\Delta)^{p-q-1}}{(p-q-1)!}\Delta L_n\right) \tag{3.3.5}$$

where, for $h \in (0,1)$ *and* $\Delta \downarrow 0$*,* $\chi_{2,1}(h) = (h-1)/h + o(1)$ *and*

$$\chi_{3,j}(h) = \frac{2(h-1)^2}{2(h-1)h - 1 - (-1)^j\sqrt{1 - 4(h-1)h}} + o(1), \quad j = 1, 2.$$

Proof. Since $p \leq 3$, $\tilde{\Theta}_{\Delta,h}(z)$ is a polynomial of order $p-1$ with real coefficients; therefore the roots, if any, can be calculated from the coefficients, and asymptotic expressions can be obtained by computing the Taylor expansions of the roots around $\Delta = 0$.

If $p = 1$, the statement follows directly from Eq. (3.3.3). For $p = 2, 3$, the roots of Eq. (3.3.4) are $\{1 + \Delta\mu_i + o(\Delta)\}_{i=1,\dots,q}$ and $\{1/\chi_{p-q,i}(h)\}_{i=1,\dots p-q-1}$, giving that

$$\tilde{\Theta}_{\Delta,h}(z) = \tilde{\theta}_{p-1}^{\Delta,h}\prod_{i=1}^{q}(1 + \Delta\mu_i + o(\Delta) - z)\prod_{i=1}^{p-q-1}(1/\chi_{p-q,i}(h) - z), \quad z \in \mathbb{C}.$$

Vieta theorem gives that the product of the roots of Eq. (3.3.4) is equal to $\tilde{\theta}_0^{\Delta,h}/\tilde{\theta}_{p-1}^{\Delta,h}$, which yields

$$\tilde{\Theta}_{\Delta,h}(z) = \tilde{\theta}_0^{\Delta,h} \prod_{i=1}^{q}(1-(1-\Delta\mu_i+o(\Delta))z) \prod_{i=1}^{p-q-1}(1-\chi_{p-q,i}(h)z).$$

Since $\tilde{\theta}_0^{\Delta,h} = g(h\Delta) = \sigma(h\Delta)^{p-q-1}/(p-q-1)!(1+o(1))$, we have established the result. □

In general the autocorrelation structure will depend on h through the parameters $\chi_{p-q,i}(h)$, $i = 1, \ldots, p-q-1$. In a time-series context, it is reasonable to require that the approximating Riemann sum process has the same asymptotic autocorrelation structure as the CARMA process we want to approximate.

Corollary 3.3.5. *Let the assumptions of Proposition 3.3.4 hold. Then* $\Phi_\Delta(B)Y^\Delta$ *and* $\Phi_\Delta(B)\tilde{Y}^{\Delta,h}$ *have the same asymptotic autocovariance structure as* $\Delta \downarrow 0$

$$\begin{aligned} &\text{for every } h \in (0,1), && \text{if } p-q=1,\\ &\text{for } h = (3\pm\sqrt{3})/6, && \text{if } p-q=2,\\ &\text{and for } h = \left(15 \pm \sqrt{225-30\sqrt{30}}\right)/30, && \text{if } p-q=3. \end{aligned}$$

Moreover, the MA *polynomials in Eqs.* (3.1.9) *and* (3.3.5) *coincide if and only if the* CARMA *process is invertible and* $|\chi_{p-q,i}(h)| < 1$*, that is*

$$\begin{aligned} &\text{for every } h \in (0,1), && \text{if } p-q=1,\\ &\text{for } h = (3+\sqrt{3})/6, && \text{if } p-q=2. \end{aligned}$$

For $p-q=3$*, such* h *does not exist.*

Proof. The claim for $p-q=1$ follows immediately from Proposition 3.3.4 and Eqs. (3.1.9)-(3.1.10). For $p=2$ and $q=0$, we have to solve the spectral factorization problem

$$\begin{aligned} \sigma_\Delta^2(1+\eta(\xi_1)^2) &= \sigma^2\Delta^3(1+\chi_{2,1}(h)^2)h^2\\ \sigma_\Delta^2\eta(\xi_1) &= -\sigma^2\Delta^3\chi_{2,1}(h)h^2 \end{aligned}$$

with $\eta(\xi_1) = 2-\sqrt{3}+o(1)$ and $\chi_{2,1}(h) = (h-1)/h+o(1)$. Eq. (3.1.10) then yields the two solutions $h = (3\pm\sqrt{3})/6$. For $p=3$ and $q=1$, analogous calculations lead to the same solutions. Finally, consider the case $p=3$ and $q=0$. We have to solve asymptotically the following system of equations

$$\begin{aligned} \sigma_\Delta^2(1+(\eta(\xi_1)+\eta(\xi_2))^2+\eta(\xi_1)^2\eta(\xi_2)^2) &= \frac{\sigma^2\Delta^5}{4}(1+(\chi_{3,1}(h)+\chi_{3,2}(h))^2+\chi_{3,1}(h)^2\chi_{3,2}(h)^2)h^4\\ \sigma_\Delta^2(\eta(\xi_1)+\eta(\xi_2))(1+\eta(\xi_1)\eta(\xi_2)) &= -\frac{\sigma^2\Delta^5}{4}(\chi_{3,1}(h)+\chi_{3,2}(h))(1+\chi_{3,1}(h)\chi_{3,2}(h))h^4\\ \sigma_\Delta^2\eta(\xi_1)\eta(\xi_2) &= \frac{\sigma^2\Delta^5}{4}\chi_{3,1}(h)\chi_{3,2}(h)h^4 \end{aligned}$$

where $\eta(\xi_{1,2}) = \left(13 \pm \sqrt{105} - \sqrt{270 \pm 26\sqrt{105}}\right)/2 + o(1)$ and $\chi_{3,1}(h)$ and $\chi_{3,2}(h)$ are as in Proposition 3.3.4. Solving that system for h gives the claimed values.

To prove the second part of the Corollary, we start observing that, under the assumption of an invertible CARMA process, the coefficients depending on μ_i will coincide automatically, if any. Then it remains to check whether the coefficients depending on h can be smaller than 1 in absolute value. The cases $p - q = 1, 2$ follow immediately. Moreover, to see that there is no such h for $p - q = 3$, it is enough to notice that, for $h \in (0, 1)$, $|\chi_{3,1}(h)| > 1$ and $0 < |\chi_{3,2}(h)| < 1$, i.e. they do never satisfy the sought requirement for $h \in (0, 1)$. □

Corollary 3.3.5 can be interpreted as a criterion to choose an h such that the Riemann sum approximates the continuous-time process Y in a stronger sense than the simple convergence as a random variable for every fixed t. The second part of the corollary says that there is an even more restrictive way to choose h such that Eqs. (3.1.9) and (3.3.5) will coincide. If the two processes satisfy asymptotically the same causal and invertible ARMA equation, they will have the same coefficients in their Wold representations as $\Delta \downarrow 0$, which are given in the case of the approximating Riemann sum explicitly by definition in (3.3.1).

In the light of (3.2.2) and Theorem 3.2.1, the sampled CARMA process will asymptotically behave like its approximating Riemann sum process for some specific $h = \bar{h}$, which might not even exist, as in the case $p = 3$, $q = 0$. However, if such an $\bar{h}$ exists, the kernel estimators (3.2.2) can be improved to

$$\frac{\sigma_\Delta}{\sqrt{\Delta}} \psi^\Delta_{\lfloor t/\Delta \rfloor} = g(\Delta(\lfloor t/\Delta \rfloor + \bar{h})) + o(\Delta), \quad t \in \mathbb{R}.$$

For invertible CARMA(p, q) processes with $p - q = 1$, any choice of h would accomplish that. In principle an $\bar{h}$ can be found matching a higher order expansion in Δ, where higher order terms will depend on h.

For $p - q = 2$, there is only a specific value $h = \bar{h} := (3 + \sqrt{3})/6$, such that $\tilde{Y}^{\Delta,\bar{h}}$ behaves as Y^Δ in this particular sense, and therefore it advocates for a unique, optimal value for, e.g., simulation purposes.

Finally, for $p - q = 3$, a similar value does not exist, meaning that it is not possible to mimic Y^Δ in this sense with any approximating Riemann sum.

In order to confirm this, we now give a small numerical study. We consider three different causal and invertible processes, a CARMA(2, 1), a CAR(2) and a CAR(3) process, with parameters $\lambda_1 = -0.7$, $\lambda_2 = -1.2$, $\lambda_3 = -2.6$ and $\mu_1 = 3$. Of course, for the CARMA(2, 1) we use only λ_1, λ_2 and μ_1, while for the CAR processes there is no need for μ_1. Then we estimate the kernel functions from the theoretical autocorrelation functions using (3.2.2) as in Chapter 2, for moderately high sampling rates, namely $2^2 = 4$ (Figure 3.1) and $2^6 = 64$ samplings per unit of time (Figure 3.2). In order to see where the kernel is being estimated, we plot the kernel estimations on different grids. The small circles denote the

extremal cases $h = 0$ and $h = 1$, the vertical sign the mid-point rule $h = 0.5$, and the diamond and the square are the values given in Corollary 3.3.5, if any. The true kernel function is then plotted with a solid, continuous line. For the sake of clarity, only the first 8 estimates are plotted.

For the CARMA$(2, 1)$ process, the kernel estimation seems to follow a mid-point rule (i.e. $h = 1/2$). For the CAR(2) process, the predicted value $\bar{h} = (3+\sqrt{3})/6$ (denoted with squares) is definitely the correct one, and for the CAR(3) for every $h \in [0, 1]$ the estimation is close but constantly biased. Of course in the limit $\Delta \downarrow 0$, the slightly weaker results given by Eq. (3.2.2) still hold, giving that the bias vanishes in the limit. The conclusion expressed above is true for both considered sampling rates, which is remarkable since they are only moderately high, in comparison with the chosen parameters.

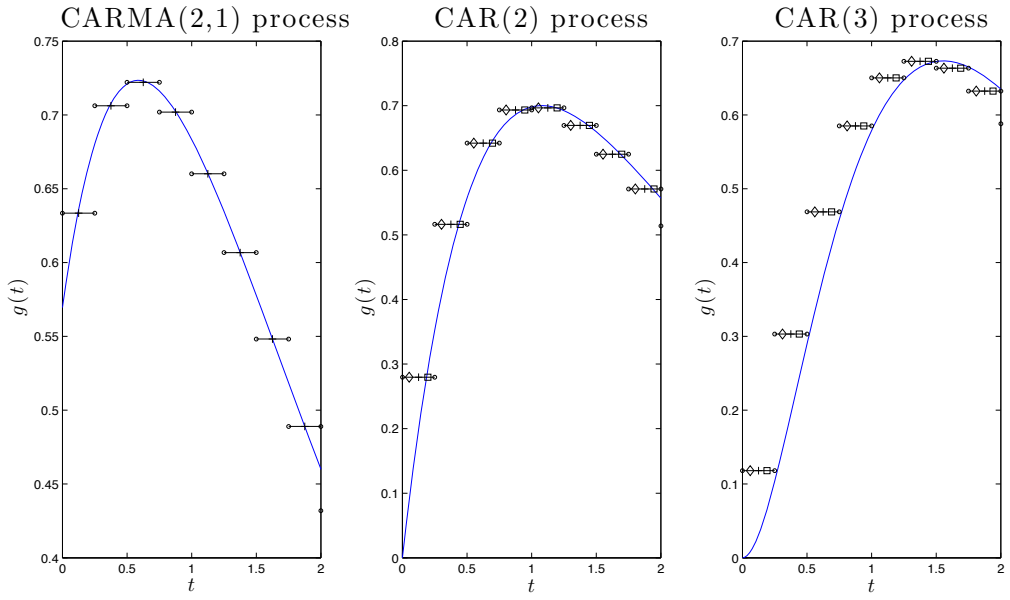

Figure 3.1.: Kernel estimation for a sampling frequency of 2^2 samplings per unit of time, i.e. $\Delta = 0.25$. The diamond and the square symbols denote, where available, the values of h suggested by Corollary 3.3.5.

3.4. Conclusion

In this Chapter we have dealt with the asymptotic behaviour of two classes of discrete-time processes closely related to the one of CARMA processes, when the sampling frequency tends to infinity.

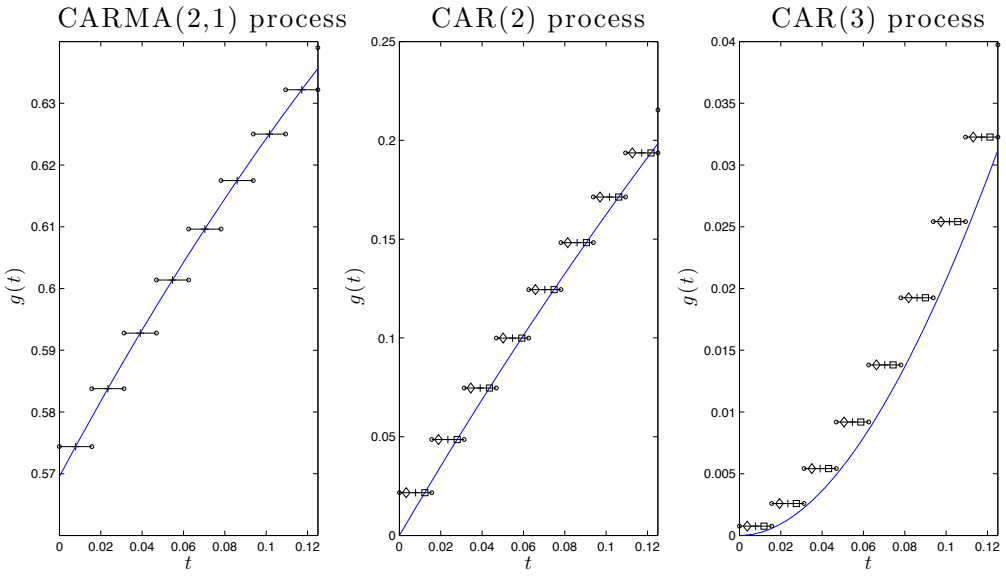

Figure 3.2.: Kernel estimation for a sampling frequency of 2^6 samplings per unit of time, i.e. $\Delta \approx 0.016$. The diamond and the square symbols denote, where available, the values of h suggested by Corollary 3.3.5.

First, we studied the behaviour of the white noise appearing in the ARMA equation solved by the sampled sequence of a CARMA process of arbitrary order. Then we showed, under a necessary and sufficient identifiability condition, that the aforementioned white noise approximates the increments of the driving Lévy process of the continuous-time model. The proposed procedure is non-parametric in nature, and it can be applied without assuming any knowledge on the order of the process. Moreover, it is argued that such results should be extendable to CMA processes with more general kernel functions. This is left for future research.

The results in the first part of this Chapter, considered jointly with those in Brockwell et al. (2013), show that the Wold representation of a sampled causal and invertible CARMA process behaves somehow like a Riemann sum as $\Delta \downarrow 0$. Then in the second part of this Chapter the converse is investigated, i.e. whether a Riemann sum approximating a causal CARMA process satisfies the same ARMA$(p, p-1)$ equation of the process we want to approximate, as the spacing of the grid tends to zero. This is in particular important for simulations, where such approximating Riemann sums constitute a natural choice.

It has been shown that these processes satisfy an ARMA$(p, p-1)$ equation, but in general they are not invertible. For $p \leq 3$, the roots of the moving average polynomial of such discrete-time processes depend, apart from the roots of $b(\cdot)$, also on the rule h. Moreover, in the case $p = 3$, $q = 0$, the Riemann sum is invertible for no choice of h, implying that the Riemann sum and the sampled process will never satisfy asymptotically

the same causal and invertible ARMA equation. Although only a finite number of cases has been considered, it shows that in general a causal and invertible CARMA process cannot be approximated by a Riemann sum, at least not in the sense of the second part of Corollary 3.3.5. Further investigations on this matter are left for future research.

3.5. Auxiliary Results

Throughout this section, we shall use the same notation as in the preceding sections.

Proposition 3.5.1. *The function $\alpha_n(x)$, as defined in Eq. (3.1.12), has the form*

$$\alpha_n(x) = \frac{1}{(2n+1)!}\frac{P_n(x)}{x^{n+1}}, \quad x \neq 0,\ n \in \mathbb{N}, \tag{3.5.1}$$

where $P_n(x)$ is a polynomial of order n in x, namely

$$\begin{aligned} P_n(x) =& \sum_{j=0}^{n} x^{n-j} \sum_{k=j+1}^{n} (2k)! \left\{ {2n+1 \atop 2k} \right\} \sum_{i=j}^{k} \left[\binom{i+1}{j+1}\binom{2k}{2i+1} - \binom{i}{j+1}\binom{2k}{2i} \right] (-2)^{j+1-2k} \\ &+ \sum_{j=0}^{n} x^{n-j} \sum_{k=j}^{n} (2k+1)! \left\{ {2n+1 \atop 2k+1} \right\} \sum_{i=j}^{k} \left[\binom{i+1}{j+1}\binom{2k+1}{2i+1} - \binom{i}{j+1}\binom{2k+1}{2i} \right] (-2)^{j-2k}, \end{aligned} \tag{3.5.2}$$

with $\left\{ {\cdot \atop \cdot} \right\}$ being the Stirling number of the second kind. Moreover, all the zeroes of $\alpha_n(x)$ are real, distinct and greater than 2.

Proof. Using the definition of the hyperbolic functions, we can write

$$\frac{\sinh(z)}{\cosh(z) - 1 + x} = \frac{e^{2z} - 1}{e^{2z} + 1 + 2(x-1)e^{z}} =: f(z,x), \quad z \in \mathbb{C}, \quad x \neq 0,$$

i.e. $f(z,x) = g(e^z, x)$, where $g(y,x) := (y^2-1)/(y^2+1+2(x-1)y)$. Then the n-th derivative of the function $f(\cdot, x)$ is, by the Faà di Bruno formula

$$\frac{\partial^n}{\partial z^n} f(z,x) = \frac{\partial^n}{\partial z^n} g(e^z, x) = \sum_{k=1}^{n} \left\{ {n \atop k} \right\} \frac{\partial^k}{\partial y^k} g(y,x) \bigg|_{y=e^z} e^{kz}, \quad z \in \mathbb{C}, \quad x \neq 0,$$

where the coefficients $\left\{ {n \atop k} \right\}$ are the Stirling numbers of the second kind. Using the previous formula and the definition of $\alpha_n(x)$, for $x \neq 0$,

$$\begin{aligned} (2n+1)!\alpha_n(x) &= \frac{\partial^{2n+1}}{\partial z^{2n+1}} f(z,x) \bigg|_{z=0} = \sum_{k=1}^{2n+1} \left\{ {2n+1 \atop k} \right\} \frac{\partial^k}{\partial y^k} g(y,x) \bigg|_{y=1} \\ &= \sum_{k=1}^{2n+1} k! \left\{ {2n+1 \atop k} \right\} \frac{1}{2\pi i} \int_{\rho} \frac{(z-1)(z+1)}{(z-a_2(x))(z-a_1(x))(z-1)^{k+1}} dz \\ &= \sum_{k=1}^{2n+1} k! \left\{ {2n+1 \atop k} \right\} \frac{1}{2\pi i} \int_{\rho} \frac{z+1}{(z-a_2(x))(z-a_1(x))(z-1)^{k}} dz \end{aligned} \tag{3.5.3}$$

where the latter equality comes from the Cauchy differentiation formula, $a_1(x) = 1 - x - \sqrt{x(x-2)}$, $a_2(x) = 1 - x + \sqrt{x(x-2)}$, i.e. they are the roots of the polynomial $y^2 + 1 + 2(x-1)y$, and ρ is a counter-clockwise oriented closed curve in the complex plane encircling $z = 1$. The case $x = 0$ has been excluded because $f(\cdot, 0)$ is not defined in $z = 0$, and $\lim_{z\to 0} |f(z, 0)| = \infty$.

Let us denote the integrand in Eq. (3.5.3) by $f_k(z, x)$; it is a rational function having one pole of order k in $z = 1$. Moreover, there are two simple poles in $z = a_1(x)$ and $z = a_2(x)$ if $x \neq 2$, or just a simple one in $z = -1$ if $x = 2$, due to cancellation with the zero at $z = -1$ in the numerator. The case $x = 2$ can be also obtained by letting the difference between $a_1(x)$ and $a_2(x)$ tend to zero in the upcoming calculations and is therefore not treated by itself.

Then by the Cauchy theorem of residues, Theorem 1, p. 24 of Mitrinović and Kečkić (1984), we have that the integral in Eq. (3.5.3) is, for $x \neq 0, 2$,

$$\frac{1}{2\pi i}\int_\rho f_k(z,x)dz = \mathrm{Res}_{z=1} f_k(z,x) = -\mathrm{Res}_{z=a_1(x)} f_k(z,x) - \mathrm{Res}_{z=a_2(x)} f_k(z,x) - \mathrm{Res}_{z=\infty} f_k(z,x),$$

where the latter identity is obtained using Theorem 2, p. 25 of Mitrinović and Kečkić (1984). Moreover, since the difference of orders between the polynomials in the denominator and in the numerator of $f_k(z, x)$ is $k + 1 > 1$, the residue at infinity is always zero (Section 3.1.2.3, pp. 27-28, Mitrinović and Kečkić (1984)). For $x \neq 0, 2$, we have that $z = a_1(x)$ and $z = a_2(x)$ are simple poles, yielding

$$\begin{aligned}
\frac{1}{2\pi i}\int_\rho f_k(z,x)dz =& \frac{1 + a_1(x)}{(a_1(x)-1)^k(a_2(x)-a_1(x))} - \frac{1 + a_2(x)}{(a_2(x)-1)^k(a_2(x)-a_1(x))} \\
=& (2x)^{-k}\sum_{i=0}^{\lfloor k/2\rfloor}\left[2\binom{k}{2i+1}(-x)^{-1} + \binom{k}{2i+1} - \binom{k}{2i}\right](-x)^{k-2i}(x(x-2))^i \\
=& \sum_{j=0}^{\lfloor k/2\rfloor - 1}\sum_{i=j}^{\lfloor k/2\rfloor}\left[\binom{i+1}{j+1}\binom{k}{2i+1} - \binom{i}{j+1}\binom{k}{2i}\right](-2)^{j+1-k}x^{-j-1} \\
&+ (k \bmod 2)(-2)^{\lfloor k/2\rfloor + 1 - k}x^{-\lfloor k/2\rfloor - 1};
\end{aligned} \tag{3.5.4}$$

where the last equality is obtained by using the Binomial theorem. Plugging Eq. (3.5.4) in Eq. (3.5.3), and dividing the outermost sum in odd and even k, we get, still for $x \neq 0, 2$,

$$\begin{aligned}
&(2n+1)!\,\alpha_n(x) \\
&= \sum_{k=1}^{n}\sum_{j=0}^{k-1}\sum_{i=j}^{k}(2k)!\left\{{2n+1 \atop 2k}\right\}\left[\binom{i+1}{j+1}\binom{2k}{2i+1} - \binom{i}{j+1}\binom{2k}{2i}\right](-2)^{j+1-2k}x^{-j-1} \\
&+ \sum_{k=0}^{n}\sum_{j=0}^{k-1}\sum_{i=j}^{k}(2k+1)!\left\{{2n+1 \atop 2k+1}\right\}\left[\binom{i+1}{j+1}\binom{2k+1}{2i+1} - \binom{i}{j+1}\binom{2k+1}{2i}\right](-2)^{j-2k}x^{-j-1} \\
&+ \sum_{k=0}^{n}(2k+1)!\left\{{2n+1 \atop 2k+1}\right\}(-2)^{-k}x^{-k-1}.
\end{aligned}$$

Then Eq. (3.5.1) can be obtained by merging the last two lines and rearranging the indices.

Using Eq. (3.5.2), we easily see that, for $P_n(x) = p_0 + p_1 x + \ldots + p_n x^n$,

$$p_0 = (-2)^{-n}(2n+1)!, \quad p_n = 1, \tag{3.5.5}$$

i.e. $P_n(x)$ will have n, potentially complex, roots, and they can not be zero. Moreover it is easy to verify that $f(z,x)$ solves the mixed partial differential equation

$$\frac{\partial^2}{\partial z^2} f(z,x) = \left[(x-1)\frac{\partial}{\partial x} + x(x-2)\frac{\partial^2}{\partial x^2}\right] f(z,x), \quad z \in \mathbb{C},\ x \neq 0. \tag{3.5.6}$$

Then we take $2n-1$, $n \in \mathbb{N}$, derivatives in z on both sides of Eq. (3.5.6); invoking the Schwarz theorem, the product rule for the derivatives and evaluating the resulting expression at $z = 0$, we obtain that the function $\alpha_n(x)$ is given by recursion, for $x \notin (0,2)$,

$$\begin{aligned} (2n+3)\,(2n+1)\,\alpha_{n+1}(x) &= \sqrt{x(x-2)}\frac{\partial}{\partial x}\left[\sqrt{x(x-2)}\frac{\partial}{\partial x}\alpha_n(x)\right], \\ \alpha_0(x) &= 1/x. \end{aligned} \tag{3.5.7}$$

We now prove by induction the claim regarding the roots being real, distinct and greater than 2. The cases $\alpha_0(x) = 1/x$ and $6\alpha_1(x) = (x-3)/x^2$ have respectively no and one zero, so the claim can only be partially verified; then we start from $\alpha_2(x) = (30 - 15x + x^2)/(120x^3)$, whose zeros are $\xi_{2,1} = 1/2\left(15 - \sqrt{105}\right) \approx 2.37652$, $\xi_{2,2} = 1/2\left(15 + \sqrt{105}\right) \approx 12.6235$, and they satisfy the claim. We now assume that the claim holds for $\alpha_n(x)$, $n \geq 2$, and its zeros are $2 < \xi_{n,1} < \xi_{n,2} < \ldots < \xi_{n,n}$.

The derivative of $\alpha_n(x)$ is of the form $Q_n(x)/x^{n+2}$, where $(2n+1)!Q_n(x) = x\frac{\partial}{\partial x}P_n(x) - (1+n)P_n(x)$. By Rolle theorem, $Q_n(x)$ has $n-1$ real roots $\chi_{n,i}$, $i = 1, \ldots, n-1$, such that $2 < \xi_{n,1} < \chi_{n,1} < \xi_{n,2} < \chi_{n,2} < \ldots < \chi_{n,n-1} < \xi_{n,n}$. Using the product rule and the value of the coefficients in Eq. (3.5.5), we get

$$\frac{\partial}{\partial x}\alpha_n(x) \sim -x^{-2}/(2n+1)! \to 0, \quad x \to \infty. \tag{3.5.8}$$

Again by Rolle theorem, since $\frac{\partial}{\partial x}\alpha_n(x) \to 0$ and $\alpha_n(x) \to 0$ as $x \to \infty$, $Q_n(x)$ has a zero at some point $\xi_{n,n} < \chi_{n,n} < \infty$. For $x \geq 2$, the function $\sqrt{x(x-2)}\frac{\partial}{\partial x}\alpha_n(x)$ is well defined and it is zero for $x = 2$ and $x = \chi_{n,i}, i = 1, \ldots, n$. With the same arguments as before, we then obtain that $\frac{\partial}{\partial x}[\sqrt{x(x-2)}\frac{\partial}{\partial x}\alpha_n(x)]$ is zero for $x = \xi_{n+1,i}$, $i = 1, \ldots, n+1$, where $2 < \xi_{n+1,1} < \chi_{n,1} < \xi_{n+1,2} < \chi_{n,2} < \ldots < \chi_{n,n} < \xi_{n+1,n+1} < \infty$. Then by Eq. (3.5.7), those zeros are also roots of, respectively, $\alpha_{n+1}(x)$ and $P_{n+1}(x)$. Since $P_{n+1}(x)$ is a polynomial of order $n+1$, it can have only $n+1$ roots, which were already found. Moreover, they are all real, distinct and strictly greater than 2, and the claim is proven. □

Lemma 3.5.2. *Suppose that* $\Re(\mu_j) \neq 0$ *for all* $j = 1, \dots, q$. *Then we have, for any* $t \in (0, \infty)$ *and* $\omega \in \mathbb{R}\backslash\{0\}$,

$$\lim_{\Delta \downarrow 0} \sigma \frac{\sqrt{\Delta}}{\sigma_\Delta} \frac{1 - \cos(\omega \lfloor t/\Delta \rfloor \Delta)}{\omega} \frac{\sin(\omega\Delta)}{1 - \cos(\omega\Delta)} \Re\left(\frac{\prod_{j=1}^p (1 - e^{\Delta(\lambda_j + i\omega)})}{\Theta_\Delta(e^{i\omega\Delta})} \frac{b(-i\omega)}{a(-i\omega)} \right) = \frac{2 - 2\cos(\omega t)}{\omega^2} \big(1 + \Re(D(\omega))\big)$$

and

$$\lim_{\Delta \downarrow 0} \sigma \frac{\sqrt{\Delta}}{\sigma_\Delta} \frac{1 - \cos(\omega \lfloor t/\Delta \rfloor \Delta)}{\omega} \Im\left(\frac{\prod_{j=1}^p (1 - e^{\Delta(\lambda_j + i\omega)})}{\Theta_\Delta(e^{i\omega\Delta})} \frac{b(-i\omega)}{a(-i\omega)} \right) = 0,$$

where $D(\omega) := -1 + \prod_{j \in J} (\mu_j - i\omega)/(-\mu_j - i\omega)$ *and* $J := \{j = 1, \dots, q : \ \Re(\mu_j) < 0\}$. *Obviously, if* $\Re(\mu_j) > 0$ *for all* $j = 1, \dots, q$, *then* $D(\omega) = 0$ *for all* $\omega \in \mathbb{R}$.

Proof. By Proposition 3.1.2, we have that $\eta(\xi_j) \in (0, 1)$ for sufficiently small Δ. Hence, for any $\omega \in \mathbb{R}$,

$$\begin{aligned} \frac{\prod_{j=1}^p (1 - e^{\Delta(\lambda_j + i\omega)})}{\Theta_\Delta(e^{i\omega\Delta})} \frac{b(-i\omega)}{a(-i\omega)} &= \frac{1}{\prod_{j=1}^{p-q-1} (1 + \eta(\xi_j) e^{i\omega\Delta})} \prod_{j=1}^p \frac{e^{\Delta(\lambda_j + i\omega)} - 1}{i\omega + \lambda_j} \prod_{j=1}^q \frac{\mu_j - i\omega}{1 - \zeta_j e^{i\omega\Delta}} \\ &= \Delta^{p-q} (1 + D(\omega)) \prod_{j=1}^{p-q-1} (1 + \eta(\xi_j))^{-1} \cdot (1 + o(1)) \quad \text{as } \Delta \downarrow 0. \end{aligned}$$

Moreover, using Eq. (3.1.10), we obtain

$$\sigma \frac{\sqrt{\Delta}}{\sigma_\Delta} = \frac{\sqrt{[2(p-q)-1]! \cdot \prod_{j=1}^{p-q-1} \eta(\xi_j)}}{\Delta^{p-q-1}} (1 + o(1)) \quad \text{as } \Delta \downarrow 0.$$

Since $\cos(\omega \lfloor t/\Delta \rfloor \Delta) \to \cos(\omega t)$ and $\Delta \sin(\omega\Delta)/(1 - \cos(\omega\Delta)) \to 2/\omega$ as $\Delta \downarrow 0$ for any $\omega \in \mathbb{R}\backslash\{0\}$, we can use the equality (cf. (Brockwell et al. 2013, proof of Theorem 3.2))

$$\frac{\sqrt{[2(p-q)-1]! \cdot \prod_{j=1}^{p-q-1} \eta(\xi_j)}}{\prod_{j=1}^{p-q-1} (1 + \eta(\xi_j))} = \frac{\prod_{j=1}^{p-q-1} |1 + \eta(\xi_j)|}{\prod_{j=1}^{p-q-1} (1 + \eta(\xi_j))} \cdot (1 + o(1)) = 1 + o(1) \quad \text{as } \Delta \downarrow 0$$

to conclude the proof. □

Lemma 3.5.3. *Suppose that* $t \in (0, \infty)$ *and* $\Re(\mu_j) \neq 0$ *for all* $j = 1, \dots, q$, *and let the functions* $h^{\Delta,1}(\cdot), h^{\Delta,2}(\cdot)$ *and* $h^{\Delta,3}_{\lfloor t/\Delta \rfloor}(\cdot)$ *be defined as in the proof of Theorem 3.2.1. Then there is a* $C > 0$ *such that, for any* $\omega \in \mathbb{R}$ *and any sufficiently small* Δ,

$$\left| 2\Re\left(h^{\Delta,1} \cdot h^{\Delta,3}_{\lfloor t/\Delta \rfloor}(\omega) \cdot \overline{h^{\Delta,2} \cdot h^{\Delta,3}_{\lfloor t/\Delta \rfloor}(\omega)} \right) \right| \leq h(\omega),$$

where $h(\omega) := \big(7^{2p}/2^{2p+q} + 1\big) t^2 \mathbf{1}_{(-1,1)}(\omega) + C\omega^{-2} \mathbf{1}_{\mathbb{R}\backslash(-1,1)}(\omega)$. *Moreover,* h *is integrable over the real line.*

Proof. We obviously have

$$\left|2\Re\left(h^{\Delta,1}\cdot h^{\Delta,3}_{\lfloor t/\Delta\rfloor}(\omega)\cdot\overline{h^{\Delta,2}\cdot h^{\Delta,3}_{\lfloor t/\Delta\rfloor}(\omega)}\right)\right|\leq\left|h^{\Delta,1}\cdot h^{\Delta,3}_{\lfloor t/\Delta\rfloor}(\omega)\right|^2+\left|h^{\Delta,2}\cdot h^{\Delta,3}_{\lfloor t/\Delta\rfloor}(\omega)\right|^2 \tag{3.5.9}$$

for any $\omega\in\mathbb{R}$ and any Δ. Let us first consider the second addend on the RHS of Eq. (3.5.9).

We obtain $|h^{\Delta,2}\cdot h^{\Delta,3}_{\lfloor t/\Delta\rfloor}(\omega)|^2=2(1-\cos(\omega\lfloor t/\Delta\rfloor\Delta))/\omega^2$ and since $\lfloor t/\Delta\rfloor\Delta\leq t$ holds, we can bound, for any Δ, the latter function by t^2 on the interval $(-1,1)$ and by $4/\omega^2$ on $\mathbb{R}\backslash(-1,1)$.

As to the first addend on the RHS of Eq. (3.5.9), we calculate

$$\left|h^{\Delta,1}\cdot h^{\Delta,3}_{\lfloor t/\Delta\rfloor}(\omega)\right|^2=\sigma^2\frac{\Delta}{\sigma_\Delta^2}\frac{\prod_{j=1}^p\left|1-e^{\Delta(\lambda_j+i\omega)}\right|^2}{\left|\Theta_\Delta(e^{i\omega\Delta})\right|^2}\frac{|b(-i\omega)|^2}{|a(-i\omega)|^2}\cdot\frac{1-\cos(\omega\lfloor t/\Delta\rfloor\Delta)}{1-\cos(\omega\Delta)}. \tag{3.5.10}$$

Let now $|\omega|<1$ and suppose that Δ is sufficiently small, i.e. the following inequalities will be true for any $|\omega|<1$ whenever Δ is sufficiently small. Using $|1-e^z|\leq 7/4|z|$ for $|z|<1$ (see, e.g., (Abramowitz and Stegun 1974, 4.2.38)) yields

$$\frac{\prod_{j=1}^p\left|1-e^{\Delta(\lambda_j+i\omega)}\right|^2}{|a(-i\omega)|^2}\leq\left(\frac{7}{4}\Delta\right)^{2p}.$$

Then, $(1-\cos(\omega\Delta))/(\omega\Delta)^2\geq 1/4$ together with $4(1-\cos(\omega\lfloor t/\Delta\rfloor\Delta))/\omega^2\leq 2t^2$ (see above) implies

$$\frac{1-\cos(\omega\lfloor t/\Delta\rfloor\Delta)}{1-\cos(\omega\Delta)}\leq 2\left(\frac{t}{\Delta}\right)^2.$$

As in the proof of Lemma 3.5.2 we write $\Theta_\Delta(z)=\prod_{j=1}^{p-q-1}(1+\eta(\xi_j)z)\cdot\prod_{j=1}^q(1-\zeta_j z)$, where $\zeta_j=1-\operatorname{sgn}(\Re(\mu_j))\,\mu_j\,\Delta+o(\Delta)$ (see Chapter 2, Theorem 2.1). Since $\prod_{j=1}^q\left(\left|1-\zeta_j e^{i\omega\Delta}\right|/\Delta\right)^2\geq\prod_{j=1}^q 1/2\left|\operatorname{sgn}(\Re(\mu_j))\,\mu_j-i\omega\right|^2$, we further deduce

$$\frac{|b(-i\omega)|^2}{\prod_{j=1}^q|1-\zeta_j e^{i\omega\Delta}|^2}\leq\frac{2^q}{\Delta^{2q}}.$$

Again due to Eq. (3.1.10), we obtain

$$\sigma^2\frac{\Delta}{\sigma_\Delta^2}\prod_{j=1}^{p-q-1}\left|1+\eta(\xi_j)e^{i\omega\Delta}\right|^{-2}\leq\frac{2\cdot[2(p-q)-1]!}{\Delta^{2(p-q-1)}}\prod_{j=1}^{p-q-1}\frac{|\eta(\xi_j)|}{|1+\eta(\xi_j)e^{i\omega\Delta}|^2}$$

and since $|\eta(\xi_j)|<1$ for all j (see Proposition 3.1.2) we also have that $|1+\eta(\xi_j)e^{i\omega\Delta}|\geq\frac{1}{2}|1+\eta(\xi_j)|$ for all j, resulting in

$$\sigma^2\frac{\Delta}{\sigma_\Delta^2}\prod_{j=1}^{p-q-1}\left|1+\eta(\xi_j)e^{i\omega\Delta}\right|^{-2}\leq\frac{2^{2(p-q)-1}}{\Delta^{2(p-q-1)}}\cdot[2(p-q)-1]!\prod_{j=1}^{p-q-1}\frac{|\eta(\xi_j)|}{|1+\eta(\xi_j)|^2}=\frac{2^{2(p-q)-1}}{\Delta^{2(p-q-1)}}$$

where the latter equality follows from (Brockwell et al. 2013, proof of Theorem 3.2). All together the RHS of Eq. (3.5.10) can be bounded for any $|\omega| < 1$ and any sufficiently small Δ by $(7/2)^{2p}\, 2^{-q} t^2$.

It remains to bound the RHS of Eq. (3.5.10) also for $|\omega| \geq 1$. Hence, for the rest of the proof let us suppose $|\omega| \geq 1$ and in addition we assume again that Δ is sufficiently small in order that all the following inequalities hold. We are going to show that

$$\sigma^2 \frac{\Delta}{\sigma_\Delta^2} \frac{\prod_{j=1}^{p} \left|1 - e^{\Delta(\lambda_j + i\omega)}\right|^2}{\left|\Theta_\Delta(e^{i\omega\Delta})\right|^2} \frac{|b(-i\omega)|^2}{|a(-i\omega)|^2} \frac{1 - \cos(\omega \lfloor t/\Delta \rfloor \Delta)}{1 - \cos(\omega\Delta)} \leq \frac{C}{\omega^2}$$

for some $C > 0$. Since $\left|\sigma^2\Delta/\sigma_\Delta^2\right| \leq \text{const.} \cdot \left|\Delta^2/\Delta^{2(p-q)}\right|$ (see (3.1.10)) and since $\prod_{j=1}^{p-q-1} |1 + \eta(\xi_j) e^{i\omega\Delta}|^{-2} \leq \prod_{j=1}^{p-q-1} (1 - |\eta(\xi_j)|)^{-2} \leq \text{const.}$ (cf. Proposition 3.1.2), it is sufficient to prove

$$\frac{(\omega\Delta)^2}{\Delta^{2(p-q)}} \frac{\prod_{j=1}^{p} \left|1 - e^{\Delta(\lambda_j + i\omega)}\right|^2}{\prod_{j=1}^{q} \left|1 - \zeta_j e^{i\omega\Delta}\right|^2} \frac{|b(-i\omega)|^2}{|a(-i\omega)|^2} \frac{1 - \cos(\omega \lfloor t/\Delta \rfloor \Delta)}{1 - \cos(\omega\Delta)} \leq C \tag{3.5.11}$$

for some $C > 0$. The power transfer function satisfies $|b(-i\omega)|^2/|a(-i\omega)|^2 \leq \text{const.}/(\omega^{2(p-q)} + 1)$ for any $\omega \in \mathbb{R}$. Thus, Eq. (3.5.11) will follow from

$$\frac{(\omega\Delta)^2}{(\omega\Delta)^{2(p-q)} + \Delta^{2(p-q)}} \frac{\prod_{j=1}^{p} \left|1 - e^{\Delta(\lambda_j + i\omega)}\right|^2}{\prod_{j=1}^{q} \left|1 - \zeta_j e^{i\omega\Delta}\right|^2} \frac{1 - \cos(\omega \lfloor t/\Delta \rfloor \Delta)}{1 - \cos(\omega\Delta)} \leq C. \tag{3.5.12}$$

We even show that Eq. (3.5.12) is true for any $\omega \in \mathbb{R}$. However, using symmetry and periodicity arguments it is sufficient to prove Eq. (3.5.12) on the interval $[0, \frac{2\pi}{\Delta}]$. We split that interval into the following six subintervals

$$I_1 := \left[0, \min_{j=1,\ldots,q} \frac{|\mu_j|}{2}\right], \; I_2 := \left[\min_{j=1,\ldots,q} \frac{|\mu_j|}{2}, \max_{j=1,\ldots,q} 2|\mu_j|\right], \; I_3 := \left[\max_{j=1,\ldots,q} 2|\mu_j|, \frac{\pi}{\Delta}\right],$$

$$I_4 := \left[\frac{\pi}{\Delta}, \frac{2\pi}{\Delta} - \max_{j=1,\ldots,q} 2|\mu_j|\right], \; I_5 := \left[\frac{2\pi}{\Delta} - \max_{j=1,\ldots,q} 2|\mu_j|, \frac{2\pi}{\Delta} - \min_{j=1,\ldots,q} \frac{|\mu_j|}{2}\right] \text{ and}$$

$$I_6 := \left[\frac{2\pi}{\Delta} - \min_{j=1,\ldots,q} \frac{|\mu_j|}{2}, \frac{2\pi}{\Delta}\right].$$

For any $\omega \in I_1 \cup I_6$, the fraction $\frac{1-\cos(\omega \lfloor t/\Delta \rfloor \Delta)}{1-\cos(\omega\Delta)}$ can be bounded by $\lfloor t/\Delta \rfloor^2$. In the other intervals we have the obvious bound $\frac{2}{1-\cos(\omega\Delta)}$ for that term.

Now, for any $j = 1, \ldots, p$, we have, as $\Delta \downarrow 0$,

$$\left|1 - e^{\Delta\lambda_j} \cdot e^{i\omega\Delta}\right|^2 \leq 2\left|1 - e^{i\omega\Delta}\right|^2 + 4\Delta^2 |\lambda_j|^2 = 8 \sin^2\left(\frac{\omega\Delta}{2}\right) + 4\Delta^2 |\lambda_j|^2 \leq 4\Delta^2 \left(\omega^2 + |\lambda_j|^2\right)$$

if $\omega \in I_1 \cup I_2 \cup I_3$, and $\left|1 - e^{\Delta\lambda_j} \cdot e^{i\omega\Delta}\right|^2 \leq 4\Delta^2 \left((2\pi/\Delta - \omega)^2 + |\lambda_j|^2\right)$ if $\omega \in I_4 \cup I_5 \cup I_6$.

The first fraction on the LHS of Eq. (3.5.12) satisfies

$$\frac{(\omega\Delta)^2}{(\omega\Delta)^{2(p-q)} + \Delta^{2(p-q)}} \leq \begin{cases} \min\limits_{j=1,\ldots,q} \frac{|\mu_j|}{2} \cdot \frac{\Delta^2}{\Delta^{2(p-q)}}, & \text{if } \omega \in I_1, \\ \frac{(\omega\Delta)^2}{(\omega\Delta)^{2(p-q)}}, & \text{if } \omega \in I_2 \cup I_3, \\ \frac{(2\pi)^2}{\pi^{2(p-q)}}, & \text{if } \omega \in I_4 \cup I_5 \cup I_6. \end{cases}$$

Then, for any $j = 1, \ldots, q$ and $\omega \in I_1 \cup I_6$, we obtain

$$\begin{aligned} \left|1 - \zeta_j e^{i\omega\Delta}\right|^2 &= \left|1 - (1 - \operatorname{sgn}(\Re(\mu_j))\,\mu_j\Delta + o(\Delta))e^{i\omega\Delta}\right|^2 \geq \frac{1}{2}\Delta^2 \left|\operatorname{sgn}(\Re(\mu_j))\,\mu_j - i\omega\right|^2 \\ &\geq \frac{1}{8}\Delta^2 \left|\mu_j\right|^2. \end{aligned}$$

If $\omega \in I_3$, then we have

$$\begin{aligned} \left|1 - \zeta_j e^{i\omega\Delta}\right|^2 &\geq \left(\left|1 - e^{i\omega\Delta}\right| - \left|\mu_j + o(1)\right|\Delta\right)^2 = \left(2\sin\left(\frac{\omega\Delta}{2}\right) - \left|\mu_j + o(1)\right|\Delta\right)^2 \\ &\geq \Delta^2 \left(\frac{3}{5}\omega - \left|\mu_j + o(1)\right|\right)^2 \end{aligned}$$

and likewise, for $\omega \in I_4$, we deduce $\left|1 - \zeta_j e^{i\omega\Delta}\right|^2 \geq \Delta^2 \left(\frac{3}{5}(\frac{2\pi}{\Delta} - \omega) - \left|\mu_j + o(1)\right|\right)^2$. On I_2 we get for arbitrary $\varepsilon > 0$

$$\begin{aligned} \left|1 - \zeta_j e^{i\omega\Delta}\right|^2 &= 2(1 - \cos(\omega\Delta)) \cdot (1 - \Delta \operatorname{sgn}(\Re(\mu_j))\,\Re(\mu_j) + o(\Delta)) \\ &\qquad + 2\sin(\omega\Delta) \cdot (-\Delta \operatorname{sgn}(\Re(\mu_j))\,\Im(\mu_j) + o(\Delta)) + \Delta^2|\mu_j|^2 + o(\Delta^2) \\ &\geq (\omega\Delta)^2 \cdot (1 - \varepsilon) - 2(\omega\Delta) \cdot \Delta\,|\Im(\mu_j)| \cdot (1 + \varepsilon) + \Delta^2 \left(|\mu_j|^2 + o(1)\right) =: f_\varepsilon^\Delta(\omega\Delta). \end{aligned}$$

Since $f_\varepsilon^\Delta(\omega)/\omega^2 \to 1 - \varepsilon$ $(\omega \to \infty)$ and $f_\varepsilon^\Delta(\omega)/\omega^2 \to \infty$ $(\omega \to 0)$, a (global) minimum of $f_\varepsilon^\Delta(\omega)/\omega^2$ on $(0, \infty)$ could be achieved in any ω^* with $\left(\frac{\mathrm{d}}{\mathrm{d}\omega}\frac{f_\varepsilon^\Delta(\omega)}{\omega^2}\right)(\omega^*) = 0$. The only such value is $\omega^* = \frac{\Delta(|\mu_j|^2 + o(1))}{(1+\varepsilon)|\Im(\mu_j)|}$. Since

$$\frac{f_\varepsilon^\Delta(\omega^*)}{(\omega^*)^2} = 1 - \varepsilon - (1+\varepsilon)^2 \frac{|\Im(\mu_j)|^2}{|\mu_j|^2 + o(1)} \geq (1+\varepsilon)\frac{\Re(\mu_j)^2}{|\mu_j|^2} - 3\varepsilon - \varepsilon^2 \geq \frac{1}{2}\frac{\Re(\mu_j)^2}{|\mu_j|^2};$$

if we choose $\varepsilon = \frac{1}{6}\frac{\Re(\mu_j)^2}{|\mu_j|^2}$, we obtain $\frac{f_\varepsilon^\Delta(\omega)}{\omega^2} \geq \frac{1}{2}\frac{\Re(\mu_j)^2}{|\mu_j|^2}$ for any $\omega \in (0, \infty)$. Hence,

$$\left|1 - \zeta_j e^{i\omega\Delta}\right|^2 \geq f_\varepsilon^\Delta(\omega\Delta) \geq \frac{1}{2}\frac{\Re(\mu_j)^2}{|\mu_j|^2}(\omega\Delta)^2 \quad \text{for all } \omega \in I_2.$$

Using periodic properties of the sine and cosine terms, we likewise get

$$\left|1 - \zeta_j e^{i\omega\Delta}\right|^2 \geq \frac{1}{2}\frac{\Re(\mu_j)^2}{|\mu_j|^2}\Delta^2 \left(\frac{2\pi}{\Delta} - \omega\right)^2 \quad \text{for any } \omega \in I_5.$$

Putting all together, we can bound the LHS of Eq. (3.5.12) in I_1 by

$$\min_{j=1,\dots,q} \frac{|\mu_j|}{2} \cdot \frac{(\lfloor t/\Delta \rfloor \Delta)^2}{\Delta^{2(p-q)}} \frac{4^p \Delta^{2p} \cdot \prod_{j=1}^{p} \left(\min_{k=1,\dots,q} |\mu_k|^2/4 + |\lambda_j|^2 \right)}{8^{-q} \Delta^{2q} \prod_{j=1}^{q} |\mu_j|^2}$$
$$\leq \min_{j=1,\dots,q} \frac{|\mu_j|}{2} \cdot t^2 \cdot \frac{4^{p+q} \cdot \prod_{j=1}^{p} \left(\min_{k=1,\dots,q} |\mu_k|^2/4 + |\lambda_j|^2 \right)}{\prod_{j=1}^{q} \frac{1}{2} |\mu_j|^2} = C,$$

in I_2 by

$$\frac{2(\omega\Delta)^2}{1-\cos(\omega\Delta)} \frac{4^p \Delta^{2p} \cdot \prod_{j=1}^{p} \left(4 \max_{k=1,\dots,q} |\mu_k|^2 + |\lambda_j|^2 \right)}{(\omega\Delta)^{2p} \cdot \prod_{j=1}^{q} \frac{1}{2} \frac{\Re(\mu_j)^2}{|\mu_j|^2}}$$
$$\leq \frac{5 \cdot 4^{2p} \cdot \prod_{j=1}^{p} \left(4 \max_{k=1,\dots,q} |\mu_k|^2 + |\lambda_j|^2 \right)}{\min_{j=1,\dots,q} |\mu_j|^{2p} \cdot \prod_{j=1}^{q} \frac{1}{2} \frac{\Re(\mu_j)^2}{|\mu_j|^2}} = C,$$

in I_3 by

$$\frac{2(\omega\Delta)^2}{1-\cos(\omega\Delta)} \frac{4^p (\omega\Delta)^{2p} \cdot \prod_{j=1}^{p} \left(1 + \frac{|\lambda_j|^2}{4 \max_{k=1,\dots,q} |\mu_k|^2} \right)}{(\omega\Delta)^{2(p-q)} \cdot (\frac{1}{20}\omega\Delta)^{2q}}$$
$$\leq \pi^2 \, 4^p \, 20^{2q} \prod_{j=1}^{p} \left(1 + \frac{|\lambda_j|^2}{4 \max_{k=1,\dots,q} |\mu_k|^2} \right) = C,$$

in I_4 by

$$\frac{(2\pi)^2}{\pi^{2(p-q)}} \frac{2}{1-\cos(\omega\Delta)} \frac{4^p (2\pi - \omega\Delta)^{2p} \cdot \prod_{j=1}^{p} \left(1 + \frac{|\lambda_j|^2}{4 \max_{k=1,\dots,q} |\mu_k|^2} \right)}{20^{-2q} \, (2\pi - \omega\Delta)^{2q}}$$
$$\leq 4^{p+1} \, 20^{2q} \prod_{j=1}^{p} \left(1 + \frac{|\lambda_j|^2}{4 \max_{k=1,\dots,q} |\mu_k|^2} \right) \frac{2 \cdot (2\pi - \omega\Delta)^2}{1 - \cos(2\pi - \omega\Delta)}$$
$$\leq \pi^2 \, 4^{p+1} \, 20^{2q} \prod_{j=1}^{p} \left(1 + \frac{|\lambda_j|^2}{4 \max_{k=1,\dots,q} |\mu_k|^2} \right) = C,$$

in I_5 by

$$\frac{(2\pi)^2}{\pi^{2(p-q)}} \frac{2}{1-\cos(\omega\Delta)} \frac{4^p \Delta^{2p} \cdot \prod_{j=1}^{p} \left(4 \max_{k=1,\dots,q} |\mu_k|^2 + |\lambda_j|^2 \right)}{\Delta^{2q} \prod_{j=1}^{q} \frac{1}{8} \min_{k=1,\dots,q} |\mu_k|^2 (\Re(\mu_j)/|\mu_j|)^2}$$
$$\leq \frac{(2\pi)^2}{\pi^{2(p-q)}} \frac{4^p \cdot \prod_{j=1}^{p} \left(4 \max_{k=1,\dots,q} |\mu_k|^2 + |\lambda_j|^2 \right)}{\prod_{j=1}^{q} \frac{1}{8} \min_{k=1,\dots,q} |\mu_k|^2 (\Re(\mu_j)/|\mu_j|)^2} \frac{2\Delta^2}{1 - \cos(2\pi - \omega\Delta)}$$
$$\leq \frac{(2\pi)^2}{\pi^{2(p-q)}} \frac{4^p \cdot \prod_{j=1}^{p} \left(4 \max_{k=1,\dots,q} |\mu_k|^2 + |\lambda_j|^2 \right)}{\prod_{j=1}^{q} \frac{1}{8} \min_{k=1,\dots,q} |\mu_k|^2 (\Re(\mu_j)/|\mu_j|)^2} \frac{5 \cdot 4}{\min_{j=1,\dots,q} |\mu_j|^2} = C,$$

and, finally, in I_6 by

$$\frac{(2\pi\lfloor t/\Delta \rfloor)^2}{\pi^{2(p-q)}} \frac{4^p \Delta^{2p} \cdot \prod_{j=1}^{p} \left(\min_{k=1,\dots,q} |\mu_k|^2/4 + |\lambda_j|^2 \right)}{8^{-q} \Delta^{2q} \prod_{j=1}^{q} |\mu_j|^2}$$
$$\leq \frac{(2\pi t)^2}{\pi^{2(p-q)}} \frac{4^{p+q} \cdot \prod_{j=1}^{p} \left(\min_{k=1,\dots,q} |\mu_k|^2/4 + |\lambda_j|^2 \right)}{\prod_{j=1}^{q} \frac{1}{2} |\mu_j|^2} = C.$$

This shows Eq. (3.5.12) and thus concludes the proof. □

4. On the data acquisition process in turbulence experiments

The recording process of windspeed data and subsequent data processing are discussed. Those operations can lead to artefacts that can be misinterpreted or can affect the estimation of physically meaningful quantities.

4.1. Introduction

This Chapter is organised as follows: in Section 2 we review the data acquisition process and we present possible issues that can arise in the analysis of the data; in Section 3 we show that the discretisation error is approximately uniform and independent of the measured value if the discretisation level is small and it can be safely ignored in the estimation of second order quantities. In Section 4 we analyse the Brookhaven dataset, which presents a very pathological histogram of the increments, especially for small increments.

4.2. Experimental data

A direct measurement of a physical quantity is often difficult or impossible to perform directly. Therefore, the interested quantity must be indirectly inferred from other, more accessible measurements. The inference mostly involves electronic devices, whose output can be related with the quantity of interest.

To measure turbulent velocities for scientific purposes hot-wire anemometery is widely employed. A hot-wire consists of a thin wire of metal, with two or more prongs, characterised by a high electric resistance, being flown through by an electric current. The wire is heathen up to a temperature much higher than the one of the flow being measured, and this temperature will be kept constant by an ad-hoc circuitry. Finally, the hotwire is immersed in the fluid and its temperature will drop as the colder fluid flows around it. This cooling effect, which is proportional to the flow velocity, will be compensated with a variation of the voltage at one end of the circuitry. What we actually observe is then a function of the velocity of the flow. The whole process is afflicted by various errors, which can be kept at bay, but not eliminated, by a correct preparation of the experiment. For further reference and details we refer to Tropea et al. (2008) and Bruun (1995).

4.2.1. Data acquisition process: hotwire anemometer

Here we schematise the operations performed to collect windspeed data. We will denote the voltage, which is the actual output of the hotwire, with V^0. Moreover, to stress when a quantity X is a continuous time signal, we will use X_t, where $t \in \mathbb{R}$. For the discrete time values, the notation X_i, for $i \in \mathbb{Z}$, is used.

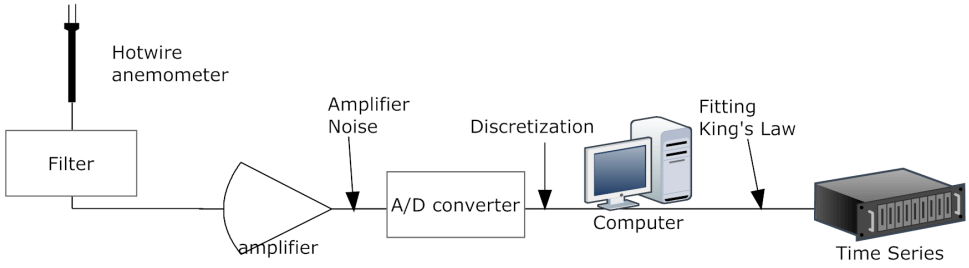

Figure 4.1.: Succession of typical operations performed on the data, as reported in Bruun (1995).

As mentioned before, the output of a hotwire is not a windspeed, but the voltage difference V_t^0 between the two ends of the anemometer. This signal will be filtered by applying a low-pass filter, with cut off frequency set at half (or less) of the sampling frequency. The rationale for this operation is the Shannon-Nyquist theorem that assures that a good reconstruction of the signal in the time domain can be obtained only for information contained in the part of the spectrum with frequency $f < f_0/2$. All those operations are applied to the analog (i.e. continuous time) signal through electronic devices.

The filtered signal $\tilde{V}_t^0$ is passed through an amplifier, yielding the amplified signal $V_t^1 = a\tilde{V}_t^0$, where $a > 0$ is the gain factor.

After these manipulations the amplified signal is passed through an analog-to-digital converter (A/C) in order to get a discretised sequence of values, to be used by a computer. The output of the A/C can only assume a discrete number p of values, called bits. Let us assume that the signal to be sampled is included in the interval $E = [\underline{V}, \overline{V}]$, then we call $|E| = \overline{V} - \underline{V}$ the voltage scale. The voltage scale can be adjusted, depending on the amplitude of the incoming signal, remaining fixed during the experiment. Since only signals with values in E can be properly sampled, it is necessary to consider $|E|$ large enough in order such that

$$\underline{V} \leq a\tilde{V}_t^0 \leq \overline{V} \quad t \in [0, T],$$

otherwise the experiment must be performed again, since the exceeding values will be censored, i.e. set to the nearest value inside E. Then the digital data will have a truncation

level of

$$\alpha = \frac{|E|}{2^p - 1}, \tag{4.2.1}$$

that is, every variation of the voltage smaller than α will not be visible in the discretised data. Now we obtain discrete-time data V_i, for $i = 0, \ldots, \lfloor T/n \rfloor$:

$$V_i^{\{\alpha\}} = \alpha \left\lfloor \frac{\tilde{V}^1(i/n)}{\alpha} + 1/2 \right\rfloor = \alpha \left\lfloor \frac{\tilde{V}^0(i/n)}{\alpha'} + 1/2 \right\rfloor ; \tag{4.2.2}$$

where $\alpha' = |E|/a(2^p - 1)$ is the equivalent truncation level of the signal V_t^0.

In general, the behaviour of the A/C converter is non-linear, i.e. the output and the input are not related by a simple linear dependence. The voltage scale $|E|$ and the amplifier gain have to be chosen in order to minimise the truncation level but considering the specifics of the electronic equipment. In fact, every electronic device has precise operative ranges, where the behaviour of each instrument is, to a satisfying level, linear. Usual values in the field of hotwire anemometry are $p = 12$ bit, $|E| = 20$ volt, implying $\alpha \approx 0.005$, i.e. the voltage increment has no more than 2 reliable decimal places.

The last step to get velocity data is the calibration curve: there exists a deterministic relationship between voltage and windspeed, which has to be determined for each anemometer. An anemometer is normally tested in a turbulence facility, like a wind tunnel, with a stable, constant and known speed and turbulence; the output voltage is then recorded. The procedure is repeated for some wind speeds (usually 10-30 values) and then results are interpolated, to obtain a calibration curve which is a continuous function $f_\theta : [V_l, V_h] \to [0, v_{max}]$ depending on a vector θ of parameters.

Example 4.2.1. *The most common interpolating function is given by King law*

$$V_t^2 = k_0 + k_1 v_t^r, \quad V \in E, \tag{4.2.3}$$

where the exponent n depends on the geometry of the sensor. Then, for real positive k_0, k_1 and r,

$$f_\theta\left(V_t\right) = \left(\left(V_t^2 - k_0\right)/k_1\right)^{1/r}$$

and the vector is $\theta = (k_0, k_1, r)$. Note also that f_θ is increasing and concave. Even if the voltage signal had symmetric increments, the windspeed will in general not.

This procedure is normally too expensive to be performed for each commercially available anemometer, therefore it is reserved only to those to be employed in high precision scientific measurements. For all other purposes the producer provides a standard calibration curve, i.e. factory values for the parameter list θ.

Although the discretisation procedure in the voltage data is clear, for wind data it is not the case. That can be seen by using the chain rule

$$\frac{\partial v}{\partial t} = \frac{\partial v}{\partial V}\frac{\partial V}{\partial t} \approx f'_\theta(V_i^{\{\alpha\}})\frac{V_{(i+1)}^{\{\alpha\}} - V_i^{\{\alpha\}}}{\Delta}.$$

Now the discretisation step depends on the derivatives of the calibration curve, which is not usually available with the time-series. We shall now use an argument to recover the original voltage data.

4.2.2. Recovering the parameters

Let us suppose that the interpolation function f_θ is smooth enough to have all the needed derivatives. Using the Taylor expansion for $f_\theta(V)$ we obtain, for some integer K and a small ΔV,

$$\Delta v = f_\theta(V^{\{\alpha\}} + \Delta V) - f_\theta(V^{\{\alpha\}}) = \sum_{i=1}^{K} \frac{1}{i!} f_\theta^{(i)}(V^{\{\alpha\}})(\Delta V)^i + o\left((\Delta V)^K\right). \tag{4.2.4}$$

We conclude from the RHS of (4.2.4) that the new discretisation steps depend on the derivatives of the calibration curve f at voltage V and on the discrete increments ΔV. Since Taylor formula is precise only for small ΔV and, by smoothness of f, for small Δv, it makes sense to consider only the increments smaller than a threshold β. Then for all $j_i \in \mathbb{N}$ such that $|\Delta_{j_i} v| < \beta$:

$$\Delta^{[\beta]} v = (\Delta_{j_0} v, \ldots, \Delta_{j_n} v)$$

where $\Delta_j v = v_{j+1} - v_j$. Then we summarise the associated levels $v^{[\beta]}$ as

$$v^{[\beta]} = (v_{j_0}, \ldots, v_{j_n}).$$

Plotting $\Delta^{[\beta]} v$ versus $v^{[\beta]}$ a striking visualisation of the discretisation effect can be observed, as shown in Figure 4.2.

Null increments are of course distributed along all the measurement levels, but other increments move along solid curves, as the speed varies; this is due to the variation of the derivatives of f_θ. Then we fix V and we get discretised increments $\delta^i v := f_\theta(V + i\Delta V) - f_\theta(V)$; using Taylor formula:

$$\begin{array}{rcl} \delta^1 v & = & \sum_{i=1}^{K} \frac{1}{i!} f_\theta^{(i)}(V)(\Delta V)^i + o\left((\Delta V)^K\right) \\ \vdots & & \vdots \\ \delta^K v & = & \sum_{i=1}^{K} \frac{1}{i!} f_\theta^{(i)}(V)(K\Delta V)^i + o\left((\Delta V)^K\right) \end{array} \tag{4.2.5}$$

Since we only have velocity data, we express the formulas above in terms of the latter with the change of variable $V = f_\theta^{-1}(v)$. Then, in the light of (4.2.5) we can interpret Figure 4.2 in two different manners:

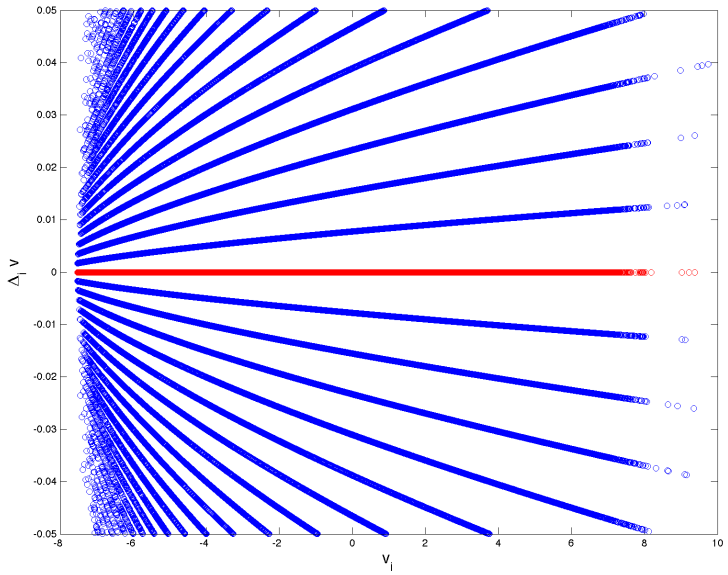

Figure 4.2.: $\Delta^{[\beta]}v$ vs. $v^{[\beta]}$ for the Brookhaven dataset (see Section 4.3), $\beta = 0.05$. The non-linear behaviour of the curves is given by derivatives of King law. Note that 92.36% of all increments of Brookhaven dataset belongs to $\Delta^{0.05}v$, including the already mentioned 23% of null increments (in red).

- We fix v and we look at the different branches of the increments: here we see how the velocity can only discretely jump to some predefined values. That happens because the voltage is moving with step ΔV.
- We look only at the first, upper branch (i.e. the one composed by the smallest non-null increments). If we move along this curve, we have fixed ΔV and we vary v, that is, we see how the derivatives of f_θ influence the increments.

The first outlook gives us an immediate feeling of the discreteness of our data, but the second one is more productive. Since $\Delta V \sim (2^{12} - 1)^{-1} = 2.4420 \cdot 10^{-4}$, we should be able to reach a good approximation with low order Taylor series.

We propose the following strategy to recover the parameter vector θ.

Take increments $\Delta^{(1)}v := \{\Delta v : \text{belongs to the first branch}\}$ and the levels $v^{(1)} := \{v : \text{belongs to the first branch}\}$. Furthermore, let $\phi = (\theta, \Delta V)$ be the extended parameter vector of the Taylor series and let $\phi^{(0)}$ be a guess on ϕ, which we take as initial value.

Then we perform a non-linear least squares fitting on the first order Taylor series

$$\Delta^{(1)}v = f'_\theta(f_\theta^{-1}(v^{(1)}))\Delta V \tag{4.2.6}$$

returning the estimate $\phi^{(1)} + o(\Delta V)$. If the estimate is too crude, we may need to take

higher order Taylor polynomials into account, getting the estimate, for instance, $\phi^{(2)}$ from a least squares fitting on the second order:

$$\Delta^{(1)}v = f'_\theta(f_\theta^{-1}(v^{(1)}))\Delta V + f''_\theta(f_\theta^{-1}(v^{(1)}))\frac{\Delta V^2}{2} + o((\Delta V)^2) \tag{4.2.7}$$

improving $\phi^{(1)}$, and so on. If the function f_θ is complicated, as the one in Example 4.2.1, it may be a good idea to start with a Taylor expansion to the first order. If the interpolating function f_θ is polynomial, we can directly use the Taylor series of the same order as f_θ.

4.3. A concrete example

We shall recover the voltage data from an atmospheric turbulence time-series, the Brookhaven dataset. It is a high frequency dataset, recorded via hot-wire anemometry techniques; a full account of the data can be found in Drhuva (2000) and in Chapter 5. The Brookhaven dataset consists of $20 \cdot 10^6$ data points sampled at 5 kHz (i.e. $5 \cdot 10^3$ points per second). The acquisition process with this kind of technique was described in Section 4.2.

We will use the strategy explained in Section 4.2.2 on the Brookhaven dataset, in order to recover its true discretisation pattern. As stated in Drhuva (2000), the Brookhaven data were obtained by using King law (Example 4.2.1). For this interpolating function we report here the derivatives up to order 3:

$$\begin{aligned}
f'_\theta(f_\theta^{-1}(v)) &= \frac{2v^{1-r}\sqrt{k_0 + k_1 v^r}}{k_1 r} \\
f''_\theta(f_\theta^{-1}(v)) &= \frac{2v^{1-r}}{k_1 r} + \frac{4\,(1-r)\,v^{1-2r}\,(k_0 + k_1 v^r)}{k_1^2} \\
f'''_\theta(f_\theta^{-1}(v)) &= \frac{12\,(1-r)\,v^{1-2r}\sqrt{k_0 + k_1 v^r}}{k_1^2} + \frac{8r\,(1-2r)\,(1-r)\,v^{1-3r}\,(k_0 + k_1 v^r)^{3/2}}{k_1^3}
\end{aligned}$$

For the first branch the behaviour mainly depends on the first derivative, allowing us to make a guess on the parameter r, which gives the shape of the curve. For small values of v the curve tends to zero, and for big values of v it grows somehow linearly, we can then suppose $r \in (0, 1)$, with an initial guess $r^{(0)} = 0.5$.

Since the mean value of the windspeed was unfortunately subtracted from the Brookhaven data, instead of the actual velocities v, we have to consider the Reynolds decomposition

$$v_t = u_t + v_0, \quad t \in [0, T],$$

where v_0 is the unknown average windspeed. Since the derivatives depend in a nonlinear way on the values of the windspeed, this information is important and it has to be recovered as well.

In Drhuva (2000), Table 1, for entry 3 (BNL) $v_0 = 8.3$ is reported, but it was calculated on 4×10^7 values, while our dataset has "only" 2×10^7 data points. Two strategies are viable: we can either assume that the average speed given in Drhuva (2000) is correct, or we can use it as a guess, increasing the numbers of parameters to be fitted by 1.

We tried both strategies, getting similar results; it is very interesting to notice how a slight variation in the value of v_0 causes a relatively better fit, similarly for the residuals listed in Table 1. Nonetheless, the really close estimation of average windspeed on only half the dataset is, at least, a good indication of the stationarity of this dataset.

Table 4.1.: Non-linear least squares fitting for Brookhaven dataset.

	k_0	k_1	r	ΔV	v_0	max(res)	max(res/$\Delta^{(1)}v$)
$\phi^{(0)}$	12	12	0.5	$10 \cdot (2^{12} - 1)^{-1}$	8.3	-	-
$\phi^{(1)}$	13.0084	10.4190	0.5005	13.40×10^{-4}	8.3	8.78×10^{-6}	0.0051
$\phi^{(2)}$	12.9990	10.4449	0.5010	13.40×10^{-4}	8.3	8.97×10^{-6}	0.0052
$\phi^{(1)}$	13.0386	10.5953	0.5000	13.31×10^{-4}	8.3115	9.87×10^{-9}	3.23×10^{-6}
$\phi^{(2)}$	13.0316	10.5653	0.4999	13.32×10^{-4}	8.3120	1.05×10^{-8}	3.21×10^{-6}

Once we have estimated θ, we can proceed to reconstruct the voltage data and to compare them to the windspeed data. In Figure 4.3 a,d) we report the histogram of the increments, for increments within three standard deviations. We divide the data in 10000 bins in order to highlight the fine discretised structure of the considered data. In Figure 4.3 a) the peculiar structure already seen in Figure 4.2 produce an erratic behaviour in the density for the increments smaller than a standard deviation. On the other hand, the voltage data now clearly show the neat discretised structure imposed by the sampling process described in Section 4.2.

From the voltage data we obtain that $\Delta V = 0.0011$, which is not that far from the value estimated by the least squares fitting. We do stress that the parameter ΔV is not a parameter of King law, but it is necessary, since it gives the scaling in the Taylor series. Eq. (4.2.1) yields a voltage scale $|E| = 0.0011 \cdot (2^{12} - 1) \approx 4.5V$. This is in agreement with the recovered data, as

$$\max_{i=1,\dots,n} V_i - \min_{i=1,\dots,n} V_i = 2.8763.$$

It suggests that the experimenter took a large, but reasonable voltage scale to be able to sample the whole signal, sacrificing some accuracy.

4.3.1. Comparison of voltage and windspeed

Since we have voltage and windspeed, we can perform a standard analysis on both of them, in order to understand how we can profit from the additional knowledge of the sampling process. Due to some inertia of the components of every electric device, a circuitry reacts to a generic input with a smoother output. Therefore, the voltage (and as a consequence the windspeed) must enjoy a rather strong form of continuity. A first comparison between

Table 4.2.: normalized moments of ΔV and Δv.

	mean	variance	μ_3	μ_4	μ_5	μ_6	μ_7
ΔV	-1.54×10^{-8}	1.87×10^{-5}	0.62	31.48	143.61	1.84×10^4	3.76×10^5
Δv	-1.22×10^{-7}	9.62×10^{-4}	0.64	25.93	82.37	4.69×10^3	3.55×10^4

the two datasets can be performed by looking at their normalised moments. In general, the voltage increments have higher normalised moments (see Table 4.2) than the windspeed, suggesting that the voltage increments are more heavy tailed than windspeed ones. This is clearly showed by the log-histograms of both considered increments, Figure 4.3 b, e).

A popular choice for fitting the distribution of the time increments of turbulence is the Normal-Inverse Gaussian distribution (Barndorff-Nielsen and Schmiegel (2008b)) and the Generalised Hyperbolic distribution (Birnir (2013)), which are able to capture skewness and semi-heavy tails. Within our CMA framework, we will propose and fit a model for the distribution of the driving noise W in Chapter 5. Since the second-order properties are of paramount importance in this dissertation, especially in Chapter 2 and 3 and we compare the spectral densities of both voltage and wind data. As customary in physics, we show in Figure 4.3 c, f) the so called compensated spectral densities, which are defined to be $\varphi^{5/3} f^{\Delta}(\varphi)$. Through the compensation, the region where the spectral density decays as prescribed by the 5/3-law should appear flat. Regardless of the non-linearity of the relation linking the voltage and the windspeed, the respective spectral density look similar, with a well-developed inertial range, and a fast decaying dissipation range for high frequencies.

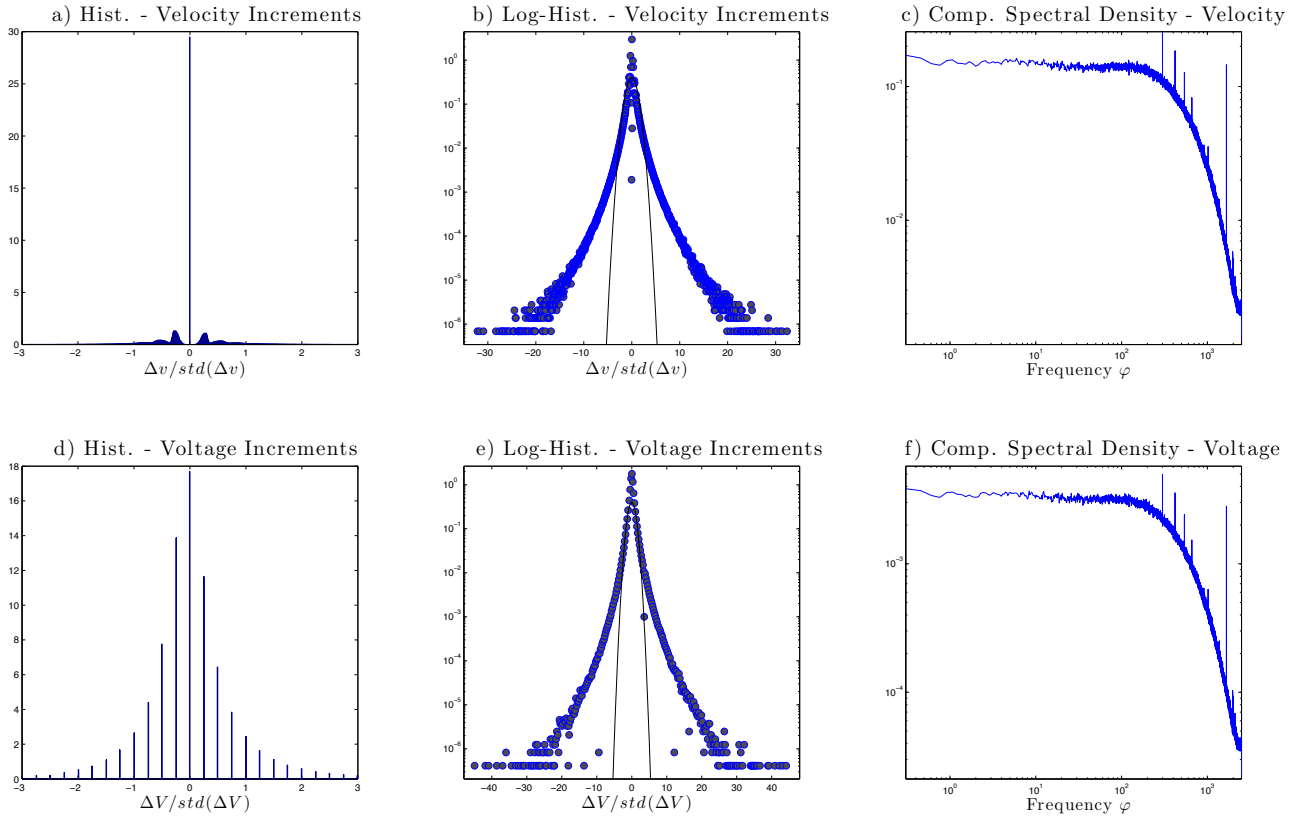

Figure 4.3.: Statistical comparison between voltage and wind data. a, d) Histograms of the increments of the voltage and the windspeed (10000 bins). Only values between $\pm 3\sqrt{\mathbb{E}[(\Delta V)^2]}$ and $\pm 3\sqrt{\mathbb{E}[\Delta v]^2}$ are shown. b, e) Log-histograms of the increments (1000 bins). The solid line denotes a standard Gaussian distribution. c, f) Compensated spectral density $\hat{f}^{\Delta}(\varphi)\varphi^{5/3}$ for the velocity and the voltage. The spectral density is estimated with the Welch method (Welch (1967)). The flat regions denote where the Kolmogorov 5/3 law holds. The spikes can be attributed to some periodicity effects in the experimental settings.

5. Empirical modelling of turbulence

A general model for stationary, time-wise turbulent velocity is presented and discussed. This approach, inspired by modelling ideas of Barndorff-Nielsen and Schmiegel (2008a), is coherent with the K41 hypothesis of local isotropy, and it allows us to separate second order statistics from higher order ones. The model can be motivated by Taylor hypothesis and a relation between time and spatial spectra. The non-parametric method analysed in Chapter 3 will be employed to estimate the increments of the driving noise of the CMA model. A parametric model for the driving noise is proposed, able to reproduce the main features of the non-parametric estimate.

5.1. Introduction

The Wold-Karhunen representation (Doob (1990), p. 588) states that every non-deterministic, one dimensional, stationary stochastic process $X = \{X_h\}_{h\in\mathbb{R}}$, whose two-sided power spectrum $E(\xi)$ satisfyies the Paley-Wiener condition

$$\int_{-\infty}^{\infty} \frac{|\log E(\xi)|}{1+\xi^2} d\xi < \infty, \tag{5.1.1}$$

can be written as a causal moving average (CMA)

$$X_h = \mathbb{E}[X] + \int_{-\infty}^{h} g(h-s)dW_s, \quad h \in \mathbb{R}, \tag{5.1.2}$$

where $W = \{W_h\}_{h\in\mathbb{R}}$ is a process with uncorrelated and weakly stationary increments, $\mathbb{E}[dW_h] = 0$ and $\mathbb{E}[(dW_h)^2] = dh$. The kernel g is an element of the Hilbert space L^2, i.e. $\|g\|_{L^2}^2 := \int_0^\infty |g(s)|^2 ds < \infty$ and it is causal, i.e. it vanishes on $(-\infty, 0)$.

The converse is also true, i.e. every stationary stochastic process of form (5.1.2) satisfies (5.1.1). If we consider h to be time, the representation (5.1.2) has the physically amenable feature of being causal, i.e. X depends only on the past values of W. The autocovariance function of X has a simple expression: for $\tau \in \mathbb{R}$,

$$\gamma_X(\tau) = \mathbb{E}[(X_{h+\tau} - \mathbb{E}[X])(X_h - \mathbb{E}[X])] = \int_0^\infty g(s+|\tau|)g(s)ds, \tag{5.1.3}$$

while the two-sided power spectrum is $E(\xi) = (2/\pi)\int_0^\infty \gamma_X(s)\cos(\xi s)ds = |\mathcal{F}\{g(\cdot)\}|^2(\xi)$, where

$$\mathcal{F}\{g(\cdot)\}(\xi) = \frac{1}{\sqrt{2\pi}}\int_0^\infty g(s)e^{-i\xi s}ds, \quad \xi \in \mathbb{R},$$

denotes the Fourier operator. Condition (5.1.1) is crucial, since for a general stationary process a representation similar to (5.1.2) holds, but the kernel g may not vanish on $(-\infty, 0)$ and the integrals in (5.1.2) and (5.1.3) are extended to the whole real line (Yaglom (2005), Ch. 26). The rate of decay of the spectrum plays a pivotal role in determining whether a given process has representation (5.1.2) or not, since (5.1.1) excludes spectra decaying at infinity as $\exp(-\xi)$ or faster. In this context h or ξ do not necessarily denote time or frequency. In the following x will denote a stream-wise spatial coordinate, κ_1 the associate wavenumber, t a time coordinate, and $\omega = 2\pi f$ the associated angular velocity with frequency f.

In the turbulence literature the spectral properties of turbulent velocity fields were intensively investigated, starting from Kolmogorov K41 theory (Kolmogorov (1941b,a, 1942)). In the Wold-Karhunen representation (5.1.2) the second order properties of X depend only on the function g, with no necessity to specify the driving noise W. This is analogous to K41 theory, where the second order properties of the velocity field can be handled without considering the intermittent behaviour of the turbulent flow.

From now on, we shall denote the mean flow velocity component by V. Moreover, we work with the usual Reynolds decomposition $V = U + u$, where U denotes the mean velocity and u is the time-varying part of V. Then $\mathrm{Re} := UL/\nu$ is the Reynolds number of the flow, by L we denote a typical length, and ν is the kinematic viscosity of the flow.

In K41 the first universality hypothesis claims that, for locally isotropic and fully developed turbulence (i.e. $\mathrm{Re} \gg 1$), the spatial power spectrum E_L of the mean flow velocity fluctuations, has the universal form (see e.g. Pope (2000), Section 6.5.4)

$$E_L(\kappa_1) = (\varepsilon\nu^5)^{1/4}\Phi_L(\eta\kappa_1) = v_\eta^2\eta\Phi_L(\eta\kappa_1), \tag{5.1.4}$$

where $\eta = (\nu^3/\varepsilon)^{1/4}$ and $v_\eta = (\varepsilon\nu)^{1/4}$ are, respectively, Kolmogorov length and velocity, and $\Phi_L(\cdot)$ is a universal, a-dimensional function of a-dimensional argument. As a cornerstone of the K41 theory, much effort has been devoted to verify Eq. (5.1.4) and to determine the functional form of Φ_L. For finite Re we stress the dependence of Φ_L in (5.1.4) on Re with the notation Φ_L^{Re}.

In an experimental setting with a probe in a fixed position, the Taylor hypothesis (Taylor (1938)) can be used to estimate the spatial power spectrum with the time spectrum E_L^τ, with the formula (Gledzer (1997), Eq. (7))

$$E_L(\kappa_1) = UE_L^\tau(U\kappa_1), \tag{5.1.5}$$

where $\kappa_1 = 2\pi f/U$. This is regarded as a good approximation, when the turbulence intensity $I = \sqrt{\mathbb{E}[u^2]}/U \ll 1$ (Wyngaard and Clifford (1977), Lumley (1965)). Relation

(5.1.5) is a first order approximation, where in general higher order corrections are feasible (Gledzer (1997), Lumley (1965)), and also error bounds can be obtained.

Comparison of a large number of experimental low-intensity data sets (Gibson and Schwarz (1963), Saddoughi and Veeravalli (1994), Saddoughi (1997)) shows that in the dissipation range Φ_L^{Re} is unvarying on a wide range of Reynolds numbers. On the other hand, the inertial range does not exist for small Reynolds number (Champagne (1978)), however, its length increases with the Reynolds number. The supposed infinite differentiability of the solution of the Navier-Stokes equation yields Φ_L to decrease faster than any power in the far dissipation range ($\kappa_1\eta > 1$) (Von Neumann (1961-1963)). Moreover, the link between second order properties and third order ones is given by von Kármán-Howart-Monin relation (Kolmogorov (1941a), Pope (2000), Eq. 6.83, Lindborg (1999))

$$S_3(x,t) = -\frac{4}{5}\epsilon x + 6\nu\frac{dS_2}{dx} - \frac{3}{x^4}\int_0^x z^4\frac{dS_2}{dt}dz, \tag{5.1.6}$$

where $S_n(x,t) = \mathbb{E}[(u(s+x,t)-u(s,t))^n]$ is the n-th order longitudinal structure function. Formula (5.1.6) has been used in Sirovich et al. (1994) to determine an expression for the spatial spectrum which decreases like $\kappa_1^\alpha \exp(-\beta\kappa_1)$ as κ_1 tends to infinity and α and β depend on the Reynolds number. Numerical (see e.g. Chen et al. (1993), Martínez et al. (1997), Ishihara et al. (2007), Schumacher (2007), Lohse and Müller-Groeling (1995)) and experimental (Saddoughi and Veeravalli (1994), Saddoughi (1997)) studies confirmed such exponential decay in the dissipation range. Under the hypothesis of local isotropy the *local* rate of energy dissipation is (see e.g. Pope (2000), Eq. 6.314)

$$\epsilon_x = 15\nu(\partial_x V)^2 \approx \frac{15\nu}{U^2}(\partial_t V)^2 = \varepsilon_t, \quad t \in \mathbb{R}, \tag{5.1.7}$$

where the approximation with the *instantaneous* rate of energy dissipation ε_t follows from Taylor hypothesis (see e.g. Gledzer (1997), Eq. (1)). As customary in physics literature, we will drop the term rate for the sake of simplicity. The average energy dissipation can be calculated directly from the spatial spectrum (Batchelor (1953)) as (see e.g. Pope (2000), Section 6.5.4)

$$\epsilon := \mathbb{E}[\epsilon_x] = 15\nu\int_{\mathbb{R}} \kappa_1^2 E_L(\kappa_1)d\kappa_1 \approx \mathbb{E}[\varepsilon_t], \tag{5.1.8}$$

where the integrand $\kappa_1^2 E_L(\kappa_1)$ for $\kappa_1 > 0$ is the dissipation spectrum. An important fingerprint of the non-linearity of turbulence is given by it intermittent behaviour, that is, that the energy dissipation is highly correlated. That means that we observe period of high energy dissipation and periods of low energy dissipation, in analogy to what is called volatility clustering in finance. The estimated autocovariance function of the surrogated energy dissipation usually behaves as power law, decaying almost universally with exponent -0.25 (Sreenivasan and Kailasnath (1993), Pope (2000), Eq. 6.317), with a weak dependence on the Reynolds number. The observed power law behaviour of the

empirical autocovariance function cannot hold for every lag, but it must not near to the origin and for large lags. The matter was studied in great detail by Cleve (2004).

Since the model (5.1.2) is a linear model, and the surrogate energy dissipation (5.1.7) is a non-linear function of the velocity, this behaviour cannot be reproduced by the kernel only. Therefore we advocate that the intermittency process $W = \{W_t\}_{t\in\mathbb{R}}$ can be appropriately modelled by a two-sided, time-changed Lévy process

$$W_t = L_{\int_0^t Y_s ds}, \quad t \in \mathbb{R}, \tag{5.1.9}$$

where L is a purely discontinuous martingale with tempered stable Lévy measure (see Rosiński 2007) and Y is itself a positive, ergodic, causal continuous-time moving average process − independent of L. In detail: we suppose there exists an $0 < \alpha < 2$ and there are two completely monotone functions $q_+, q_- : \mathbb{R}_+ \to \mathbb{R}_+$, called the *tempering functions*, such that the Lévy measure of L is given by

$$F(dx) = \frac{q_+(x)}{x^{1+\alpha}}\mathbf{1}_{\{x>0\}}(x)dx + \frac{q_-(|x|)}{|x|^{1+\alpha}}\mathbf{1}_{\{x<0\}}(x)dx; \tag{5.1.10}$$

and we suppose that Y is – again – a CMA process.

To model volatility clustering, time-changed Lévy processes have been introduced to mathematical finance by Geman et al. (2001) and Carr and Wu (2004). Likewise, these processes have been introduced to turbulence modelling by Barndorff-Nielsen et al. (2004) and Barndorff-Nielsen and Schmiegel (2004, 2008a). Since the processes $B \circ \int_0^\cdot Y_s ds$ and $\int_0^\cdot Y_s^{1/2} dB_s$ are indistinguishable in the case of a Brownian motion B, the relation to other stochastic volatility models like the BNS Ornstein–Uhlenbeck (Barndorff-Nielsen and Shephard 2001, 2002) and the COGARCH model (Klüppelberg et al. 2004) is apparent. Treating these estimated increments as true observations, first, we estimated the time-change using a Method of Momentsapproach (see Kallsen and Muhle-Karbe 2011). Second, we estimated the Lévy density of the Lévy process L using the projection estimator of Figueroa-López (2009), Figueroa-López (2011) and the penalisation method which Ueltzhöfer and Klüppelberg (2011) studied in the case of Lévy processes. Third, under a constraint on the moments of the time-changed Lévy process, we calculate least squares fits of certain parametric families of tempered stable Lévy densities to our non-parametric estimate. We minimise an information criterion to find an optimal choice of parameters.

The generality of the CMA model (5.1.2) requires in the context of turbulence modelling some interpretation of the parameters, in particular, the kernel function g. This Chapter is articulated in two parts. In the first we characterise the model (5.1.2) from a physical point of view, focussing on the kernel function g. In the second part we focus on modelling the increments of the driving noise W; we propose a model that is able to reproduce certain features of turbulence, and we fit it to the increments of W, which have been recovered using the method illustrated in Chapter 3.

In Section 5.2 the model (5.1.2) for the time-wise behaviour of the time-varying component u of a turbulent velocity field is motivated first by an analysis of the literature yielding a discussion on the errors of Taylor hypothesis and consequences for our model. Physical scaling properties of the kernel lead to a model for g in the inertial and energy containing range. In Section 5.3 the estimation methods of Section 5.2 are applied, using a non-parametric estimation of the kernel on 13 turbulent data sets, having Reynolds numbers Re spanning over 5 orders of magnitude. In Section 5.4 we illustrate a parametric model for the intermittency process, inside the larger class of time-changed Lévy processes. More specifically, we will propose and fit to the data a parametric model, motivating it by the physical point of view. In order to validated the fitted model, in Section 5.5 we simulate it and we compare the results with the original data.

5.2. Time-wise turbulence model

In this Section we present the theoretical aspects of our turbulence model. Section 5.2.1 is devoted to motivating the model by a discussion of Taylor hypothesis and certain refinements. In Section 5.2.2 a rescaling of the kernel similar to (5.1.4) is obtained, such that the rescaled kernel depends on the Reynolds number Re and the turbulence intensity I only. In Section 5.2.3 we present a model for the inertial range and the energy containing range in order to deduce the scaling with Re of some features of the rescaled kernel.

5.2.1. Does the Paley-Wiener condition hold?

First note that an exponentially decaying power spectrum E violates (5.1.1) and, therefore, it leads to a non-causal representation, regardless of any power-law factors. For spatial spectra this is not against intuition: the basic balance relations leading to the Navier-Stokes equation must hold in every spatial direction; on the other hand, the causality of representation (5.1.2) makes sense, when considering the time-wise turbulence behaviour.

It is known that the spatial spectra estimated via Taylor hypothesis (5.1.5) give larger errors in the dissipation range rather than in the inertial range, and that the error is in general positive, i.e. the time spectrum decays at a slower rate than the spatial spectrum. Lumley (1965) derived from a specific model an ordinary differential equation relating time and space spectra. Lumley ODE was solved in Champagne (1978) and used on jet data with $I = 0.30$, resulting that the time spectrum obtained via (5.1.5) at $\kappa_1\eta \approx 1$ is 238% higher than the spectrum obtained with Lumley model. Moreover, Gledzer (1997) showed that the power-law scaling in the inertial range is substantially left unchanged by Lumley model. A similar effect has been already observed in Tennekes (1975), comparing Eulerian and Lagrangian spectra; such spectra decay as ω^{-2} and $\omega^{-5/3}$, respectively.

Based on such facts we postulate that the time spectrum for every flow with turbulence

intensity $I > 0$ satisfies (5.1.1), and it is related to the spatial spectrum by

$$E_L(\kappa_1) = UE_L^\tau(\Lambda_I(U\kappa_1)), \tag{5.2.1}$$

where Λ depends on I, such that $\Lambda_I(\kappa_1)/\kappa_1 \to 1$ uniformly in κ_1 as $I \downarrow 0$. The classical Taylor hypothesis in (5.1.5) assumes that *all* eddies are convected at velocity U; however, it is likely that larger eddies propagate with a velocity of the order U, whilst the smaller eddies travel at lower velocity, resulting in a less steep decay (Moin (2009), del Álamo and Jiménez (2009)). The function Λ_I accounts for such spectral distortion. In our framework we will not take the limit $I \downarrow 0$ for two reasons: firstly, since the variance $\mathbb{E}[u^2]$ is finite, $I \downarrow 0$ would imply that the mean velocity tends to infinity, and, secondly, if $I \downarrow 0$, in virtue of Taylor hypothesis, the time spectrum (5.1.5) would decay exponentially like the spatial one, violating the Paley-Wiener condition (5.1.1). Therefore, in the considered setting, the limit $I \downarrow 0$ is singular, and we shall consider only the approximation for $I \ll 1$. We shall do the same with the singular limit for Re tending to infinity (Frisch (1996), Section 5.2), denoting it by $\mathrm{Re} \gg 1$.

To date the resolution of experimental data is limited to scales in the order of η but, if the data are not too noisy in the dissipation range, it is still possible to check, whether (5.1.1) holds. In Figure 5.1a) the time spectrum for the data set h3 is depicted; Figure 5.1b) shows that the integral in (5.1.1) converges and that the dissipation range does not make any significant contribution to the integral.

5.2.2. Rescaling the model

The CMA representation (5.1.2) for the time-wise behaviour of the mean flow velocity component of a fully developed turbulent flow in the universal equilibrium range (i.e. inertial and dissipation ranges) can be rewritten as

$$V_t = U + C_2 \int_{-\infty}^{t} g(C_1(t-s))dW_s, \quad t \in \mathbb{R}, \tag{5.2.2}$$

where g is a positive universal function, depending on the Reynolds number Re and the turbulence intensity I; C_1 and C_2 are normalising constants to be determined. The integral represents the time-varying part u in the Reynolds decomposition. The scaling property of the Fourier transform, i.e. that for $c > 0$, $c\mathcal{F}\{g(c\,\cdot)\}(\xi) = \mathcal{F}\{g(\cdot)\}(\xi/c)$, gives

$$E_L^\tau(\omega) = (C_2/C_1)^2 |\mathcal{F}\{g(\cdot)\}|^2 \,(\omega/C_1)\,.$$

Using (5.1.4) replacing Φ_L with Φ_L^{Re}, i.e. without considering the limit for $\mathrm{Re} \gg 1$, and (5.2.1), the relation between the rescaled spatial spectrum and the time spectrum is given by

$$v_\eta^2 \eta \Phi_L^{\mathrm{Re}}(\eta\kappa_1) = U(C_2/C_1)^2 |\mathcal{F}\{g(\cdot)\}|^2 \,(\Lambda_I(U\kappa_1/C_1))\,. \tag{5.2.3}$$

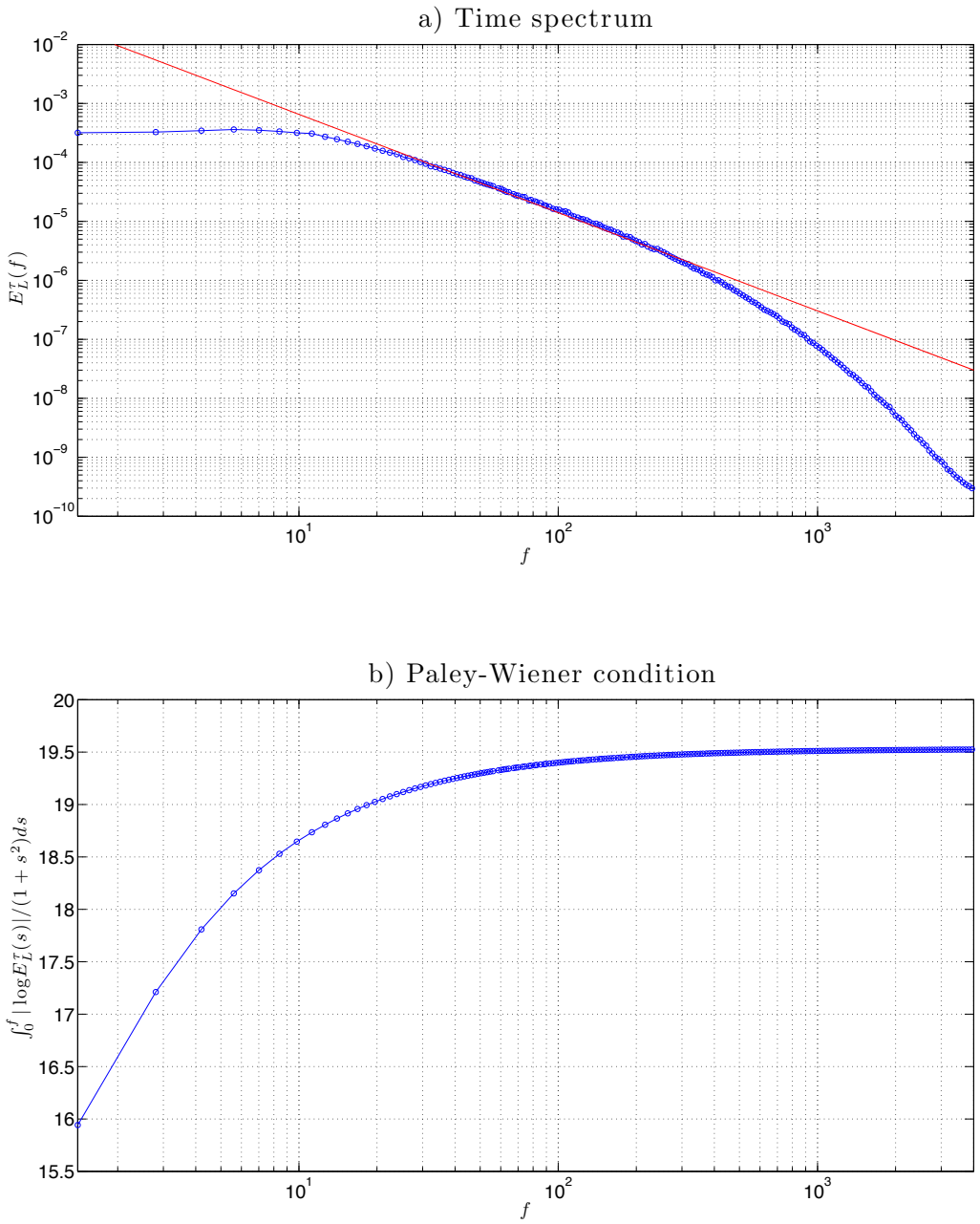

Figure 5.1.: a) Time spectrum for data set h3, the solid line indicates Kolmogorov 5/3 law. b) Convergence of the Paley-Wiener integral (5.1.1). The spectral density is estimated with the Welch method, using a Hamming window of 2^{14} data points and 60% overlap.

Matching both sides of (5.2.3), we get $C_1 = U/(2\pi\eta) = f_\eta$, i.e. the Kolomogorov frequency, and $C_2^2 = U/v_\eta\epsilon$. The Reynolds decomposition can be rewritten as

$$V_t = U + \sqrt{\frac{U}{v_\eta}} \int_{-\infty}^{t} g(f_\eta(t-s))d\tilde{W}_s, \tag{5.2.4}$$

where $d\tilde{W}_s = \sqrt{\epsilon}dW_s$ such that $\mathbb{E}[(d\tilde{W}_s)^2] = \epsilon ds$. The time-wise increments of the mean flow velocity, at time scale Δ, can be calculated from (5.2.4) as

$$\delta_t^\Delta V = V_t - V_{t-\Delta} = \int_{-\infty}^{t-\Delta} [\bar{g}(t-s) - \bar{g}(t-\Delta-s)]d\tilde{W}_s + \int_{t-\Delta}^{t} \bar{g}(t-s)d\tilde{W}_s,$$

where $\bar{g}(\cdot) := \sqrt{U/v_\eta}\; g(f_\eta \cdot)$. If $\Delta^{-1}\int_{t-\Delta}^{t} \bar{g}(t-s)d\tilde{W}_s \to 0$ a.s. as $\Delta \downarrow 0$, we have that the derivative process is, with the limit assumed to exist a.s.,

$$\partial_t V = \lim_{\Delta\downarrow 0} \Delta^{-1}\delta_t^\Delta V = \sqrt{\frac{U}{v_\eta}} f_\eta \int_{-\infty}^{t} g'(f_\eta(t-s))d\tilde{W}_s,$$

i.e. it is again a model of the form (5.1.2) and we essentially exchanged integration and differentiation. Moreover, plugging (5.1.4) into (5.1.8) we obtain

$$\epsilon = 15\nu\frac{v_\eta^2}{\eta^2}\int_{\mathbb{R}} s^2\Phi_L(s)ds,$$

and, recalling the definition of v_η and η and (5.2.3), we get

$$\|\mathcal{F}\{g(\cdot)\}(\Lambda_I(\cdot))\;\cdot\|_{L^2}^{-2} = 15. \tag{5.2.5}$$

The Plancherel theorem, the fact that

$$i\xi\mathcal{F}\{g(\cdot)\}(\xi) = \mathcal{F}\{g'(\cdot)\}(\xi)$$

and (5.2.5) give that $\|g'\|_{L^2}^{-2} \approx 15/2\pi$ for $I \ll 1$.

Eq. (5.1.7) gives the instantaneous energy dissipation

$$\varepsilon_t := \frac{15\nu}{U^2}(\partial_t V)^2 = \frac{15 f_\eta}{2\pi}\int_{-\infty}^{t}\int_{-\infty}^{t} g'(f_\eta(t-s_2))g'(f_\eta(t-s_1))d\tilde{W}_{s_1}d\tilde{W}_{s_2}, \tag{5.2.6}$$

whose mean value is $\varepsilon = \mathbb{E}[\varepsilon_t] = 15/2\pi\|g'\|_{L^2}^2\epsilon \approx \epsilon$ when $I \ll 1$.

The constant U/v_η is a-dimensional, serving as a scaling factor of the model. Moreover, the rescaled model (5.2.4) indicates that $\{(d\tilde{W}_s)^2\}_{s\in\mathbb{R}}$ can account for the observed intermittency, i.e. it must provide all the higher order features of turbulence that can not be reproduced by a Gaussian model, as, for instance, the non-Gaussian behaviour of the

instantaneous energy dissipation $\{\varepsilon_t\}_{t\in\mathbb{R}}$ as indicated by (5.2.6). Moreover, we stress that g is a second order parameter of V, and so is g'.

The model $d\tilde{W}_s = \sqrt{\sigma_s}dB_s$ with Brownian motion $\{B_t\}_{t\in\mathbb{R}}$ has been suggested in Barndorff-Nielsen and Schmiegel (2008a), where $\sqrt{\sigma_s}$ is the random intermittency process, assumed to be independent of B, and $\{\sigma_s\}_{s\in\mathbb{R}}$ is the instantaneous energy dissipation, with mean rate $\mathbb{E}[\sigma_s] = \epsilon$. The major shortcoming of this model is that the Brownian motion assumption implies that the distribution of the increment process $\{\delta_t^\Delta V\}_{t\in\mathbb{R}}$ is symmetric around zero for every scale Δ, which is against experimental and theoretical findings, especially at small scales (see e.g. Frisch (1996), Section 8.9.3). Such shortcoming amended in Barndorff-Nielsen and Schmiegel (2009) by assuming the presence of a possibly non-stationary drift Z, in addiction to the CMA X, where Z is smoother than X (see e.g. Barndorff-Nielsen and Schmiegel (2009), Remark 6). The assumed smoothness of Z implies that the drift has a negligible effect on small scales increments, and is therefore more suitable for modelling phenomena at larger scales, such as the energy containing range.

From a second order point of view, everything depends on U, Re, ϵ and ν, which are the parameters of (5.2.4). Moreover, given that the dependence of g on Re is known, it is easy to simulate a process having the prescribed time spectrum. As long as only second order properties are of interest, one can indeed take $\{W_t\}_{t\in\mathbb{R}} = \{B_t\}_{t\in\mathbb{R}}$. If realistic higher order properties are desired, a realistic model for W is needed.

5.2.3. Dependence of the kernel function on the Reynolds number

It has been observed from experimental evidence (see e.g. Frisch (1996), Section 5.2) that the mean energy dissipation ϵ is independent of the Reynolds number provided $\mathrm{Re} \gg 1$.

Since $v_\eta\eta/\nu = 1$, as in (4), $U/v_\eta = \mathrm{Re}\,\eta/L$ holds. From Eq. (6.8) of Pope (2000) we have that $U/v_\eta \propto \mathrm{Re}^{1/4}$. From (5.1.3), the variance of the mean flow velocity V is

$$\mathbb{E}[u^2] = \mathbb{E}[(V-U)^2] = v_\eta^2\|g\|_{L^2}^2, \tag{5.2.7}$$

where v_η is independent of Re, when $\mathrm{Re} \gg 1$, and $\|g\|_{L^2}$ depends on Re (and to a lesser extent on I). Then the turbulence intensity of (5.2.4) is, using (5.2.7),

$$I = \frac{\sqrt{\mathbb{E}[u^2]}}{U} = \frac{v_\eta}{U}\|g\|_{L^2} \propto \mathrm{Re}^{-1/4}\|g\|_{L^2}.$$

Since I must be independent of Re, we have $\|g\|_{L^2} \propto \mathrm{Re}^{1/4}$.

A parametric model, suggested in Barndorff-Nielsen and Schmiegel (2008a) for the kernel g, is the gamma model

$$g(t) = C_{\mathrm{Re}}t^{\mu_{\mathrm{Re}}-1}e^{-\delta_{\mathrm{Re}}t}, \quad t \geq 0, \tag{5.2.8}$$

where $\mu_{\mathrm{Re}} > 1/2$ and $\delta_{\mathrm{Re}}, C_{\mathrm{Re}} > 0$. This model yields a power-law time spectrum Pope (2000)

$$E_L^\tau(\omega) = (2\pi)^{-1} C_{\mathrm{Re}}^2 \Gamma^2(\mu_{\mathrm{Re}})(\delta_{\mathrm{Re}}^2 + \omega^2)^{-\mu_{\mathrm{Re}}}, \tag{5.2.9}$$

where $\Gamma(\cdot)$ is Euler gamma function. For instance, the von Kármán spectrum von Kármán (1948) is a special case of (5.2.9), where $\mu_{\mathrm{Re}} = 5/6$ and $C_{\mathrm{Re}} = \sqrt{\pi C}/\Gamma(\mu_{\mathrm{Re}}) \approx 1.1431$, and C is the Kolmogorov constant, which has been found to be around 0.53 over a large number of flows and Reynolds numbers, and therefore universal and independent of the Reynolds number Sreenivasan (1995). For $\omega \ll \delta_{\mathrm{Re}}$, the spectrum (5.2.9) is constant; hence $\omega \approx \delta_{\mathrm{Re}}$ can be interpreted as the *transition frequency* from the inertial range to the energy containing range; moreover, since the upper limit of the inertial range is independent of the Reynolds number, the size of the inertial range varies as $\delta_{\mathrm{Re}}^{-1}$.

The gamma model has two essential shortcomings: firstly, it fails to model the steeper spectral decay in the dissipation range, but can be regarded as a good model for the inertial range. Secondly, the kernel has unbounded support, implying that the process is significantly autocorrelated even for large times, although the autocorrelation is exponentially decaying.

From now on, we shall assume that the kernel function g has compact support, i.e. $g(t) = 0$ for $t > T_{\mathrm{Re}}$ and $t < 0$, where T_{Re} is the decorrelation time (O'Neill et al. (2004)). Since the inertial range increases with Re (see e.g. Pope (2000), p. 242) we expect δ_{Re} to decrease. For the same reason we expect T_{Re} to increase with Re.

Explicit computations can be carried out for the truncated gamma model, considering a truncation at T_{Re} and assuming that the failure of the gamma model in the dissipation range does not significantly affect $\|g\|_{L^2}$. Then

$$\|g\|_{L^2}^2 = C_{\mathrm{Re}}^2 \int_0^{T_{\mathrm{Re}}} s^{2(\mu_{\mathrm{Re}}-1)} e^{-2\delta_{\mathrm{Re}} s} ds = \frac{\Gamma\left(2\mu_{\mathrm{Re}} - 1\right) - \Gamma\left(2\mu_{\mathrm{Re}} - 1, 2T_{\mathrm{Re}}\delta_{\mathrm{Re}}\right)}{C_{\mathrm{Re}}^{-2} 2^{2\mu_{\mathrm{Re}}-1}} (\delta_{\mathrm{Re}})^{1-2\mu_{\mathrm{Re}}},$$

where $\Gamma(a, z) := \int_z^\infty s^{a-1} e^{-s} ds$. If $T_{\mathrm{Re}}\delta_{\mathrm{Re}} \gg 0$ and it does not vary too much with Re, with the choice of the parameters as in the von Kármán spectrum and the fact that $\|g\|_{L^2} \propto \mathrm{Re}^{1/2}$, we get $\delta_{\mathrm{Re}} \propto \mathrm{Re}^{-3/4}$.

5.3. Estimation of the kernel function

5.3.1. The data

In this Section we estimate the kernel function g non-parametrically, the parameters of model (5.2.4), and the increments of the driving noise W. Not surprisingly, the quality of the data in the present study does not allow us to perform a reliable estimation in the dissipation range. For the kernel in the universal equilibrium range, the gamma model (5.2.8) is estimated by the non-parametric kernel estimation method as suggested in Chapter 2.

Data	$\epsilon \cdot 10^2$ $m^2 s^{-3}$	η μm	λ mm	R_λ	F kHz	f_η kHz	I %	$\|g\|_{L^2}$	μ_{Re}	$\delta_{Re} \cdot 10^4$	$T_{Re} \cdot 10^{-2}$	C_2
h1	2.72	36.42	0.76	112	5.74	1.14	20.56	5.37	0.76	363.85	0.98	0.84
h2	0.52	55.07	1.11	105	2.87	0.52	19.19	5.21	0.73	387.11	1.05	0.38
h3	20.14	22.08	0.55	162	22.97	3.57	21.47	6.46	0.85	276.51	1.38	2.46
h4	0.85	15.7	0.49	253	5.74	1.74	24.04	8.08	0.81	120.81	3.06	0.53
h5	13.14	24.56	0.66	184	45.94	6.01	10.98	6.9	0.95	316.1	1.25	2.87
h6	10.98	8.28	0.36	495	22.97	9.02	23.34	11.31	0.83	63.57	5.95	2.31
h7	64.37	5.32	0.26	640	91.88	25.66	22.58	12.85	0.87	49.87	7.53	6.05
h8	1995.62	2.25	0.14	930	367.5	175.68	22.15	15.5	0.84	22.95	13.81	37.37
h9	2120.81	2.22	0.14	978	367.5	190.05	21.64	15.89	0.84	21.78	15.79	39.46
h10	5192.01	1.78	0.11	1005	367.5	285.13	22.88	16.11	0.83	18.13	18.42	60.46
h11	13580.72	1.4	0.1	1336	735	570.02	21.34	18.58	0.8	11.76	26.57	108.72
a1	1.38	837.47	140.01	7216	10	1.21	15.29	43.16	0.77	0.55	282.72	1.97
a2	9.41	442.42	115.85	17706	5	2.99	28.23	67.61	0.81	0.24	882.39	4.75

Table 5.1.: h1-h11: Helium data (Chanal et al. (2000)), a1: Sils-Maria data (Gulitski et al. (2007)), a2: Brookhaven data (Drhuva (2000)). The norm $\|g\|_{L^2}$ is evaluated using (5.2.7).

We analysed 13 different data sets, whose characteristics are summarised in Table 5.1. Also dependence of the parameters on Re is considered. Two of the data sets examined here come from the atmospheric boundary layer (a1, described in Gulitski et al. (2007), and a2, see Drhuva (2000)) and eleven from a gaseous helium jet flow (records h1 to h11, see Chanal et al. (2000)). Since the data sets come from different experimental designs, characteristic quantities such as Taylor microscale Reynolds number $R_\lambda = \sqrt{\mathbb{E}[u^2]}\lambda/\nu$ based on Taylor microscale $\lambda = \sqrt{15\mathbb{E}[u^2]\nu/\epsilon}$ are considered. This Reynolds number is unambiguously defined and the rough estimate $R_\lambda \propto \sqrt{2\,\mathrm{Re}}$ holds (Pope (2000), p. 245). In all data sets the turbulence intensity I is rather high and, therefore, the expectation of the RHS of (5.1.7) would not be a good approximation for ϵ. Moreover, in most of the data sets the inertial range is hard to identify due to low Reynolds numbers. The mean energy dissipation ϵ has been estimated from (5.1.6), following Lindborg (1999). Estimation of ϵ is a challenging and a central task, since the rescaling constants in (5.2.4) depend, in the K41 spirit, only on ϵ, ν and U.

5.3.2. Kernel estimation

The kernel function g characterises the second order properties of the mean flow velocity V, i.e. spectrum, autocovariance and second order structure function. Classical time-series methods have been employed to estimate the kernel function of high frequency data Chapter 2 with a non-parametric method. The method is essentially based on finding the unique function g solving (5.1.3), when the autocovariance function γ_X is given. We estimate the discrete autocovariances $\gamma_X^\Delta(i) := \gamma_X(i\Delta)$, where Δ is the sampling grid size and i are integer values. It has been shown in Chapter 2 that the coefficients of a high order discrete-time moving average process fitted to such closely observed autocovariance func-

tion, when properly rescaled, estimate consistently the kernel function. We shall assume that the estimation of the kernel function is on the mid-point grid; i.e, $\hat{g}(i) \approx g((i+1/2)\Delta)$ for integers i.

The results are presented in Figure 5.2a), where all the estimated kernels are plotted on a logarithmic time axis. Due to instrumental noise, the high turbulence intensity of the data sets and the non-infinitesimal dimension of the hot-wires, estimates in the dissipation range ($tf_\eta < 1$) differ significantly from one data set to another. In general we notice that the steeper decay of the spectrum in the dissipation range is reflected by the fact that the kernel functions tend to 0 for $tf_\eta \ll 1$, instead of exploding as the gamma model for $\mu_{\mathrm{Re}} = 5/6$. The only estimation of the kernel that is not perfectly aligned with the others is the one for h5, which looks slightly shifted to the left. This can be attributed to the difficulty in estimating ϵ, and consequently f_η. In Figure 5.2c) the estimated $\|g\|_{L^2}$ based on (5.2.7) are plotted against R_λ, and the power-law fitting shown in the figure returned $\|g\|_{L^2} = 0.5081\,\mathrm{R}_\lambda{}^{0.5} \propto \mathrm{Re}^{0.25}$.

The decorrelation time T_{Re} has been estimated by the first zero-crossing of the estimated g. It increases with R_λ (Figure 5.2a)) and it follows empirically the law $T_{\mathrm{Re}} = 0.1408\,\mathrm{R}_\lambda{}^{1.3613} \propto \mathrm{Re}^{0.6806}$ (Figure 5.2c)).

The transition frequency δ_{Re} is obtained via least squares fitting of the gamma model (5.2.8) to the non-parametric estimate of g for $tf_\eta > 5$ (Figure 5.2b)). The statistical fits in Figure 5.2b) are very good for all data sets considered, at least when not too close to T_{Re}. The transition frequency follows the empirical law $\delta_{\mathrm{Re}} = 61.4917\,\mathrm{R}_\lambda{}^{-1.5127} \propto \mathrm{Re}^{-0.7564}$ (Figure 5.2e)), which is exceptionally close to the exponent $-3/4$ obtained from the gamma model, and $\delta_{\mathrm{Re}} T_{\mathrm{Re}}$ is between 1.5 and 4.1 in all data sets. The estimated values of μ_{Re} are also close to the reference value of $5/6 \approx 0.834$, with a mean value of 0.8218. The only notable outlier is the data set h5, which has been already proven to be somewhat anomalous.

As said in Section 2.3, the truncated gamma model is not able to capture the sharp cutoff in the neighbourhood of T_{Re} nor the rapid decrease in the dissipation range.

To estimate how the variance of the model (5.1.2) is affect by the truncation at T_{Re}, we consider the quantity

$$H(\mathrm{Re}) = \frac{\|g(\cdot)\Theta(T_{\mathrm{Re}} - \cdot)\|_{L^2}^2}{\|g(\cdot)\|_{L^2}^2} = 1 - \frac{\Gamma(2/3, 2c_1c_2\mathrm{Re}^{\beta-\alpha})}{\Gamma(2/3)}$$

where the latter is obtained using the gamma kernel (5.2.8) with parameters $\mu_{\mathrm{Re}} = 5/6$, $T_{\mathrm{Re}} = c_1\mathrm{Re}^{\beta}$ and $\delta_{\mathrm{Re}} = c_2\,\mathrm{Re}^{-\alpha}$, where $c_1, c_2 > 0$ and $\alpha > \beta > 0$, as indicated by the least squares in Figure 5.2. H represents the ratio between the variance (5.2.7) using a truncated gamma model and a non-truncated one, and it is a decreasing function of Re, and it tends to 0 as $\mathrm{Re} \gg 1$, indicating that the truncation is important when $\mathrm{Re} \gg 1$; i.e., when $T_{\mathrm{Re}}\delta_{\mathrm{Re}} \ll 1$. Nonetheless, using the values of c_1, c_2, α, β returned by the least squares fitting, we obtain $H \approx 0.991$ for the dataset a2, which exhibits the highest Reynolds

number among the considered datasets. Then we can conclude that, for the wide range of Reynolds numbers considered, the variance of the model (5.1.2) with a kernel following the truncated gamma model does not differ in a sensible way from the variance of the classical von Kárman model.

Finally, the behaviour of δ_{Re} as function of Re estimated via the gamma model agrees significantly with the data, showing that the dissipation range does not contribute appreciably to $\|g\|_{L^2}$, which is in agreement with the idea that there is few energy in the dissipation range.

5.4. A model for the driving noise

In this section, we present our intermittency model from Eqs. (5.1.9)-(5.1.10) in a rigorous manner. We outline its specific features in detail. In addition, we discuss the statistical methods for its estimation from discrete observations.

On the filtered probability space $(\Omega, \mathcal{F}, (\mathcal{G}_t)_{t\in\mathbb{R}}, \mathbb{P})$, let $L = \{L_t\}_{t\in\mathbb{R}}$ be a two-sided, real-valued Lévy process without Gaussian part and Lévy measure F given by (5.1.10). We suppose that $\mathbb{E}[L_t] = 0$; its characteristic exponent takes the form

$$\log \mathbb{E}[e^{itL_1}] = \int \left(e^{itx} - 1 - itx\right) F(dx)$$

and, for $n \geq 2$, its cumulants are given by $c_n := c_n[L_1] := \int x^n F(dx)$. The time-change process

$$T_t := \int_0^t Y_s ds \quad \text{is a} \mathcal{G}_t\text{-stopping time for all} t \in \mathbb{R}.$$

The process Y is, in the light of the previous formula, is called the activity process. We shall suppose, that $\mathbb{E}[Y_0] = 1$, so that $\mathbb{E}[T_t] = t$.

From now on, we shall assume that the intermittency process, which acts as driving process of the CMA process (5.2.2), is a time-changed Lévy process, that is

$$W_t = L_{T_t}, \quad t \in \mathbb{R}.$$

By Corollaire 10.12 of Jacod (1979), the time-changed Lévy process $W = \{W_t\}_{t\in\mathbb{R}}$ given by 5.1.9 is a purely discontinuous martingale w.r.t. the filtration given by $\mathcal{F}_t := \mathcal{G}_{T_t}$; the process has càdlàg sample paths and $W_0 = 0$. The integer-valued random measure $\mathfrak{m}$ on $\mathbb{R} \times \mathbb{R}$ given by

$$\mathfrak{m}(\omega; dt, dx) := \sum_{\{s:\Delta W_s(\omega)\neq 0\}} \delta_{(s,\Delta W_s(\omega))}(dt, dx),$$

where δ_x denotes the Dirac measure at x, is called its *jump measure*. By Theorem II.2.34 of Jacod and Shiryaev (2003), moreover, the increments $W_{t+s} - W_t$ can be represented as

the stochastic integral, for $s > 0$,

$$W_{t+s} - W_t = \int_{]t,t+s]\times\mathbb{R}} x(\mathfrak{m} - \mathfrak{n})(dr, dx), \quad t \in \mathbb{R}, \tag{5.4.1}$$

where $\mathfrak{n}(\omega; dt, dx) = Y_t(\omega)dtF(dx)$ is the predictable compensator of $\mathfrak{m}$. The moments and autocovariance function of the intermittency increments and their squares are determined by the cumulants of L and the mean and autocovariance of Y (see e.g. Kallsen and Muhle-Karbe (2011), Theorem 2.2).

In particular, the autocovariance function of the squared increments of the intermittency process is linked to the activity process Y by the formula

$$\begin{aligned}\bar{\gamma}_Y^{\Delta}(k\Delta) &:= \operatorname{Cov}\left[(W_{k\Delta} - W_{(k-1)\Delta})^2, (W_{(k+j)\Delta} - W_{(k+j-1)\Delta})^2\right] \\ &= \operatorname{var}[L_1]^2 \operatorname{Cov}\left[\int_0^{\Delta} Y_{(k-1)\Delta+s}ds, \int_0^{\Delta} Y_{(k+j-1)\Delta+r}dr\right]\end{aligned} \tag{5.4.2}$$

for every $k \in \mathbb{Z}$, $j \in \mathbb{N}$ and $\Delta > 0$. W.l.o.g. we assume that $\operatorname{var}[L_1] = 1$, then, for $t > 0$, we have (see, e.g., Barndorff-Nielsen and Shepard 2006, Proposition 5)

$$\begin{aligned}\bar{\gamma}_Y^{\Delta}(t) =& \int_0^{t+\Delta}\int_0^u \gamma_Y(s)dsdu - 2\int_0^t\int_0^u \gamma_Y(s)dsdu + \int_0^{t-\Delta}\int_0^u \gamma_Y(s)dsdu \\ =& \gamma_Y(t)\Delta^2 + o(\Delta^2) \quad \Delta \downarrow 0,\end{aligned}$$

where γ_Y is the autocorrelation function of the activity process Y.

By construction, we have

$$\mathbb{E}[W_t] = 0, \quad \operatorname{var}[W_t] = tc_2\mathbb{E}[Y_0], \quad t \in \mathbb{R}_+.$$

Recalling that W is supposed to be the driving process of the CMA model for the velocity V, furthermore, we assume that the intermittency process is normalised such that $c_2 = \operatorname{var}[W_1] = 1$. Under this assumptions, we note that

$$\mathbb{E}[W_t^3] = tc_3, \quad \mathbb{E}[W_t^4] = tc_4 + 3(\tilde{\gamma}_Y(t) + t^2), \quad t \in \mathbb{R}_+, \tag{5.4.3}$$

where

$$\tilde{\gamma}_Y(t) := 2\int_0^t\int_0^u \gamma_Y(s)dsdu$$

(see, e.g., Barndorff-Nielsen and Shepard 2006, Proposition 2). Dividing both sides of (5.4.2) by $\operatorname{var}[W_{\Delta}^2] = \mathbb{E}[W_{\Delta}^4] - (\mathbb{E}[W_{\Delta}^2])^2$, moreover, we obtain that the autocorrelation

$$\rho_{W^2}^{\Delta}(k) := \operatorname{cor}[(W_{\Delta} - W_0)^2, (W_{(k+1)\Delta} - W_{k\Delta})^2]$$

of the squared intermittency increments for $k \in \mathbb{N}^*$, in addition, is given by

$$\rho^{\Delta}_{W^2}(k;\theta) = \frac{\bar{\gamma}^{\Delta}_Y(k\Delta)}{c_4\Delta + 2\Delta^2 + 3\tilde{\gamma}_Y(\Delta)}. \tag{5.4.4}$$

From (5.4.4) it is clear that the autocorrelation function of the increments of the intermittency process is, for small Δ, given, up to a scaling factor, by the autocovariance of the activity process Y.

Therefore we let the activity $Y = \{Y_t\}_{t\in\mathbb{R}}$ be again a CMA process, independent of L, namely

$$Y_t := \int_{-\infty}^{t} g_Y(t-s;\theta)dZ_s, \quad t \in \mathbb{R}, \tag{5.4.5}$$

where Z is a Lévy subordinator, g_Y is square integrable function, depending on a list of parameters θ. Since the driving subordinator Z of Y satisfies $\mathrm{var}[Z_1] = 1$ by assumption, the autocovariance function $\gamma_Y : \mathbb{R} \to \mathbb{R}_+$ of Y is given by the usual formula

$$\gamma_Y(t;\theta) := \mathrm{Cov}[Y_0, Y_t] = \int_0^{\infty} g_Y(s;\theta)g_Y(|t|+s;\theta)ds, \quad t \in \mathbb{R}. \tag{5.4.6}$$

The autocorrelation given by the gamma kernel (see Example II.i) tends to a constant as the argument goes to zero, with the leading term in the Taylor expansion having order $2\nu - 1$. This model not able to reproduce the sharp decay observed autocorrelation of the squared increments of the velocity, which is widely believed to follow a power law $\tau^{-0.2}$ for τ finite and bigger than zero (Cleve (2004)). The squared increments of the intermittency process W show a rather similar behaviour(see e.g. Figure 5.4).

The most obvious choice would be to allow the gamma kernel to have $0 < \nu < 0.5$, but that would lead to a gamma kernel with infinite L^2 norm, and it would not be a legitimate kernel for a CMA process with finite variance. A solution, inspired by Cleve (2004), is to truncate the kernel near to the origin at some cut-off ζ, yielding a square-integrable kernel for every value of ν. More specifically, we assume the kernel g_Y belongs to the family

$$g_Y(t) = g_Y(t;\theta) = \begin{cases} C\sigma\zeta^{\nu-1}\exp(-\lambda\zeta) & \text{if} 0 \le t < \zeta, \\ C\sigma t^{\nu-1}\exp(-\lambda t), & \text{if} t \ge \zeta, \end{cases} \tag{5.4.7}$$

with strictly positive parameters $\theta = (\sigma, \nu, \lambda, \zeta)$, and $C = C_{\nu,\lambda,\zeta} > 0$ is a normalising constant such that $\int g_Y(t;\theta)^2 dt = \sigma^2$. Then the autocovariance function given by this kernel will be flat for $\tau \ll \zeta$ and it will behave as $\tau^{2\nu-1}$ for $\tau \gg \zeta$, as suggested in Cleve (2004), Section 4.2.

We stress that, at this point, Z remains some unspecified Lévy subordinator with $\mathrm{var}[Z_1] = 1$ such that Y is independent of L, non-negative, and with finite fourth moment.

5.4.1. Estimation of the intermittency model from discrete observations

We suppose to observe the intermittency process W on a discrete-time grid with sampling interval $\Delta > 0$. In particular for some $n \in \mathbb{N}^*$, we observe a realisation of the increments

$$\Delta_k^n W := W_{k\Delta} - W_{(k-1)\Delta}, \quad \text{for } k = 1, \dots, n.$$

The jumps of the process and the time-change are latent.

First, we turn to the estimation of the parameters $\theta = (\sigma, \nu, \lambda, \zeta)$ of the kernel g_Y given by (5.4.7). For typographical convenience, set $\mu_4 := \mathbb{E}[W_\Delta^4]$. Solving (5.4.3) for c_4 and plugging it into (5.4.4), we obtain

$$\rho_{W^2}^\Delta(k; \theta, \mu_4) = \frac{\bar{\gamma}_Y^\Delta(k; \theta)}{\mu_4 - \Delta^2}, \tag{5.4.8}$$

where we emphasise the dependence on μ_4. We estimate the parameters θ, performing a least squares fit of $\rho_{W^2}^\Delta(k; \theta, \mu_4)$ to its empirical version: In particular, let $\hat{\mu}_4$ (resp., $\hat{\rho}_{W^2}^\Delta$) denote the empirical fourth moment of the observed increments $\Delta_k^n W$ (resp., the empirical autocorrelation function of the squared increments $(\Delta_k^n W)^2$). Then, our estimator of θ is given by

$$\hat{\theta} := \operatorname*{argmin}_{\theta \in \mathbb{R}_+^4} \sum_{k \in \mathbb{N}^*} \left| \hat{\rho}_{W^2}^\Delta(k) - \rho_{W^2}^\Delta(k; \theta, \hat{\mu}_4) \right|^2.$$

Second, we turn to the estimation of the Lévy density of the Lévy process L. The class of tempered stable Lévy measures (5.1.10) is truly of semi-parametric nature. By Bernstein (1929), every bounded, completely monotone function is the Laplace transform of some finite measure Q on $\mathbb{R}_+^*$; that is, $x \mapsto \int_0^\infty e^{-\lambda x} Q(\mathrm{d}\lambda)$. In literature, parametric estimation of tempered stable Lévy densities is often based on the assumption that – for known orders $p_+, p_- \in \mathbb{N}^*$ – it belongs to the $2(p_+ + p_-) + 1$-parametric sub-family

$$f(x; \theta_{p_+,p_-}) = \begin{cases} x^{-1-\alpha} \sum_{k=1}^{p_+} c_k^+ \exp(-\lambda_k^+ x) & \text{for } x > 0, \\ |x|^{-1-\alpha} \sum_{k=1}^{p_-} c_k^- \exp(-\lambda_k^- |x|) & \text{for } x < 0, \end{cases} \tag{5.4.9}$$

where all parameters $\theta_{p_+,p_-} := (\alpha, (c_k^+, \lambda_k^+)_{k=1,\dots,p_+}, (c_k^-, \lambda_k^-)_{k=1,\dots,p_-})$ are strictly positive and, in addition, $\alpha < 2$. In view of the number of parameters, (5.4.9) is frequently used for low orders. The issue of order selection is rarely addressed. We use a two-step approach to circumvent the latter issue. First, we estimate the Lévy density employing an adaptive non-parametric method. Second, we calculate the least squares fits of the parametric model (5.4.9) to our non-parametric estimate for orders $p_+ + p_-$ up to some constant; we normalise our estimates so that the variance $\mathrm{var}[W_1]$ of our fitted model is equal to one; and we penalise for deviations from the third and fourth empirical moments. Last, we minimise an information criterion to find our optimal choice for p_+ and p_-.

Various non-parametric estimators for the Lévy density of a Lévy process have been suggested in literature. Here, we focus on the projection estimator of Figueroa-López (2009), Figueroa-López (2011) which employs Grenander method of sieves. In particular, let μ be some absolutely continuous Borel measure on $\mathbb{R}^*$, called the *reference measure*. We denote the μ-density of the Lévy measure F by f_μ; that is $F(dx) = f_\mu(x)\mu(dx)$. Moreover, let $D \subset \mathbb{R}^*$ be a compact interval not containing zero, called the *domain of estimation*. Throughout, we suppose that f_μ is μ-square integrable over D. For each $m \in \mathbb{N}^*$, let $K_m := \{y_{m,0}, \dots, y_{m,m}\} \subset D$ be such that $\{[y_{m,k-1}, y_{m,k}] : k = 1, \dots, m\}$ forms a μ-uniform partition of D. Then the space $\mathcal{S}_m := \mathcal{S}(3, K_m)$ of cubical $\mathcal{C}^2$-splines with control points K_m is an $m+3$-dimensional subspace of $\mathcal{L}^2(D, \mathcal{D}, \mu)$. The minimum contrast estimator $\hat{f}_\mu^m$ of f_μ w.r.t the sieve $\mathcal{S}_m$, given by

$$\hat{f}_\mu^m := \operatorname*{argmin}_{h \in \mathcal{S}_m} -\frac{2}{n\Delta} \sum_{k=1}^{n} h(\Delta_k^n W) + \int_D h(x)^2 \mu(dx), \tag{5.4.10}$$

coincides with the respective projection estimator (cf. Lemma 2.1 of Ueltzhöfer and Klüppelberg 2011).

By Figueroa-López (2009), under some hypothesis on Y, the estimator $\hat{f}_\mu^m$ is consistent for the μ-density f_μ of the Lévy measure F if $n\Delta \to \infty$, $\Delta \to 0$ fast enough, and $m \to \infty$. For some related, pointwise central limit theorem, we refer to Figueroa-López (2011).

For a numerically stable computation of $\hat{f}_\mu^m$, we construct the B-spline basis $\mathcal{B}_m := \{h_{m,j} : j = 1, \dots, m+3\}$ of the space $\mathcal{S}_m := \mathcal{S}(3, K_m)$, and denote the Gramian matrix w.r.t μ by $A = (a_{ij})_{i,j=1,\dots,m+3}$; that is,

$$a_{ij} := \int_D h_{m,i}(x) h_{m,j}(x) \mu(dx).$$

Let $h_m : \mathbb{R} \to \mathbb{R}^{m+3}$ be the mapping with components $h_{m,j}$. Then the unique minimiser in (5.4.10) is given by

$$\hat{f}_\mu^m(x) = \sum_{j=1}^{m+3} \hat{c}_{mj} h_{m,j}(x), \quad \text{where} \quad \hat{c}_m := A^{-1} \left(\frac{1}{n\Delta} \sum_{k=1}^{n} h_m(\Delta_k^n W) \right).$$

For each $m \in \mathbb{N}^*$, we are given an estimator $\hat{f}_\mu^m$ of f_μ on D; its associated contrast value is equal to $-(\hat{c}_m)^\top A \hat{c}_m$. As a data driven sieve selection method, we employ the penalisation method which Ueltzhöfer and Klüppelberg (2011) studied in the pure Lévy case. For $\zeta_1 \geq 1$ and $\zeta_2, \zeta_3, \zeta_4 > 0$, in particular, let $\mathrm{pen} : \mathbb{N}^* \to \mathbb{R}$ be the penalty function given by

$$\begin{aligned} \mathrm{pen}(m) := {} & \zeta_1 (n\Delta)^{-2} \operatorname{tr}\left((h_m(\Delta_k^n W))_{k \leq n}^\top A^{-1} (h_m(\Delta_k^n W))_{k \leq n} \right) \\ & + \zeta_2 \left(\frac{\mathfrak{D}_m}{n\Delta} \vee \frac{\mathfrak{D}_m^3}{(n\Delta)^4} \right) + \zeta_3 \left(\frac{\mathfrak{D}'_m}{n\Delta} \vee \frac{\mathfrak{D}_m'^3}{(n\Delta)^4} \right) + \zeta_4 \left(\frac{m+3}{n\Delta} \vee \frac{(m+3)^3}{(n\Delta)^4} \right), \end{aligned}$$

where

$$\mathfrak{D}_m := \sup_{h\in\mathcal{S}_m} \frac{\sup_{x\in D}|h(x)|^2}{\int_D h(x)^2\mu(dx)}, \quad \text{and} \quad \mathfrak{D}'_m := \sup_{h\in\mathcal{S}_m} \frac{(\int_D |h'(x)|\mu(dx))^2}{\int_D h(x)^2\mu(dx)}. \tag{5.4.11}$$

Then the estimator $\hat{f}_\mu^{\hat{m}}$ where

$$\hat{m} := \operatorname*{argmin}_{m\in\mathbb{N}^*} \left\{-(\hat{c}_m)^\top A\hat{c}_m + \mathrm{pen}(m)\right\}, \tag{5.4.12}$$

is called the *minimum penalised contrast estimator* of f_μ (w.r.t the penalty pen). We plug-in this estimator into the least squares fitting of the parametric family (5.4.9).

In practice, we calculate an estimator $\hat{f}_\mu^{\hat{m}_+}$ on some domain $D_+ \subset]0,\infty[$ and, separately, an estimator $\hat{f}_\mu^{\hat{m}_-}$ on some domain $D_- \subset]-\infty,0[$. For the Lebesgue density f of the Lévy measure F, we are thereby given the non-parametric estimate

$$\hat{f}(x) = \hat{f}_\mu^{\hat{m}_+}(x)\mu'(x)\mathbf{1}_{D_+}(x) + \hat{f}_\mu^{\hat{m}_-}(x)\mu'(x)\mathbf{1}_{D_-}(x). \tag{5.4.13}$$

In general, this estimate is not the restriction of a tempered stable Lévy density to the domain $D_+ \cup D_-$. For orders p_+, p_- up to a specified order, we calculate the least squares fit of the parametric family given by (5.4.9) to our estimate given by (5.4.13) under the constraint that the variance $\mathrm{var}[W_1]$ of our fitted model equals one; and we penalise for deviations of the fitted third and fourth cumulant from the empirical ones (recall (5.4.3)). In particular, our estimator of θ_{p_+,p_-} is given by

$$\begin{aligned}\hat{\theta}_{p_+,p_-} := \operatorname*{argmin}_{\{\theta_{p_+,p_-}:c_2(\theta_{p_+,p_-})=1\}} \Bigg\{ &\int_{D_+\cup D_-} |\hat{f}(x) - f(x;\theta_{p_+,p_-})|^2 dx \\ &+ \zeta\left(\left|\frac{c_3(\theta_{p_+,p_-})\Delta}{\hat{\mu}_3} - 1\right| + \left|\frac{c_4(\theta_{p_+,p_-})\Delta}{\hat{\mu}_4 - 3\Delta^2(\hat{\sigma}^2+1)} - 1\right|\right)\Bigg\},\end{aligned} \tag{5.4.14}$$

where

$$c_n(\theta_{p_+,p_-}) := \Gamma(n-\alpha)\sum_{k=1}^{p_+} c_k^+(\lambda_k^+)^{\alpha-n} + (-1)^n\Gamma(n-\alpha)\sum_{k=1}^{p_-} c_k^-(\lambda_k^-)^{\alpha-n}$$

denotes the n-th cumulant of L_1 corresponding to the Lévy density $f(\cdot,\theta_{p_+,p_-})$, $\zeta > 0$ denotes some penalisation constant, $\hat{\mu}_n$ denotes the n-th empirical moment of the observed increments, and $\hat{\sigma}^2$ belongs to the fitted parameters $\hat{\theta}$ of the kernel g_Y.

5.4.2. An empirical study of the Brookhaven data set

We shall employ the methods illustrated in the Subsection 5.4.1 on the estimation of the noise W for the Brookhaven dataset (entry a2 of Table 5.1). The estimation is carried out

the method illustrate in Chapter 3. This dataset consists of $n = 20 \times 10^6$ measurements taken at a frequency of 5000Hz; the data covers a total time interval of 4000s (66min 40s). We remark that the data set displays a Taylor microscale Reynolds number of approximately 17 000 and is regarded a good representative of fully developed turbulence.

The coefficients of the AR filter in (3.2.5) has been estimated from the sample autocorrelation function of the windspeed with the Durbin-Levinson algorithm, up to a time-lag of 78.8424 s. Consequently, the estimated increments of the intermittency process cover a total time interval of 65 min 21.1276 s. For the remainder, we treat these estimates as if they were observed true increments of the intermittency process; henceforth, we refer to them as the "(intermittency) data" W.

We summarise the data in Figure 5.3: at the top, we plotted the intermittency increments; the clustering of the increments is clearly observable. At the bottom, we present histograms of the increments $W_{k\Delta} - W_{(k-j)\Delta}$ of the intermittency process at time-lags $j\Delta$ for $j = 1, 1000, 10\,000$; for comparison, we also present the densities of a Gaussian random variable scaled to the empirical variance of the intermittency increments. At small-scale, we observe a heavy-tailed distribution; at large-scale, we observe an approximately Gaussian distribution.

For the estimation of the parameters θ of the moving-average kernel g_Y of the CMA process Y given by (5.4.5), first, we calculated the empirical autocorrelation function $\hat{\rho}^{\Delta}_{W^2}$ of the squared, observed intermittency increments $(\Delta^n_k W)^2$. We obtain from Cleve et al. (2004, Table I, data set "a2") that the surrogacy cutoff time is given by 2.5Δ; for this reasons we regard $\hat{\rho}^{\Delta}_{W^2}(k)$ reliable for $k \geq 3$ only. In addition, we observe a significant influence on the empirical autocorrelation function by non-stationary, large scale effects. For the estimation, thus, we consider $\hat{\rho}^{\Delta}_{W^2}(k)$ reliable up to one tenth of the de-correlation time – the lag $\hat{p} := 26\,698$ – only as well. We note that the empirical fourth moment of the increments is given by $\hat{\mu}_4 = 2.166 \times 10^{-6}$. With these considerations in mind, in practice, our estimator for the parameters θ is given by

$$\hat{\theta} := \operatorname*{argmin}_{\theta \in \mathbb{R}^4_+} \sum_{k=3}^{\hat{p}} \left| \hat{\rho}^{\Delta}_{W^2}(k) - \rho^{\Delta}_{W^2}(k; \theta, \hat{\mu}_4) \right|^2,$$

where $\rho^{\Delta}_{W^2}(k; \theta, \hat{\mu}_4)$ is given by (5.4.8). We remark that no closed-form solution is known for the autocorrelation $\gamma_Y(\cdot; \theta)$ of Y given by (5.4.6). In practice, hence, we utilise the convolution theorem, and employ the numerical approximation

$$\left(\gamma_Y(k\Delta/100; \theta)\right)_{|k| \leq 250\hat{p}} \approx \mathcal{D}^{-1} \left| \mathcal{D}\left[\left(g_Y(k\Delta/100; \theta) \right)_{k=0,\ldots,500\hat{p}} \right] \right|^2,$$

where we sample g_Y with a 100-times higher frequency and on a 5-times longer interval than used afterwards; $\mathcal{D}$ denotes the discrete Fourier transform, and $|\cdot|^2$ is understood component-wise. Our estimate is summarised in Figure 5.4 and Table 5.2. We plotted the

Table 5.2.: Least squares estimates of the parameters $\hat{\theta}$ of $g_Y(\cdot;\theta)$

σ	ν	λ	ζ
3.6017	0.2881	0.0325	$1.152 \cdot 10^{-3}$

empirical autocorrelation function $\hat{\rho}^{\Delta}_{W^2}(k)$ (black points) for the lags $k = 1, \ldots, \hat{p}$ and compare it to the estimated autocorrelation function $\rho^{\Delta}_{W^2}(k; \hat{\theta}, \hat{\mu}_4)$ (red solid line). We observe an excellent fit.

Estimation of the Lévy density

For the non-parametric estimation of the Lévy measure, we choose $\mu(dx) = x^{-4}dx$ as reference measure. The main advantage of our particular choice for μ over Lebesgue measure is that the μ-density f_μ of a tempered stable Lévy measure F does not have a pole at zero; in particular,

$$f_\mu(x) = q_+(x)x^{3-\alpha}\mathbf{1}_{\{x>0\}} + q_-(|x|)|x|^{3-\alpha}\mathbf{1}_{\{x<0\}}.$$

We employ the minimum penalised contrast method (5.4.10) and (5.4.12) to estimate f_μ separately on the domains $D_+ = [0.015, 0.8]$ and $D_- = [-0.8, -0.015]$; we choose the end points ± 0.8 as there are no observations with absolute value larger than 0.8 and we choose the end points $\pm 0.015 \approx \pm\sqrt{\Delta}$ to exclude an interval with a radius of about one standard deviation centred at the origin. As penalty coefficients we choose $\zeta_1 = 2$, $\zeta_2 = 1$, $\zeta_3 = 0.5$ and $\zeta_4 = 0.1$. As no closed-form solution is known for the constants $\mathfrak{D}_m$ and $\mathfrak{D}'_m$ in (5.4.11), in practice, we replaced their true value by numerical approximations. In (5.3), we summarised the penalised contrast values (PCV) for the estimators $(\hat{f}^m_\mu)_{m=1,\ldots,5}$ on D_+ and D_-. We note that a local minimum is attained at $\hat{m}_+ = 4$ and $\hat{m}_- = 1$, respectively.

For the Lebesgue density f of the Lévy measure F of the Lévy process L, we are given the non-parametric estimate

$$\hat{f}(x) := \hat{f}^{\hat{m}_+}_\mu(x)x^{-4}\mathbf{1}_{D_+}(x) + \hat{f}^{\hat{m}_-}_\mu(x)x^{-4}\mathbf{1}_{D_-}(x);$$

(recall (5.4.13)). We observe that the non-parametric estimate oscillates around zero for $|x| > 0.3$; since no more than 591 observations – that is, 0.003% of the data – are larger in absolute value than 0.3, for the remainder, we consider our estimate reliable on the set $D = [-0.3, -0.015] \cup [0.015, 0.3]$ only. For all orders $p_+ + p_- \leq 4$, we calculated the penalised least squares estimator $\hat{\theta}_{p_+,p_-}$ defined in (5.4.14); we replaced the integral over the set D by the discrete residual sum of squares given by

$$\mathrm{RSS}(\theta_{p_+,p_-}) := \sum_{k=15}^{300} \left|\hat{f}(x_k) - f(x_k;\theta_{p_+,p_-})\right|^2 + \left|\hat{f}(-x_k) - f(-x_k;\theta_{p_+,p_-})\right|^2,$$

Table 5.3.: Penalised contrast value (PCV) for the estimator $\hat{f}_\mu^m$ on D_+ and D_-

m	PCV on D_+	PCV on D_-
1	-1.283414	-1.016977
2	-1.283749	-1.016962
3	-1.283912	-1.016947
4	-1.283924	-1.016933
5	-1.283870	-1.016879

where $x_k = k/1000$; and chose the penalty constant $\zeta = 5 \times 10^5$. To find an optimal choice for (p_+, p_-), we also calculated the corrected Akaike information criterion

$$\mathrm{AIC_c}(p_+, p_-) := N \log(\mathrm{RSS}(\hat{\theta}_{p_+,p_-})/N) + 2K_{p_+,p_-} + \frac{2K_{p_+,p_-}(K_{p_+,p_-}+1)}{N - K_{p_+,p_-} - 1},$$

where $K_{p_+,p_-} := 2(p_+ + p_-) + 1$ is the number of parameters and $N := 572$ is the number of squared residuals evaluated for RSS. Our results are summarised in Table 5.4.

We observe that $\mathrm{AIC_c}$ is minimised for $p_+ = 1$ and $p_- = 2$. We present the corresponding estimated density in (5.5). The parametric fit $f(x; \hat{\theta}_{1,2})$ (red solid line) is compared to the non-parametric estimate $\hat{f}(x)$ (black points). On the left, both axes are in linear scale whereas, on the right, the y-axis is in logarithmic scale. In linear scale, the parametric and the non-parametric estimate are indistinguishable to the eye.

5.5. Simulation study

First, we specify the Lévy process Z and simulate the CMA process Y of the time change. Second, we simulate the increments of the time-changed Lévy process $W_t = L(\int_0^t Y_s ds)$ based on the realisation of Y. Finally, we compare our simulated path and the intermittency data.

In our model, the activity process Y is a causal continuous-time moving-average. We simulate from it using some numerical approximations. In particular, we approximate the stochastic integral defining the CMA process by a stochastic Riemann sum: for $\Delta_1 > 0$, let $\{\tilde{Y}_t^{\Delta_1}\}_{t\in\mathbb{R}}$ be given by

$$\tilde{Y}_t^{\Delta_1} := \sum_{k=-\infty}^{\lfloor t/\Delta_1 \rfloor} g_Y\left((\lfloor t/\Delta_1 \rfloor - k)\,\Delta_1; \hat{\theta}\right)\left(Z_{k\Delta_1} - Z_{(k-1)\Delta_1}\right); \tag{5.5.1}$$

then $\mathbb{E}[|\tilde{Y}_t^{\Delta_1} - Y_t|^2] \to 0$ as $\Delta_1 \to 0$ for every $t \in \mathbb{R}$. To achieve a good approximation of Y on some time interval $[t_1, t_2]$, we simulate from the driving process Z on a much longer

Table 5.4.: (Penalised) least square fitting of the parametric families $f(x;\theta_{p_+,p_-})$ in (5.4.9) to the non-parametric estimate $\hat{f}(x)$ given by (5.4.13).

p_+	$\hat{c}_k^+$	$\hat{\lambda}_k^+$	p_-	$\hat{c}_k^-$	$\hat{\lambda}_k^-$	$\hat{\alpha}$	$\mathrm{AIC_c}$
1	2.542	14.35	1	3.101	24.17	1.314	4361.4
1	0.618	10.33	2	0.740	19.86	1.390	3911.4
				16.879	438.58		
2	0.177	6.67	1	0.219	17.17	1.487	4059.6
	16.156	1031.79					
2	63.279	37.81	2	76.977	47.44	0.701	5544.7
	782.867	2346.48		4.229	243.94		
1	0.012	9.57	3	0.014	19.68	1.411	3937.4
				0.001	162.75		
				0.539	518.30		
3	0.180	6.74	1	0.222	17.14	1.487	4062.6
	0.000	198.51					
	15.238	928.82					

interval $[t_0, t_2]$ with $t_0 \ll t_1$ and with a smaller time-lag $\Delta_2 \ll \Delta_1$. Then, we discard the samples on $[t_0, t_1]$ which are corrupted by numerical errors, and reduce the sampling frequency of the remainder.

We remark that the Lévy subordinator Z is left unspecified apart from its mean and variance. For this simulation study, we aim for a simple, yet likely choice for Z. For two reasons, we work with a gamma process: first, subordinators with infinite activity seem appropriate to us, since turbulent motion requires permanent injection of energy. Second, the gamma process is a well-understood subordinator and, moreover, is uniquely specified by its mean and variance.

We chose $\Delta_2 = 10^{-5}\,\mathrm{s}$. On the interval $]-200\,\mathrm{s}, 1000\,\mathrm{s}]$, we simulated $1.2 \cdot 10^8$ independent and identically gamma distributed increments $Z_{k\Delta_2} - Z_{(k-1)\Delta_2}$ with mean $\Delta_2/(\|g_Y(t;\hat{\theta})\|_1)$ and variance Δ_2, where $\|g_Y(t;\hat{\theta})\|_1 = 0.1385$. To calculate the convolution (5.5.1) we truncated the MA-kernel g_Y at $t^* = 200\,\mathrm{s}$, where $g_Y(t^*;\hat{\theta})/g_Y(0^+;\hat{\theta})) < 3.4 \cdot 10^{-7}$. We discarded the observations on the interval $]-120\,\mathrm{s}, 0\,\mathrm{s}]$ which are corrupted by numerical errors and down-sampled to a time-lag of $\Delta_1 = 1/5000\,\mathrm{s}$. Consequently, we obtained $5 \cdot 10^6$ (approximate) observations $\tilde{Y}_{k\Delta_1}$ on the interval $]0\,\mathrm{s}, 1000\,\mathrm{s}]$.

As a time-changed Lévy process, the intermittency process W has independent increments conditionally on Y. By (5.4.1), moreover, we have

$$\log \mathbb{E}\left[e^{iu(W_{t+\Delta_1} - W_t)} \,\middle|\, Y\right] = \int_t^{t+\Delta_1} Y_s ds \int \left(e^{iux} - 1 - iux\right) f(x; \hat{\theta}_{p_+,p_-}) dx.$$

For each k, approximating the increment of the time-change by $\Delta_1 \tilde{Y}_{k\Delta_1}$, we simulated the increment $W_{(k+1)\Delta_1} - W_{k\Delta_1}$ using the shot-noise representation (5.19) of Rosiński (2007). All jumps with absolute value larger than 10^{-6} where simulated exactly; the small jumps where approximated by a Gaussian random variable of appropriate variance. Consequently, we obtained a sample of $5 \cdot 10^6$ (approximate) increments $\Delta_k^n \tilde{W}$ on the interval $]0\,\mathrm{s}, 1000\,\mathrm{s}]$. We present our simulation result in Figure 5.6. At the top, we plotted the increments of the intermittency at the sampling frequency of 5000 Hz. In comparison to the data as presented in 5.3, we observe a convincing similarity. At the bottom, we compare the simulation and the data in more detail: On the left, we present a quantile-quantile plot comparing the empirical quantiles of the data (x-axis) to those of the simulation (y-axis). On the interval $[-0.3, 0.3]$, which carries more than 99.996% of the data, the fit is excellent. Since the least squares fitting of the Lévy density has been performed on the domain $[-0.3, -0.015] \cup [0.015, 0.3]$ only, we are very satisfied with the fit of the stationary distribution of the intermittency increments. On the right, we compare the empirical autocorrelation function of the squared intermittency data (black points) to the empirical autocorrelation of the square simulated increments (red solid line). Both axes are in logarithmic scale. Again, their agreement is excellent.

5.6. Discussion and conclusion

In this Chapter we proposed application of a large class of stochastic processes in the context of time-wise turbulence modelling. The class of CMA processes (5.1.2) is rather flexible, with the only constraint of having a spectral density satisfying the Paley-Wiener condition (5.1.1), which excludes processes with spectrum decaying too fast but it still allows them to have sample path infinitely differentiable with probability 1. Although causality is a reasonable feature of time-wise behaviour of turbulence, it is not in the spacial one, and the link between the two is the often criticised Taylor frozen field hypothesis. To the authors' knowledge, this is the first time the question is raised and it is worthy to be studied in more detail, e.g. using DNS simulation as in del Álamo and Jiménez (2009).

Essentially the CMA model distinguishes between second order properties, accounted by the kernel function, and higher order ones, depending on the noise, which can be specified independently from each other, in agreement with the K41 theory. The dependence of the kernel function on the Reynolds number is analysed, with a special regard to its behaviour far away from the origin. The analysis in the time domain allows higher resolution of second order properties at higher lags, which corresponds to the leftmost part of the one-sided spectrum, showing in a clear way how the inertial range, proportional to $\delta_{\mathrm{Re}}^{-1}$, and the decorellation time T_{Re} increases with the Reynolds number.

We propose a modification of the gamma model of Barndorff-Nielsen and Schmiegel (2008a), with the parameters depending explicitly on the Reynolds number, modelling well the inertial range and the transition to the energy range. Unfortunately the present data, due instrumental noise, does not allow a precise analysis of the behaviour of the kernel function near to the origin, which corresponds to the dissipation range. Such an analysis would be possible using data coming from computer simulations, and it is left for future research.

Moreover, the method to recover the driving noise of Chapter 3 is employed. The obtained noise, which is dimensionally the square root of the energy dissipation, shows some of the features of the energy dissipation ε_t, collectively known as intermittency. That shows that the second order dependence does not play an important role in determining the high order statistics. Moreover, a parametric mode is proposed and fitted to the data. The distribution of the increments and the autocorrelation function of the squared increments is excellent.

We conclude mentioning that the analysis performed in this Chapter holds in great generality for one-dimensional processes. It is possible to model the full three-dimensional, time-wise behaviour of turbulent velocity field with a similar CMA model, and under the hypothesis of isotropy a model for the three-dimensional kernel function can be obtained from a one-dimensional one, since the two point correlator depends only on the longitudinal autocorrelation function (see e.g. Pope (2000), p. 196).

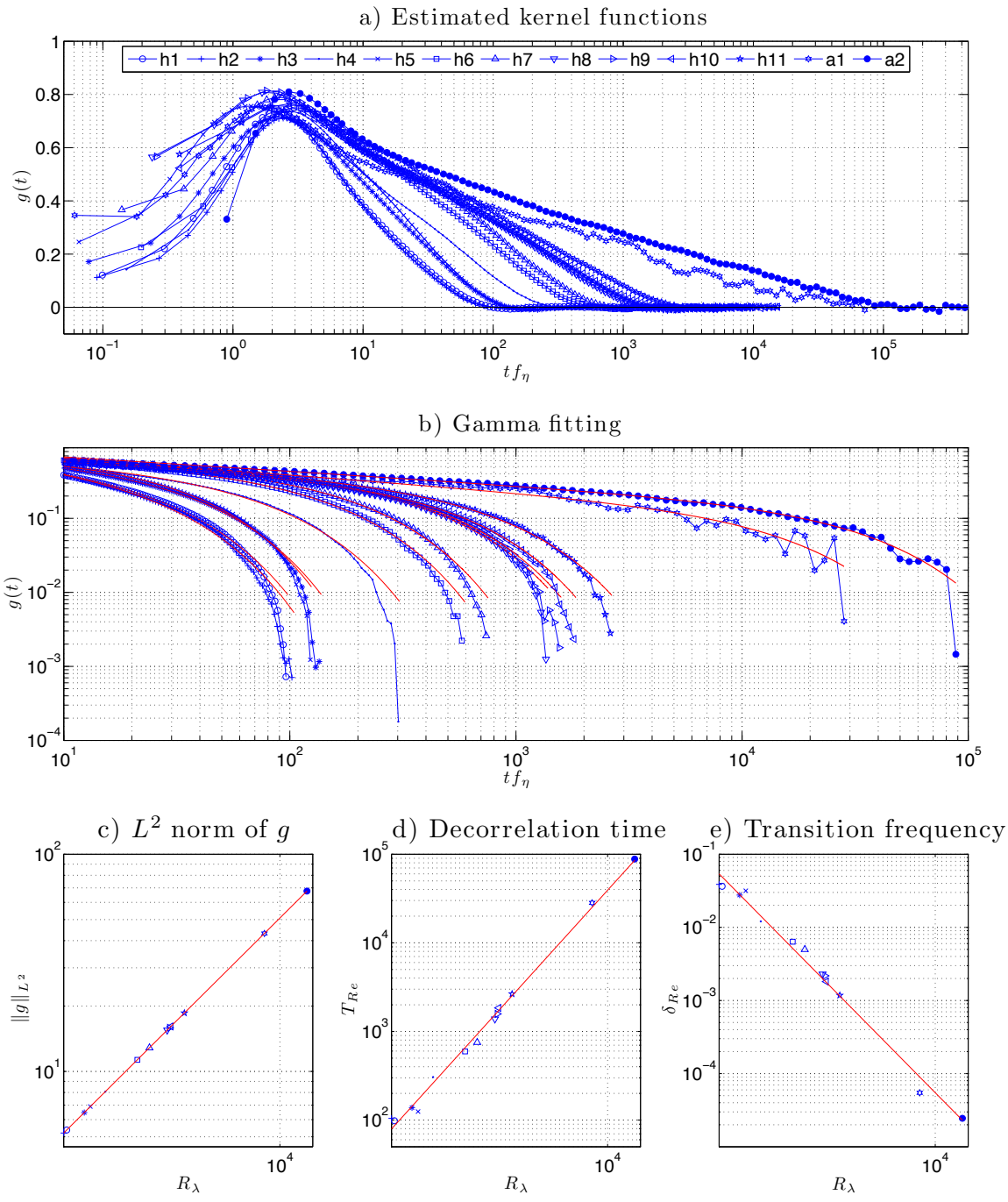

Figure 5.2.: a) Estimated kernels, against logarithmic time scale. b) Estimated kernels, plotted in log-log scale. Solid lines are the fitted gamma models (5.2.8). c-e) Decorrelation times T_{Re}, transition frequency δ_{Re} and $\|g\|_{L^2}^2$ as a function of Taylor microscale-based Reynolds number. Solid lines represents power-law fittings of the considered quantities vs. R_λ.

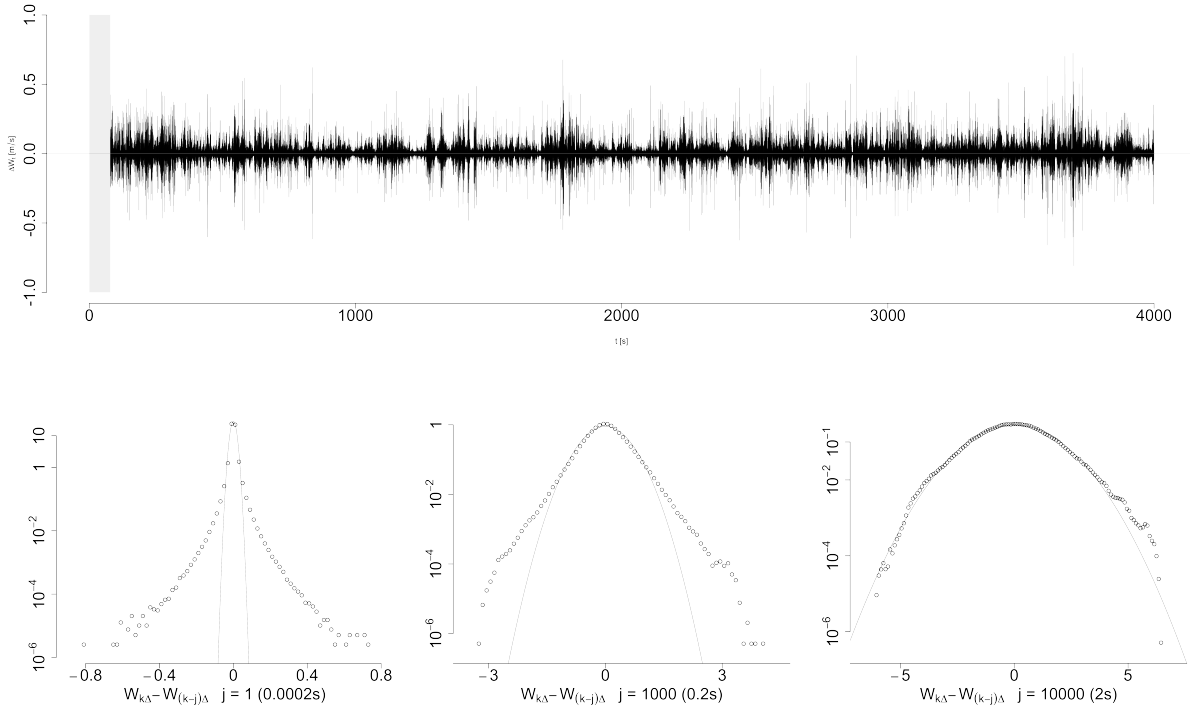

Figure 5.3.: Increments of the intermittency process W. Top: (estimated) increments $W_{k\Delta} - W_{(k-1)\Delta}$ of the intermittency process covering a total time interval of 65 min 21.1276 s. Bottom: histograms of the intermittency increments at time-lags $j\Delta$ for $j = 1$ (left), $j = 1000$ (middle) and $j = 10\,000$ (right). The y-axes are in logarithmic scale. The solid black line represents the Gaussian density scaled to the empirical variance of the intermittency increments.

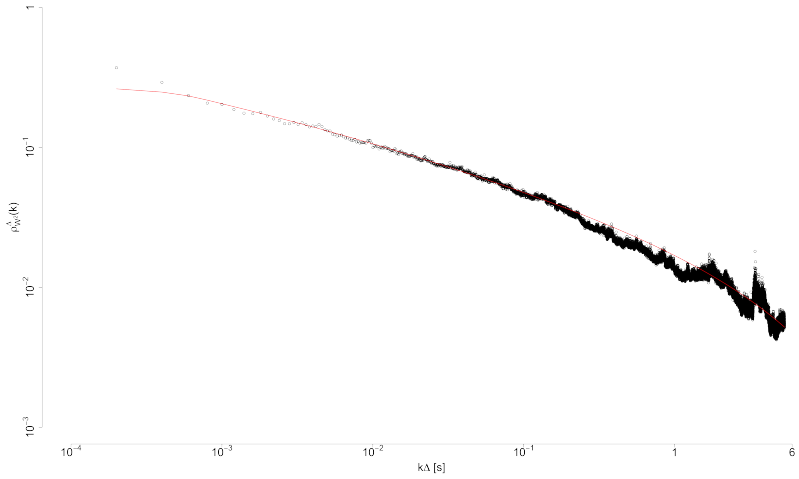

Figure 5.4.: Comparison of the empirical autocorrelation $\hat{\rho}^{\Delta}_{W^2}$ of the squared intermittency increments $(\Delta^n_k W)^2$ (black points) for lags $k = 1, \ldots, 26\,698$ corresponding to a time-lag of 5.3396s and of the parametric estimate $\rho^{\Delta}_{W^2}(\cdot; \hat{\theta})$ (red solid line). Both axes are in logarithmic scale. Right: least squares estimates of the parameters $\hat{\theta}$ of $g_Y(\cdot; \theta)$.

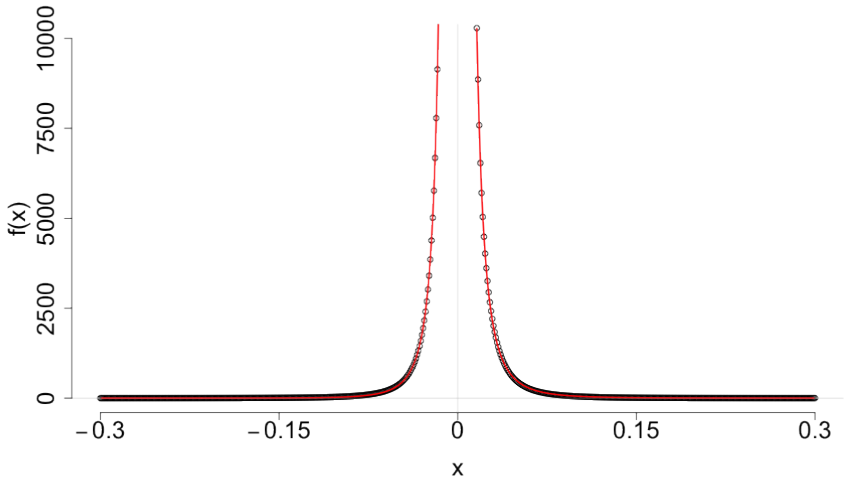

Figure 5.5.: Estimation of the tempered stable Lévy density. Left and right: the parametric estimate $f(x, \hat{\theta}_{1,2})$ (red line) and the non-parametric estimate $\hat{f}^{\hat{m}}_{\mu}(x)x^{-4}$ (black points) are compared on the domain $0.15 \leq |x| \leq 0.3$.

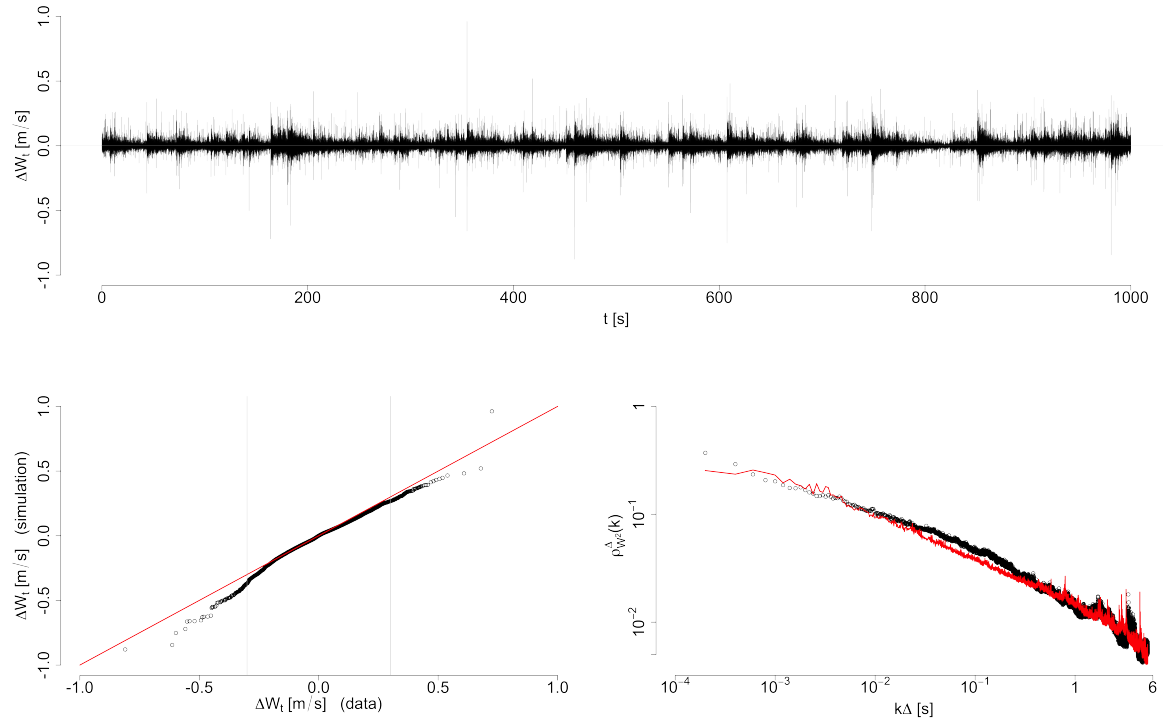

Figure 5.6.: Simulation from the fitted model. Top: simulated increments $W_{k\Delta} - W_{(k-1)\Delta}$ of the intermittency process on an interval of length 1000 s. Bottom-Left: quantile-quantile plot (black points) of the observed increments $\Delta_k^n W$ of the data (x-axis) against the simulated increments (y-axis). The red line indicates the identity diagonal. The fit is excellent on $[-0.3, 0.3]$ which carries more than 99.996% of the data. Bottom-Right: comparison of the empirical autocorrelation $\hat{\rho}^{\Delta}_{W^2}$ of the squared intermittency increments $(\Delta_k^n W)^2$ (black points) for lags $k = 1, \ldots, 26\,698$ corresponding to a time-lag of 5.3396s and of the empirical autocorrelation of the squared simulated intermittency increments (red solid line).

6. Bibliography

Abramowitz, M. and Stegun, I. A.: 1974, *Handbook of Mathematical Functions With Formulas, Graphs, and Mathematical Tables*, Dover Publications, New York.

Barndorff-Nielsen, O. E., Blæsild, P. and Schmiegel, J.: 2004, A parsimonious and universal description of turbulent velocity increments, *Eur. Phys. J. B* **41**, 345–363.

Barndorff-Nielsen, O. E., Corcuera, J. M. and Podolskij, M.: 2011, Multipower variation for Brownian semistationary processes, *Bernoulli* **17**(4), 1159–1194.

Barndorff-Nielsen, O. E. and Schmiegel, J.: 2004, Lévy based tempo-spatial modeling; with applications to turbulence, *Uspekhi Mat. Nauk* **159**, 63–90.

Barndorff-Nielsen, O. E. and Schmiegel, J.: 2008a, A stochastic differential equation framework for the timewise dynamics of turbulent velocities, *Theory of Probability and its Applications* **52**(3), 372–388.

Barndorff-Nielsen, O. E. and Schmiegel, J.: 2008b, Time change, volatility and turbulence, *Technical report*, Thiele Center for Applied Mathematics in Natural Science, Aarhus.

Barndorff-Nielsen, O. E. and Schmiegel, J.: 2009, Brownian semistationary processes and volatility/intermittency, *in* H. Albrecher, W. Runggaldier and W. Schachermayer (eds), *Advanced Financial Modelling*, Walter de Gruyter, Berlin, pp. 1–26. Radon Ser. Comput. Appl. Math. **8**.

Barndorff-Nielsen, O. E. and Shepard, N.: 2006, Impact of jumps on returns and realised variances: econometric analysis of time-deformed Lévy processes, *Journal of econometrics* **131**, 217–252.

Barndorff-Nielsen, O. E. and Shephard, N.: 2001, Non-Gaussian Ornstein-Uhlenbeck based models and some of their uses in financial economics, *J. Roy. Statist. Soc. Ser. B* **63**, 167–241.

Barndorff-Nielsen, O. E. and Shephard, N.: 2002, Econometric analysis of realised volatility and its use in estimating stochastic volatility models, *J. Roy. Statist. Soc. Ser. B* **64**, 253–280.

Batchelor, G. K.: 1953, *The Theory of Homogeneous Turbulence*, Cambridge University Press.

Beran, J.: 1992, Statistical methods for data with long-range dependence, *Statistical Science* **7**(4), 404–427.

Bernstein, S.: 1929, Sur les fonctions absolument monotones, *Acta Math.* **52**(1), 1–66.

Bingham, N., Goldie, C. and Teugels, J.: 1987, *Regular Variation*, Cambridge University Press, Cambridge.

Birnir, B.: 2013, *The Kolmogorov-Obukhov statistical theory of turbulence: a mathematical theory of turbulence*, Springer Briefs in Mathematics, Springer.

Bloomfield, P.: 2000, *Fourier Analysis of Time Series, an Introduction, 2nd ed.*, Wiley, New York.

Box, G. E. P., Jenkins, G. M. and Reinsel, G. C.: 1994, *Time Series Analysis: Forecasting and Control*, Prentice-Hall, Englewood Cliffs.

Brockwell, A. E. and Brockwell, P. J.: 1999, A class of non-embeddable ARMA processes, *J. Time Series Analysis* **20**, 483–486.

Brockwell, P. J.: 1995, A note on the embedding of discrete-time ARMA processes, *J. Time Series Analysis* **16**(5), 451–460.

Brockwell, P. J.: 2001, Lévy-driven CARMA processes, *Ann. Inst. Statist. Math.* **53**(1), 113–124.

Brockwell, P. J. and Davis, R. A.: 1988, Simple consistent estimation of the coefficients of a linear filter, *Stoch. Proc. Appl.* **28**(1), 47–59.

Brockwell, P. J. and Davis, R. A.: 1991, *Time Series: Theory and Methods*, 2nd edn, Springer, New York.

Brockwell, P. J., Davis, R. A. and Yang, Y.: 2011, Estimation for non-negative Lévy-driven CARMA processes, *J. Bus. Econom. Statist.* **29**(2), 250–259.

Brockwell, P. J., Ferrazzano, V. and Klüppelberg, C.: 2012, High-frequency sampling of a continuous-time ARMA process, *J. Time Series Analysis* **33**(1), 152–160.

Brockwell, P. J., Ferrazzano, V. and Klüppelberg, C.: 2013, High-frequency sampling and kernel estimation for continuous-time moving average processes, *J. Time Series Analysis* **34**(3), 385–403.

Brockwell, P. J. and Lindner, A.: 2009, Existence and uniqueness of stationary Lévy-driven CARMA processes, *Stoch. Proc. Appl.* **119**(8), 2660–2681.

Brockwell, P. J. and Marquardt, T.: 2005, Lévy-driven and fractionally integrated ARMA processes with continuous time parameter, *Statistica Sinica* **15**(2), 477–494.

Brockwell, P. J. and Schlemm, E.: 2013, Parametric estimation of the driving Lévy process of multivariate CARMA processes from discrete observations, *Journal of Multivariate Analysis* **115**, 217–251.

Bruun, H.: 1995, *Hot-Wire Anemometry: Principles and Signal Analysis*, Oxford University Press, Oxford.

Carr, P. and Wu, L.: 2004, Time-changed levy processes and option pricing, *Journal of Financial Economics* **71**(1), 113–141.

Champagne, F. H.: 1978, The fine structure of the turbulent velocity field, *J. Fluid Mech.* **86**(1), 67–108.

Chanal, O., Chabaud, B., Castain, B. and Hébral, B.: 2000, Intermittency in a turbulent low temperature gaseosus helium jet, *Eur. Phys. J. B* **17**, 309–317.

Chen, S., Doolen, G., Herring, J. R., Kraichnan, R. H., Orszag, S. A. and She, Z. S.: 1993, Far-dissipation range of turbulence, *Phys. Rev. Lett.* **70**(20), 3051–3054.

Cleve, J.: 2004, *Data-driven theoretical modelling of the turbulent energy cascade*, PhD thesis, Technische Universität Dresden.

Cleve, J., Greiner, M., Pearson, B. R. and Sreenivasan, K. R.: 2004, Intermittency exponent of the turbulent energy cascade, *Phys. Rev. E* **69**, 066316.

Cline, D. B. H.: 1991, Abelian and Tauberian theorems relating the local behavior of an integral function to the tail behavior of its Fourier transform, *Journal of Mathematical Analysis and Applications* **154**, 55–76.

del Álamo, J. C. and Jiménez, J.: 2009, Estimation of turbulent convection velocities and corrections to Taylor's approximation, *J. Fluid Mech.* **640**, 5–26.

Doob, J. L.: 1944, The elementary Gaussian processes, *Ann. Math. Stat.* **15**(3), 229–282.

Doob, J. L.: 1990, *Stochastic Processes*, 2nd edn, Wiley, New York.

Drhuva, B. R.: 2000, *An experimental study of high Reynolds number turbulence in the atmosphere*, PhD thesis, Yale University.

Fasen, V.: 2012, Statistical inference of spectral estimation for continuous-time ma processes with finite second moments. Submitted for publication.

Fasen, V. and Fuchs, F.: 2013, On the limit behavior of the periodogram of high-frequency sampled stable CARMA processes, *Stoch. Proc. Appl.* **123**(1), 229–273.

Ferrazzano, V.: 2010, The windspeed recording process and related issues, *Technical report*, Technische Universität München, Munich. *www-m4.ma.tum.de/en/research/preprints-publications/*.

Ferrazzano, V. and Fuchs, F.: 2013, Noise recovery for Lévy-driven carma processes and high-frequency behaviour of approximating riemann sums, *Electron. J. Statist.* **7**, 533–561.

Ferrazzano, V., Klüppelberg, C. and Ueltzhöfer, F. A. J.: 2012, Turbulence modeling by time-series methods. In preparation.

Figueroa-López, J. E.: 2009, Nonparametric estimation of time-changed Lévy models under high-frequency data, *Adv. Appl. Probability* **41**, 1161–1188.

Figueroa-López, J. E.: 2011, Central limit theorems for the nonparametric estimation of time-changed Lévy models, *Scand. J. Statist.* **38**, 748–765.

Frisch, U.: 1996, *Turbulence: the Legacy of A. N. Kolmogorov*, Cambridge University Press, Cambridge.

Geman, H., Madan, D. and Yor, M.: 2001, Time changes for Lévy processes, *Math. Finance* **11**, 79–96.

Gibson, C. and Schwarz, W.: 1963, Universal equilibrium spectra of turbulent velocity and scalar fields, *J. Fluid Mech.* **16**(3), 365–384.

Gikhman, I. I. and Skorokhod, A. V.: 2004, *The Theory of Stochastic Processes I*, reprint of the 1974 edn, Springer.

Gledzer, E.: 1997, On the Taylor hypothesis corrections for measured energy spectra of turbulence, *Physica D: Nonlinear Phenomena* **104**(2), 163–183.

Graham, R. L., Knuth, D. E. and Patashnik, O.: 1994, *Concrete Mathematics*, 2nd edn, Addison-Wesley, Reading, MA.

Gulitski, G., Kholmyansky, M., Kinzelbach, W., Lüthi, B., Tsinober, A. and Yorish, S.: 2007, Velocity and temperature derivatives in high-Reynolds-number turbulent flows in the atmospheric surface layer. Part 1. Facilities, methods and some general results, *J. Fluid Mech.* **589**, 57–81.

Guttorp, P. and Gneiting, T.: 2005, On the Whittle-Matérn correlation family, *Technical Report 80*, NRCSE Technical Report Series, Washington DC.

Hörmander, L.: 1990, *The Analysis of Linear Partial Differential Operators*, Vol. 1, Springer, Berlin.

IEC 61400-1: 1999, *Wind Turbine Generator Systems, Part 1. Safety Requirements, International Standard*, 2 edn, International Electrotechnical Commission, Geneva.

Ishihara, T., Kaneda, Y., Yokokawa, M., Itakura, K. and Uno, A.: 2007, Small-scale statistics in high-resolution direct numerical simulation of turbulence: Reynolds number dependence of one-point velocity gradient statistics, *J. Fluid Mech.* **592**, 335–366.

Jacod, J.: 1979, *Calcul Stochastique et Problèmes de Martingales*, Vol. 714 of *Lecture Notes in Mathematics*, Springer, Berlin.

Jacod, J., Klüppelberg, C. and Müller, G.: 2010, Testing for zero correlation or for a functional relationship between price and volatility jumps. Submitted for publication.

Jacod, J. and Protter, P.: 2012, *Discretization of Processes*, Stochastic Modelling and Applied Probability, Springer.

Jacod, J. and Shiryaev, A. N.: 2003, *Limit Theorems for Stochastic Processes*, Springer, Berlin. 2nd edition.

Jacod, J. and Todorov, V.: 2010, Do price and volatility jump together?, *Ann. Appl. Probab.* **20**(4), 1425–1469.

Jones, R.: 1981, Fitting a continuous time autoregression to discrete data, *in* D. Finley (ed.), *Applied Time Series Analysis II*, Academic Press, New York, pp. 651–682.

Kallsen, J. and Muhle-Karbe, J.: 2011, Method of moments estimation in time-changed Lévy models, *Statistics and Decisions* **28**(2), 169–194.

Klüppelberg, C., Lindner, A. and Maller, R.: 2004, A continuous-time GARCH process driven by a Lévy process: stationarity and second order behaviour, *J. Appl. Prob.* **41**(3), 601–622.

Kolmogorov, A. N.: 1941a, Dissipation of energy in locally isotropic turbulence, *Dokl. Akad. Nauk. SSSR* **32**, 19–21.

Kolmogorov, A. N.: 1941b, The local structure of turbulence in incompressible viscous fluid for very large Reynolds numbers, *Dokl. Akad. Nauk. SSSR* **30**, 299–303.

Kolmogorov, A. N.: 1942, The equations of turbulent motion in an incompressible viscous fluid, *Izvestia Acad. Sci. USSR* **Phys. 6**, 56–58.

Lindborg, E.: 1999, Correction to the four-fifths law due to variations of the dissipation, *Phys. Fluids* **11**(3), 510–512.

Lohse, D. and Müller-Groeling, A.: 1995, Bottleneck effects in turbulence: scaling phenomena in r versus p space, *Phys. Rev. Lett.* **74**(10), 1747–1750.

Lumley, J.: 1965, Interpretation of time spectra measured in high-intensity shear flows, *Phys. Fluids* **8**, 1056–1062.

Marquardt, T. and Stelzer, R.: 2007, Multivariate CARMA processes, *Stoch. Proc. Appl.* **117**(1), 96–120.

Martínez, D. O., Chen, S., Doolen, G., Kraichnan, R. H., Wang, L.-P. and Zhou, Y.: 1997, Energy spectrum in the dissipation range of fluid turbulence, *J. Plasma Physics* **57**(1), 195–2001.

Mitrinović, D. S. and Kečkić, J. D.: 1984, *The Cauchy Method of Residues: Theory and Applications*, Reidel, Dordrecht, Holland.

Moin, P.: 2009, Revisiting Taylor's hypothesis, *J. Fluid Mech.* **640**(1-4).

O'Neill, P., Nicolaides, D., Honnery, D. and Soria, J.: 2004, Autocorrelation functions and the determination of integral length with reference to experimental and numerical data, *in* M. Behnia, W. Lin and G. D. McBain (eds), *Proceedings of the Fifteenth Australasian Fluid Mechanics Conference*, The University of Sydney.

Paley, R. C. and Wiener, N.: 1934, *Fourier Transforms in the Complex Domain*, Vol. XIX of *Colloquium Publications*, American Mathematical Society, New York.

Pope, S.: 2000, *Turbulent Flows*, Cambridge University Press, Cambridge.

Priestley, M. B.: 1981, *Spectral Analysis and Time Series*, Vol. 1, Academic Press, London.

Richardson, L. F.: 2007, *Weather Prediction by Numerical Process*, 2nd edn, Cambridge University Press, Cambridge.

Rosiński, J.: 2007, Tempering stable processes, *Stochastic Processes and their Applications* **117**(6), 677 – 707.

Saddoughi, S. G.: 1997, Local isotropy in complex turbulent boundary layers at high Reynolds number, *J. Fluid Mech.* **348**, 201–245.

Saddoughi, S. G. and Veeravalli, S. V.: 1994, Local isotropy in turbulent boundary layers at high Reynolds number, *J. Fluid Mech.* **268**(1), 333–372.

Sato, K.: 1999, *Lévy Processes and Infinitely Divisible Distributions*, Cambridge University Press, Cambridge, U.K.

Sayed, A. H. and Kailath, T.: 2001, A survey of spectral factorization methods, *Numer. Linear Algebra Appl.* **8**, 467–496.

Schumacher, J.: 2007, Sub-Kolmogorov-scale fluctuations in fluid turbulence, *EPL* **80**, 54001.

Sirovich, L., Smith, L. and Yakhot, V.: 1994, Energy spectrum of homogeneous and isotropic turbulence in far dissipation range, *Phys. Rev. Lett.* **72**(3), 344–347.

Sreenivasan, K. R.: 1995, On the universality of the Kolmogorov constant, *Phys. Fluids* **7**(11), 2778–2784.

Sreenivasan, K. R. and Kailasnath, P.: 1993, An update on the intermittency exponent in turbulence, *Phys. Fluids A* **5**, 512–515.

Taylor, G. I.: 1938, The spectrum of turbulence, *Proc. R. Soc. London A* **164**, 476.

Tennekes, H.: 1975, Eulerian and Lagrangian time microscales in isotropic turbulence, *J. Fluid Mech.* **67**(3), 561–567.

Titchmarsh, E. C.: 1948, *Introduction to the Theory of Fourier Integrals*, 2nd edn, Oxford University Press, London, UK.

Tropea, C., Yarin, A. L. and Foss, J. F. (eds): 2008, *Handbook of experimental fluid mechanics*, Springer, Berlin.

Tsinober, A.: 2009, *An Informal Conceptual Introduction to Turbulence*, Vol. 92 of *Fluid Mechanics and its Application*, 2nd edn, Springer Verlag.

Ueltzhöfer, F. A. J. and Klüppelberg, C.: 2011, An oracle inequality for penalised projection estimation of Lévy densities from high-frequency observations, *J. Nonparametr. Statist.* **23**(4), 967–989.

von Kármán, T.: 1948, Progress in statistical theory of turbulence, *Dokl. Akad. Nauk. SSSR* **34**, 530–539.

Von Neumann, J.: 1961-1963, Recent theories of turbulence. (report made to office of naval research), *in* A. H. Taub (ed.), *Collected Works*, Vol. VI, Pergamon Press.

Welch, P.: 1967, The use of fast Fourier transform for the estimation of power spectra: A method based on time averaging over short, modified periodograms, *IEEE Transactions on Audio Electroacoustics* **15**(2), 70–73.

Whittle, P.: 1951, *Hypothesis Testing in Time Series Analysis*, Almqvist & Wiksells boktr., Uppsala.

Wyngaard, J. C. and Clifford, S. F.: 1977, Taylor's hypothesis and high-frequency turbulence spectra, *J. Atmos. Sci.* **34**, 922–929.

Yaglom, A. M.: 2005, *Correlation Theory of Stationary and Related Random Functions*, Vol. I: *Basic Results*, Springer, New York.